Neuronal Communication Mediated by Gap Junctions that Form Electrical Synapses Composed of Connexin36 in the Hippocampus

by

Deepthi Thomas

A Thesis submitted to the Faculty of Graduate Studies of

The University of Manitoba

in partial fulfilment of the requirements of the degree of

MASTER OF SCIENCE

Department of Physiology and Pathophysiology

University of Manitoba

Winnipeg

Abstract

Granule cells in the hippocampus project axons to hippocampal CA3 pyramidal cells where they form large mossy fiber terminals. We have reported the presence of gap junction protein connexin36 (Cx36) specifically in the stratum lucidum of rat ventral hippocampus, thus creating morphologically mixed synapses that have the potential for dual chemical/electrical transmission capabilities. There is some electrophysiological evidence that these terminals have a gap junction-mediated electrical transmission component under some conditions. Here, we used various approaches to further characterize molecular and electrophysiological relationships between the Cx36-containing gap junctions at mossy fiber terminals and their postsynaptic elements. In the CA3b and CA3c hippocampal regions, the vast majority of these terminals, identified by their selective expression of vesicular zinc transporter-3 (ZnT3), displayed multiple, fine immunofluorescent Cx36-puncta representing gap junctions, which were absent at mossy fiber terminals in the dorsal hippocampus. These puncta were invariably found in close proximity to the protein constituents of adherens junctions (i.e., N-cadherin and nectin-1) that are a structural hallmark of mossy fiber terminals that contact dendritic shafts of CA3 pyramidal cells, thus indicating the loci of gap junctions at these contacts. Cx36-puncta were also associated with adherens junctions at mixed synapses in other regions of the CNS. Electrophysiologically induced long-term potentiation of field responses evoked by mossy fiber stimulation was greater in the ventral than dorsal hippocampus, and it remains to be determined whether the electrical component of transmission at mossy fiber terminals contributes to the enhancement of these responses.

Acknowledgements

First, I would like to thank my supervisor, James Nagy, and co-supervisor Michael Jackson for all their support, trust and time during my MSc work. They have shown and taught me the importance of hard work, dedication and perseverance for scientific excellence, and I will always be grateful for that. I also thank my committee members, Gilbert Kirouac and Tabrez Siddiqui, for their technical help and valuable inputs at various stages of the project.

I thank Gilbert Kirouac (group member, Sa Li) for teaching me the behavioural experimental procedures and their valuable suggestions for the experimental setup. Thanks to Tabrez Siddiqui (group member, Benyamin Karimi) for teaching and assisting me with the stereotaxic surgeries.

My appreciation also goes to the lab research associate, Bruce Lynn and lab technicians, Joanne Senecal and Natalie Lavine. Completing this thesis would not have been possible without the support of my lab mates, who shared their expertise and helped me solve the everyday problems encountered in the lab. I especially thank Bruce Lynn, Joanne Senecal, Antonia Beyer, and Chetan Patil for this. I also extend my gratitude to the past lab mates, Sanwal Kaur, Albert Yeung, Prajwal Raghunatha and Hossein Tavakoli.

Many thanks also to all the people who made my life in Winnipeg a memorable one; my Indian family ‘on-site’: Vinith Yathindranath and Ramya Vinith; my dear friends: Nivedita Seshadri, Prabhisha Silwal, Joanne Senecal, Antonia Beyer, Carlos Farkas, Fangying Wang, Rony Alex and Alex Mathew and their daughters.

Finally, I express my profound gratitude to my parents and sisters, Neethu Thomas and Geethu Thomas, for motivating me and being a constant source of encouragement. This would not have been possible without you all.

Dedication

I would like to dedicate my thesis and all the good things that follow this work to my parents, M J Thomas and Rosily Thomas.

Contents

List of tables

List of figures

Chapter 1: Introduction

In the mammalian brain, different types of neurons are embedded in complex but organized networks. Normal brain function relies on the efficiency with which these neurons communicate with each other. Interneuronal communication takes place at defined minute gaps of about 20-40 nm size between neuronal elements (Tanaka et al., 2000) called synapses, where information in the form of signals is transmitted from one neuron to another within a range of milliseconds to seconds. This synaptic transmission occurs through either chemical and/or electrical signals. At chemical synapses, transmission involves action potential generation that causes the release of neurotransmitters from a presynaptic neuron, which bind to specific receptors in the postsynaptic neuron, leading to transient changes in membrane potential. At electrical synapses, two neurons are connected directly through gap junctions formed by clusters of intercellular channels, which facilitate the spread of ions and thus current between the connected neurons (Pereda, 2014). The work in this thesis is focused on electrical synapses created by the gap junction-forming protein connexin36 (Cx36) in the ventral portion of the hippocampus in rat, and specifically at highly specialized nerve endings called mossy fiber terminals, where those synapses are designated "mixed chemical/electrical synapses". Given this focus, the sections below provide a general background on gap junction and connexins, with emphasis on the distribution, structure and regulation of junctions formed by Cx36, and the nature of electrical synapses including those in mammalian CNS as well as in lower vertebrates where specifically mixed synapses were first discovered. Also presented is an overview of neuronal connections in the hippocampus in relation to what is known about electrical synapses in this structure, including current knowledge of mixed synapses at mossy fiber terminals and possible roles they play in synaptic plasticity.

1.1. Gap junctions and connexins

Gap junctions are clusters of transmembrane channels termed connexons that are hexameric assemblies of connexin (Cx) proteins (Connors and Long, 2004). Connexons between neighbouring cells appose head-to-head across the extracellular space to form transcellular pathways that permit the direct cell-to-cell transfer of ions and small metabolites (Figure 1.1). Close membrane apposition between adjacent cells is required for docking of connexons, but this apposition leaves a narrow "gap" of about 1.5-2.0 nm and hence the name gap junction (Goodenough and Paul, 2009). Gap junction channels are formed by 20 different connexin

proteins in humans and 21 in mice and rats (Willecke et al., 2002; Evans, 2015), each of which is named after its molecular weight in kDa. Multiple connexins can be present in a cell, and these may oligomerize with the same connexins to form homomeric connexons or different connexins to form heteromeric connexons (Falk et al. 1997; Segretain and Falk 2004). Also, connexons containing identical connexins can appose head-to-head to form homotypic channels or connexons containing different connexins in each of the appossing membranes to form heterotypic channels between adjacent cells. Although not all 20 or 21 connexin proteins are permissive for forming functional heterotypic channels with each other, the number of heterotypic channel combinations is large, and each combination possesses specific properties in terms of conductance and permeability. The general molecular structure or protein domains of connexins were predicted using hydropathy plots of connexin protein sequences (Evans, 2015). According to these plots, connexins span across the membrane with four hydrophobic α helical sequences. These sequences are linked by two extracellular loops and one cytosolic loop, each linked by three intramolecular disulfide bonds. At the cytoplasmic face of the protein lies a short N-terminus and a longer C-terminus tail, of which the latter varies in sequence and length across the connexin family members, thereby creating different molecular weights among these members. Gap junction channels have a high turnover rate of 3-5 hours, which is about ten times faster than most other membrane proteins (Evans, 2015). During turnover, connexons are removed from the center of the gap junction plaque, and new connexons are added to the periphery of plaques (Flores et al., 2012). Of the 20 different connexin proteins in humans (or 21 in case of the mice), about half are expressed in various cell types in the central nervous system (CNS).

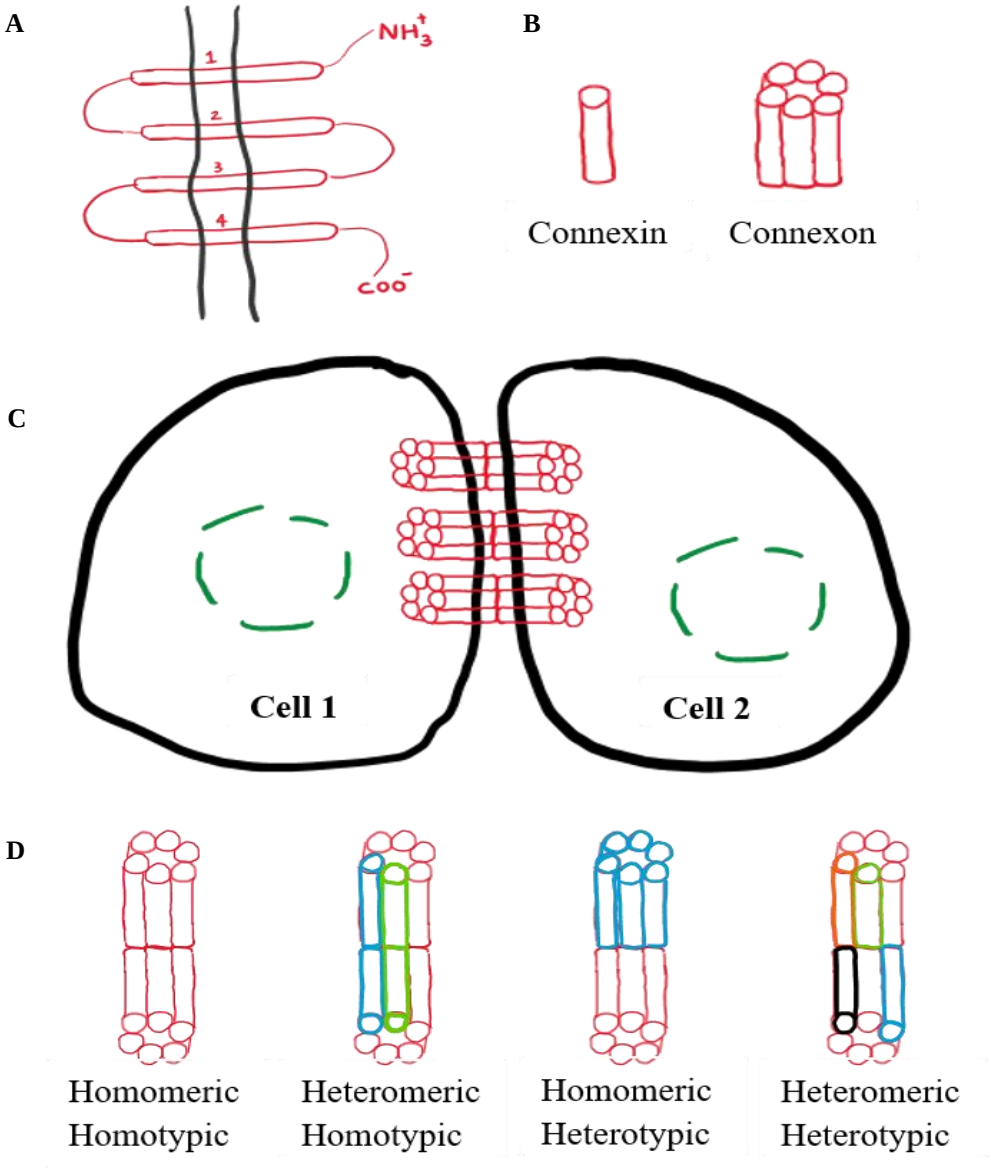

Figure 1.1. Connexins form the structural basis for gap junction channels. (A) All connexin proteins contain four transmembrane segments connected by two extracellular loops in the extracellular space and an intracellular loop in the cytoplasmic side. At the cytoplasmic face, connexins have a short N-terminus stub and a cytoplasmic tail that has variability in sequence among the connexins. (B, C) Individual connexins assemble to form connexons, which are trafficked to the surface of cell 1 and dock with connexons from cell 2 to create a complete intercellular channel. (D) Gap junction channels composed of a single connexin type are homomeric, while channels containing two or more different types of connexins are heteromeric. A homotypic gap junction channel is formed when two identical connexons dock with each other, and a heterotypic channel is formed when different connexons containing different connexins are docked. The figure is modified from Goodenough and Paul, 2009.

1.1.1. Neuronal gap junctions and electrical synapses

Gap junctions formed between non-excitable or non-neuronal cells throughout the body allow cells to share inorganic ions, metabolites and signalling molecules such as Ca^{2+} and cyclic AMP, giving rise to metabolic coupling between neighbouring cells. When formed between excitable cells like neurons, gap junctions constitute electrical synapses whose primary function is to allow the flow of current from one neuron to another (Bennett, 1997). These electrical synapses are extensively found throughout the spinal cord and brain, and between excitatory as well as inhibitory neurons (Nagy et al., 2018). Neuronal gap junctions are composed of Cx36, connexin45 (Cx45) or connexin50 (Cx50), among which Cx36 is the most abundantly expressed in a wide variety of neurons (Srinivas et al., 1999; Pereda et al., 2004). Gap junctions are often located at dendro-dendritic or dendro-somatic neuronal contacts, creating what have been called "purely electrical synapses" and referred to here as simply electrical synapses. These synapses are formed by gap junctions that have no structural association with any components of the chemical mode of neurotransmission (Nagy et al., 2018). Gap junctions forming these electrical synapses are often seen to be associated with proteins that are the structural basis of adherens junctions, as discussed further in sections below, and this association is thought to play an important role in the structural assembly and regulation of connexin channels (Derangeon et al., 2009; Lynn et al., 2012).

Neurotransmission at electrical synapses is a highly regulated, dynamic process (Goodenough and Paul, 2009), which expands the physiological complexity of these synapses, just as is known to be the case at chemical synapses. The most common function of electrical synapses includes the synchronization of subthreshold and suprathreshold electrical activity among groups of neurons (Bennett et al., 1963). Subthreshold depolarization events below that which would trigger action potentials have amplitudes and speeds much lower than action potentials themselves. Transmission of these subthreshold events are favored by electrical synapses because these synapses allow signals with a lower frequency to pass through relatively quickly without much signal attenuation, which is a distinguishing property possessed by electrical synapses that have the characteristics of a low-pass filter (Connors, 2009). The consequences of the low-pass filter properties of these synapses are profound, as seen in inferior olivary neurons and inhibitory GABAergic interneurons (Long et al., 2002; Fukuda et al., 2006). The subthreshold events determine the precise timing of the action potentials and complex spikes produced at olivary neuronal projection sites (i.e., Purkinje cells), eventually resulting in synchronous neuronal activity that plays an important role in the coordination of activities in neuronal networks (Lampl and Yarom, 1993). In Cx36 knockout

(KO) mice, electrical coupling between inferior olivary neurons, synchronization of the subthreshold potentials and their production of complex spikes were abolished, supporting the importance of the synchronization of olivary neuronal activity through electrical coupling and thereby coordinating activity in cerebellar Purkinje cells, which is critical in motor control (Long et al., 2002).

1.1.2. Historical developments on electrical synapses in vertebrates

One cannot start to write about the history of synapses without mentioning the great "soup" *vs.* "spark" controversy that existed from the 1930s to the early 1950s. This debate on whether synaptic transmission is mediated chemically as posited by the soup proponents or electrically as favoured by the spark enthusiasts was resolved in 1952 by the discovery of synaptic inhibition in motoneurons by Sir John Eccles, which completely turned the tide of thinking towards the chemical mode of neurotransmission because no means were envisoned whereby such inhibition could be mediated by electrical synapses. Nevertheless, the first convincing evidence for the electrical mode of transmission was obtained in the crayfish nerve cord by Edwin Furshpan and David Potter in 1959. Around the same time, Akira Watanabe independently showed electrical transmission in the cardiac ganglion of mantid shrimp in 1958 (Bennett, 2000). Then a flood of reports ensued describing electrical synapses in many CNS regions of lower vertebrates (Pereda and Bennett, 2017), and since the turn of the century, there has been a huge and rapid increase in reports on electrical synapses in mammalian CNS (Nagy et al., 2019).

1.2. Characterization of Cx36

Long after the discovery of electrical synaptic transmission, the ultrastructural identification of electrical synapses formed by neuronal gap junctions in lower vertebrates was possible with studies involving thin-section and freeze-fracture electron microscopy (Pereda et al., 2013). In the past two decades, the combination of freeze-fracture replica immunogold labelling (FRIL) electron microscopy and confocal immunofluorescence microscopy led to the further discoveries of many connexins expressed in various cell types of the mammalian CNS. The discovery of Cx36, its expression in neurons and in multiple CNS regions provided ample evidence for electrical synaptic transmission in mammals (Condorelli et al., 1998, Sohl et al., 1998). To date, Cx36 and its connexin35 ortholog in other species such as fish remain the most abundantly expressed neuronal connexin proteins in the CNS. Moreover, only Cx36 has been reported to be present at the mixed synapses found in CNS. For this reason, this section summarizes the discovery and distribution of

Cx36-containing gap junction channels and how they are regulated based on their turnover rate, permeability, conductance, and dynamic plasticity.

1.2.1. Discovery of Cx36

Identification of Cx36 allowed the generation of antibodies that enabled its detection using immunofluorescence and also the development of Cx36 null mice to examine functional deficits in the CNS and behavioural deficits displayed by these mice. Molecular identification of Cx36 was achieved using cloning by degenerate RT-PCR techniques (Srinivas et al., 1999). Additional studies in the same year described other relevant characteristics of Cx36 gene expression during brain development (Söhl et al., 1998). Cx36 expression was shown to be up-regulated in mouse brain before birth till postnatal day 7 and, subsequently, expression levels were reduced and reached adult levels. A couple of years later, the first ultrastructural evidence for the existence of Cx36-containing gap junctions between neurons was provided using the FRIL technique in rat inferior olive and retina (Rash et al., 2000). Also, Cx36 protein localization was examined using newly developed antibodies against Cx36 and immunofluorescence approaches and showed its presence throughout the rat brain and spinal cord (Rash et al., 2000). The application of FRIL allowed the ultrastructural visualization of gap junctions with high resolution. Also, the use of larger immunogold beads that provided a clear signal allowed quick detection of gap junctions in larger tissue areas, resulting in rapid advancement in the field as more and more neuronal gap junctions could be identified using the technique.

1.2.2. Distribution of Cx36 in CNS

In situ hybridization studies showed a complex distribution of Cx36 mRNA transcripts highly expressed in the olfactory bulb, pineal gland, inferior olive, CA3/CA4 subfields of hippocampus, cerebellum, and brain stem nuclei (Table1, Hormuzdi et al., 2004). These observations supported earlier evidence for electrical synapses and cell coupling in these structures. Although Cx36 and other connexins are present in various cell types throughout the CNS, the formation of gap junctions is highly selective. For example, in the cerebral cortex, specific types of interneurons are electrically coupled to interneurons of the same type, but not interneurons of a different type. One possible explanation for this cell specificity is the presence or absence of cell adhesion molecules that specify cell contacts with each other (Pereda et al., 2004). However, it is not always true that electrical coupling occurs only between the same type of neurons (between inhibitory or between excitatory). There is evidence that gap junctions exist between neurons of different types (an

excitatory and an inhibitory) and that these neurons are electrically coupled. For example, the excitatory fusiform cells and the inhibitory stellate interneurons in the dorsal cochlear nucleus are electrically coupled via Cx36-containing gap junctions (Apostolides and Trussell, 2013). Another example is between electrically coupled parvalbumin-positive fast-spiking interneurons and pyramidal neurons in the visual cortex, where expression of Cx36 is found (Venance et al., 2000). This heterologous coupling is rare as coupling occurs primarily between neurons of the same anatomical or functional type. One of the functional attributes of heterologous coupling is that principal cells can recruit or suppress interneurons and control the interneuron network activity or vice versa. Although mechanisms that generate this specificity are not well understood, it appears that gap junction formation and electrical coupling is highly specific.

1.2.3. Regulation of Cx36-containing gap junction channels

Electrical synapses were thought to be static structures, with minimal capacity for plasticity in their conductance or changes in rates of transmission from neuron to neuron. But, with myriad forms of regulation of gap junction function, it is now clear that electrical synapses are highly modifiable (Goodenough and Paul, 2009). As already stated, the rapid turnover rate of gap junctions indicates that they are tightly regulated with respect to connexin trafficking and assembly in the plasma membrane. The intracellular trafficking routes into and out of plasma membranes of different connexins vary. During their transit towards the plasma membrane, extensive phosphorylation occurs at amino acids in their cytoplasmic tail (Evans, 2015). Phosphorylation of different residues can make different connexins prone to degradation or stimulation of protein turnover. For example, phosphorylation at serine residue of Cx45.6 enhances its turnover and phosphorylation of Cx32 protects it from degradation (Goodenough and Paul, 2009). In the case of Cx36, there are three C-terminus serine residues - Ser293, Ser306 and Ser315 - of which Ser293 is the primary site for phosphorylation. Also, there is Ser110 at the cytoplasmic loop, which is phosphorylated by protein kinase A (PKA) as well as other kinases (Nagy et al., 2018). It has been shown that the strength of coupling between neurons can undergo modulation, depending on the state of Cx36 phosphorylation. In particular, phosphorylation may serve to induce one conductance state over another and thus impart selectivity of conductance across gap junction channels. For example, a ~50% reduction in unitary conductance was observed when Cx43 was phosphorylated at Ser368 (Goodenough and Paul, 2009). The neuronal gap junction protein Cx36 was also shown to be phosphorylated by CAMKII, causing increased junctional conductance and thus strengthening of junctional currents through Cx36 channels (Del Corsso et al., 2012).

Another important factor that can contribute to the regulation of conductance through gap junctional channels is cytoplasmic pH, suggesting a direct interaction of protons with these channels, which causes an increase or decrease in conductance (Daniel et al., 2008). Recently, pH gating of human Cx26 was extensively studied using cryo-EM and mass spectrometry, where it was found that under acidic pH, the N-terminal domains undergo extension, ordering and association that occludes the hexameric pore of Cx26 (Khan et al., 2020). But this relation cannot be generalized to all connexin isoforms. For instance, the junctional conductance of Cx36 channels is increased with the acidification of the cytoplasm, while alkalization increases the conductance of channels formed by other connexins (Daniel et al., 2008; Rimkute et al., 2018). This was shown to be the case for Cx36-containing channels formed in human and mouse cells and channels formed by Cx35 in perch, where their sensitivity to acidification sheds light on the mechanical and structural components of these connexins. Mutational studies showed that both C- and N-terminals of Cx36 interact with each other under alkaline conditions, closing the channel. Hence, intracellular proton concentration has a significant impact on Cx36 channel gating and transmission strength at electrical synapses (Daniel et al., 2008).

Changes in the strength of neuronal connections or synaptic plasticity, in general, remain one of the best cellular models for learning and memory, and the nature of these changes is dependent on the type of synapses, developmental age and stimulation parameters (Bennett, 1997; Nicoll, 2017). Synaptic plasticity of chemical synapses has been well studied and proposed to be an underlying mechanism for learning and memory in many systems. However, studies conducted on electrical synapses in fish and amphibia provided physiological evidence that various manipulations can also enhance excitability and synaptic transmission between neurons coupled with gap junctions composed of Cx35 (fish ortholog of mammalian Cx36). Gap junctions were found on auditory afferents that terminate as large, myelinated club endings on the lateral dendrite of Mauthner cells (Pereda et al., 2004). These electrical synapses were found to be modifiable by the action of neurotransmitters like dopamine as well as by activity-dependent modulation, as seen at chemical synapses. Although Mauthner cells were found to be highly innervated by dopaminergic fibers, as seen by immunolabelling with antibodies against dopamine or tyrosine hydroxylase (the rate-limiting enzyme in the synthesis of dopamine), they do not form synaptic contacts with either the primary afferents or the Mauthner cells. The dopamine released from varicose fibers activates a postsynaptic cascade by diffusing to the lateral dendrite where they interact with the dopamine D_1 receptor leading to cAMP-dependent activation and PKA-mediated

phosphorylation of Cx35, resulting in an enhancement in electrical synaptic responses. Gap junctional conductance at these terminals was also enhanced during prolonged high-frequency stimulation protocols, suggesting they exhibit activity-dependent plasticity (Pereda et al., 2004). In goldfish, high-frequency stimulation given on the posterior VIIIth nerve increased the passage of gap junction permeable dyes from Mauthner cell to primary afferents, indicating electrical synapses can undergo long-term potentiation like chemical synapses (Pereda et al., 2004; Pereda, 2014).

1.2.4. Macromolecular composition of electrical synapses

In addition to the above discussed mechanisms that contribute to regulation of transmission at electrical synapses, there are likely other still poorly defined cellular signalling pathways that govern this process, including those the orchestrate the assembly, maintenance and disassembly of neuronal gap junctions. This view is based on studies, so far largely emanating from the laboratory of my supervisor (Dr. JI Nagy), showing that electrical synapses are not just a collection of plaque-forming connexons in plasma membranes, but rather are emerging as exquisitely complex multi-molecular structures harbouring a variety of structural and regulatory proteins. Using a variety of biochemical, molecular, pull-down, co-immunoprecipitation (co-IP) and immunofluorescence approaches, it has been found that Cx36-containing neuronal gap junctions forming electrical synapses in the CNS have associated with them the scaffolding proteins zonula occludens-1 (ZO-1) and multi-PDZ protein-1 (MUPP1), the cellular signalling effector protein AF6 (aka, afadin), the E3 ubiquitin ligases LNX1 and LNX2 that ubiquitinate Cx36 for degradation, and the cytoskeleton protein cingulin. It has been demonstrated that a PDZ domain binding motif at the C-terminus of Cx36 is required and is sufficient for mediation of direct Cx36 interaction with PDZ domains contained in all of these proteins, except cingulin (Li et al., 2004; Carmen et al., 2008; Li et al., 2012; Lynn et al., 2012; Lynn et al., 2018). In addition to this complexity, neuronal gap junctions (nGJ) and specifically those forming purely electrical synapses (i.e., dendro-dendritic, dendro-somatic) in the CNS have been repeatedly shown by thin section electron microscopy to be in very close ultrastructural association and continuity with cell-cell contacts formed by adherens junctions (AJs) (Peters, 1991). Consistent with this were observations by immunofluorescence labelling that showed Cx36 and its above interacting proteins closely associate with core protein constituents of adherens junction (AJ) (N-cadherin, nectin, α-catenin, β-catenin), where AJs and nGJs occupy separate or partially overlapping domains in what were referred to as the AJ-nGJ complex (Nagy and Lynn, 2018). It is known and of note that nectins

interact with AF6, that cadherins bind α-catenin and β-catenin, and that nectin-AF6 and cadherin-catenin associate through AF6-α-catenin interaction (Harris and Tepass, 2010) and are required to cooperatively organize AJs (Miyahara et al., 2000; Takai, 2003; Mori et al., 2013). In analogy with this, the presence of AF6 at nGJs and its molecular interaction with Cx36 may also serve to anchor nGJs to AJs at the AJ-nGJ complex. In peripheral tissues, AJs promote gap junction formation in some systems (Robert et al., 1988; Derangeon et al., 2009) and may do so with respect to nGJs in the CNS, although this is not yet known. However, the presence of AF6 at nGJs provide a plausible mechanism whereby it and its associated signalling pathways may contribute not only to regulation of nGJ formation but also to efficacy of electrical synaptic transmission through control of rapid junction assembly and disassembly. In particular, AF6 is an effector of the Ras family of GTP-binding proteins such as Rap1, and Rap1 is the upstream activator of AF6 (Thomas et al., 1999; Benjamin et al., 2000; Boettner et al., 2001; Kooistra et al., 2006). Rap1 regulates cell-cell junctions, and promotes AJ formation (Caron, 2003; Kooistra et al., 2006). It is present in neurons (Xie et al., 2005), and activated by the cAMP effector Epac, a guanine nucleotide exchange factor (GEF) that is distinct from the cAMP effector protein kinase A (PKA). SynGAP1, a GTPase activating protein (GAP), which is present at nGJs (unpublished observations), is a negative regulator constraining Rap1 activity (Pena et al., 2008), and is found at chemical synapses, where it is anchored by MUPP1 (Komiyama et al., 2002; Krapivinsky et al., 2004). So far, it has been shown that cAMP via Epac increased recruitment of Cx43 to GJs in heart (Somekawa et al., 2005). Thus, although not yet directly tested, it is possible that signalling via the cAMP/Epac/Rap1 pathway to AF6 at the AJ-nGJ complex represents a novel means for regulation of AJ-nGJ assembly and maintenance and consequently electrical synaptic transmission. A diagram summarizing the above proposed scenario is shown in figure 2.

As noted above, it has been emphasized that dynamic characteristics of electrical synapses are key features of their role in neuronal circuitry (O'Brien, 2014; Pereda, 2014; Curti and O'Brien, 2016; Haas et al., 2016; Coulon and Landisman, 2017; Alcamí and Pereda, 2019; O'Brien, 2019). Mechanisms that confer those features are poorly understood, mainly because the molecular and structural organization and the protein components of those synapses and the AJ-nGJs complex is not fully known, such that those proteins identified so far likely represent only a small protion of this molecular machinery. Of relevance here is that identification of the AJ-nGJ complex and the signalling processes proposed above apply as yet only to purely electrical synapses because the existence of that complex at mixed synapses has not yet been fully examined; the presence of that

complex at mixed synapses would extend the possible occurrence of the above discussed signalling processes to these synapses.

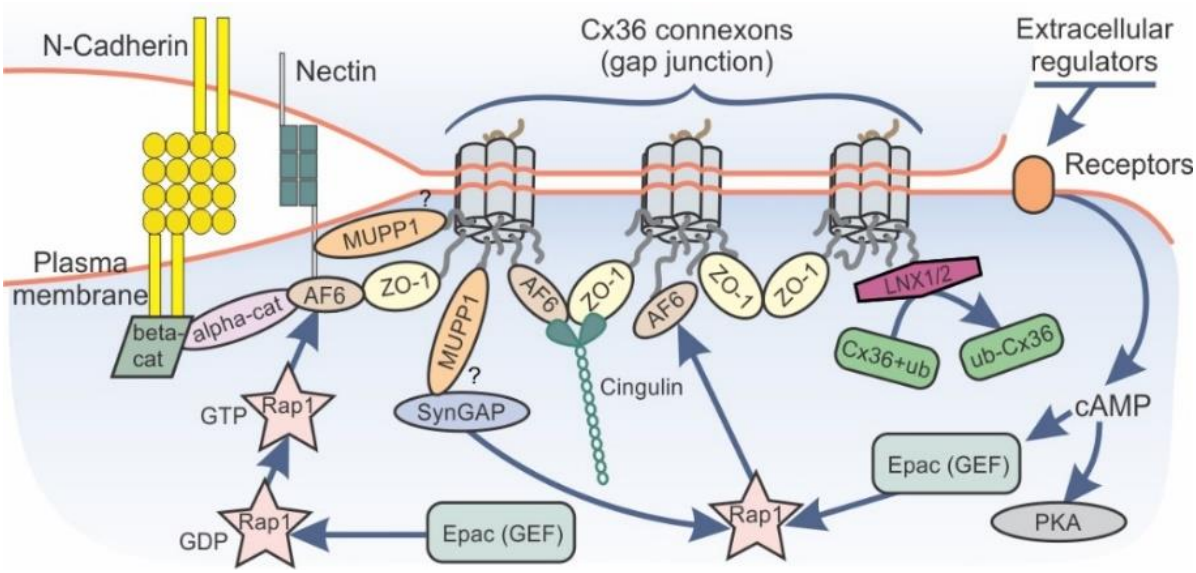

Figure 1.2. Hypothesized model of AJ-nGJ complex and cAMP-Epac-Rap1 signalling. Cx36 interactions with ZO-1, AF6 and MUPP1 via its C-terminus stabilize nGJs and nGJ-AJ interactions. cAMP activates Epac leading to Rap1 activation, recruitment of AF6 to AJ-nGJs and promotion of junctional stability and coupling capacity. SynGAP1 at AJ-nGJs interacts with MUPP1 and mediates down-regulation of Rap1 activity. AF6 interactions with catenins and ZO-1 anchor AJs to nGJs. The figure is modified from Lynn et al., 2012.

1.3. Mixed synapses: chemical/electrical

Although gap junctions, as noted, are often located at dendro-dendritic or dendro-somatic neuronal contacts, they are also found at nerve terminal synaptic contacts with dendrites and neuronal somata where chemical transmission occurs. This scenario, where a chemical synapse co-exists with an electrical synapse, is considered a mixed synapse. These were identified in lower vertebrates (Pereda et al., 2003; Pereda et al., 2004) and in mammalian CNS (Korn et al., 1973; Rash et al., 1996).

1.3.1. Distribution of mixed synapses in lower vertebrates

In lower vertebrates, mixed synapses are often found between neurons with larger somata and larger diameter axons, making them amenable to *in vivo* electrophysiological studies. At mixed synapses on Mauthner cells formed by primary afferent terminals on these cells, it is estimated that gap junctions occupy 10-20% of the synaptic contact, which is higher than that occupied by chemical transmitter release sites (Tuttle et al., 1986), and this could be why mixed synapses are seen to be preferentially associated with larger terminals where they contribute the bulk of the synaptic transmission load. Species in which mixed synapses were found include electric fish, lamprey, toadfish, frog, lizard, pigeon and chick. The most elaborately studied was the circuitry in goldfish involving the large club ending gap junctions with Mauthner cells (Nagy et al., 2019). These gap junctions composed of Cx35 were seen to be closely associated with postsynaptic specializations that contain NMDA receptors (Pereda et al., 2004). Stimulation given to the posterior VIIIth nerve afferents evoked a mixed field excitatory postsynaptic potential (fEPSP) when recorded from the lateral dendrite on Mauthner cells. This mixed synaptic potential contained a fast electrical component followed by a slower chemical component, thus providing early physiological evidence for electrical transmission in vertebrates (Figure 1.2). Mauthner cells are a pair of reticulospinal neurons with their apposing club ending axon terminals having diameters as large as 5 - 10 µm. Ultrastructural studies revealed that each of these terminals contained 24,0000 to 106,000 gap junction channels (Nakajima, 1974; Tuttle et al., 1986). Compared with estimates from electrophysiological data, the average number of open gap junction channels at a single club ending synapse is 350, suggesting most of the gap junction channels at the large myelinated club ending are closed at any given time (Tuttle et al., 1986).

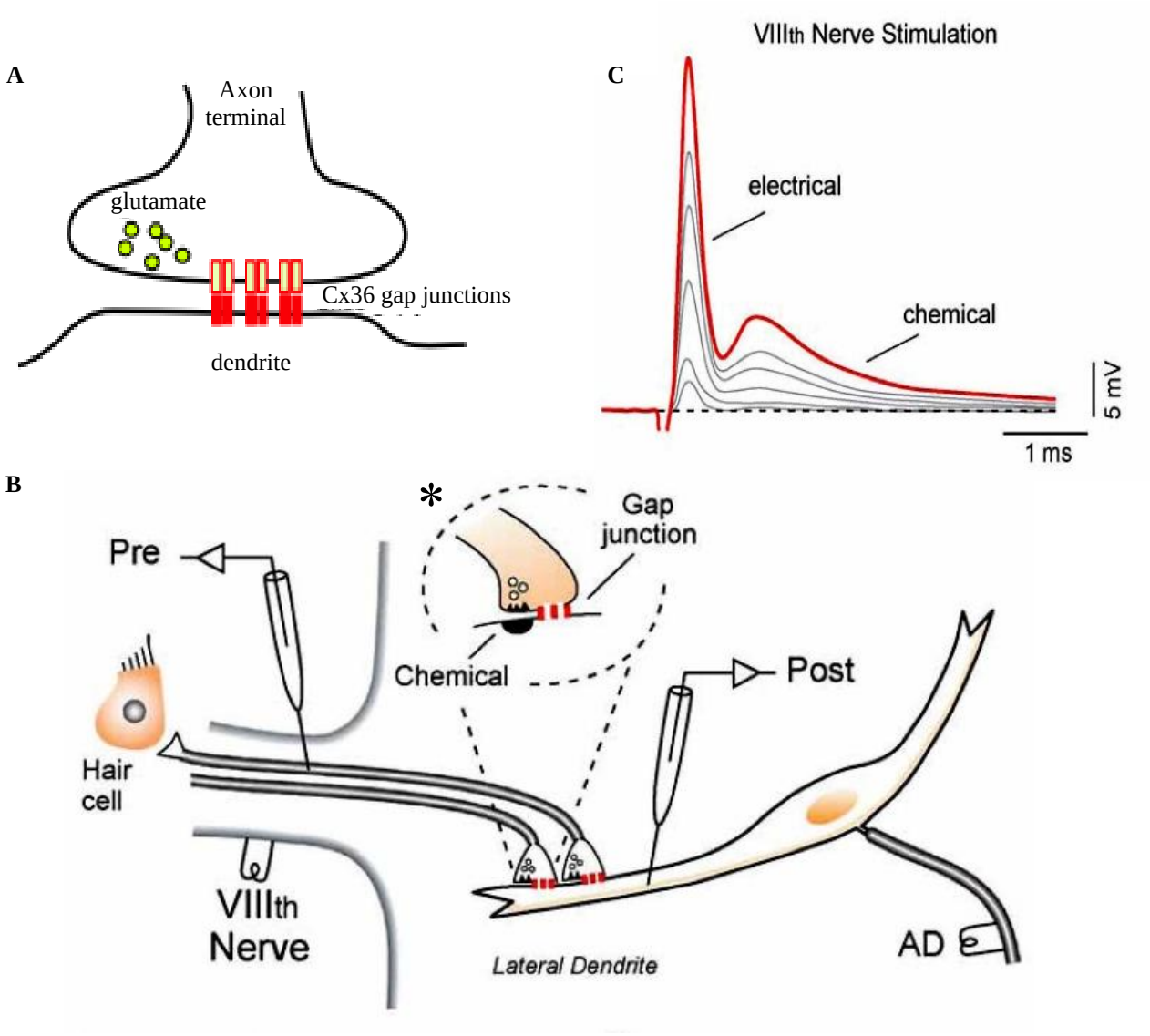

Figure 1.3. Mauthner cell endings display mixed synaptic transmission. (A) Cartoon diagram showing the presence of gap junctions between a presynaptic axon terminal, filled with glutamate-containing synaptic vesicles, and the postsynaptic dendrite. (B) The experimental arrangement showing the electrode positioning at presynaptic VIIIth nerve and postsynaptic lateral dendrite. A club ending is shown in the inset where both components of chemical and electrical transmission are present. (C) Stimulation at the VIIIth nerve produced a mixed EPSP containing contributions from both chemical and electrical components of the transmission. Graded stimulations evoked graded mixed EPSPs from the postsynaptic dendrite (Pereda et al., 2004). The figure is taken from Pereda et al., 2004.

1.3.2. Functional relevance of mixed synapses in lower vertebrates

Mauthner cells are involved in tail flip escape responses, which are triggered by sensory stimuli mediated by the VIIIth cranial nerve. Synaptic potentials recorded from the lateral dendrite of the Mauthner cell provided early physiological evidence for specifically mixed synaptic transmission in lower vertebrates. Extracellular stimulation of a single afferent of the VIIIth nerve evoked mixed synaptic potentials, indicating that the two components do not arise from the activation of purely electrical or chemical synapses associated with separate fibers. In cold-blooded species like fish, the temporal separation between the electrical and chemical components is pronounced in part resulting from the lower speed of chemical neurotransmission at their lower body temperature. Therefore, the primary advantage of combining chemical signals with electrical signals is that the electrical synapse could compensate for chemical transmission delays in cold-blooded species. Thus, the additional presence of electrical synapses provides higher fidelity to Mauthner cell networks governing behaviours such as fast escape from predators.

1.3.3. Mixed synapses at rat hippocampal mossy fiber terminals

In the search for mixed synapses in mammalian CNS, one particular region that was found to contain these was the hippocampus. Their presence in this forebrain structure came as a surprise because other mixed synapses in mammalian CNS were found exclusively in the hindbrain (i.e., brainstem) and spinal cord areas. The presence of Cx36 in the interneurons within hippocampus is well characterized both by ultrastructural (Ribak et al., 1993; Fukuda and Kosaka, 2000) and electrophysiological (Zsiros and Maccaferri, 2005) studies. Distal dendrites of parvalbumin containing GABAergic interneurons in CA1 region, hilus, stratum oriens are shown to form dendrodendritic gap junctions (Ribak et al., 1993; Fukuda and Kosaka, 2000). However, a high density of immunofluorescence labelling for Cx36 was observed in axon terminals of hippocampal granule cells in the rat ventral hippocampus (Nagy, 2012), which was not reported previously. As noted elsewhere, the labelling of Cx36 appeared as typical immunopositive Cx36-puncta that extended to the CA3b and CA3c subfields but were absent in the CA3a subfield (Nagy, 2012). The high density of fine Cx36-puncta observed at mossy fiber terminals were seen to be co-localized with various proteins - vesicular glutamate transporter 1 (vglut1) and bassoon- that were highly concentrated in the mossy fiber terminals. It was estimated from quantitative analysis of Cx36-positive puncta along the stratum lucidum region of rat hippocampus that this area posseses 40% of the density of Cx36-puncta seen in the inferior olivary nucleus, which displays among the

highest levels of Cx36 in rodent CNS (Nagy, 2012). This high density of electrical synapses associated with mossy fiber terminals could have functional and physiological implications for electrical transmission at these terminals.

1.3.4. Anatomy of the hippocampus

Given the focus of this thesis on gap junctions present in the axon terminals of hippocampal granule cells, the following is a brief account of basic hippocampal neural circuitry. Ramón y Cajal was the first to depict the main hippocampal neuronal organization using drawings based on his histological data. A massive expansion of data in hippocampus neuroanatomy occurred with the introduction of techniques such as immunohistochemistry, intracellular labelling, and anterograde and retrograde tracing methods.

The hippocampus region contains two sets of cortical structures - the hippocampal formation (HF) and the parahippocampal region (PHR) that lies adjacent to the HF. These two regions differ from each other based on their number of cortical layers and their connectivity. The rat HF is a C-shaped structure located in the caudal part of the brain with three distinctive areas – the dentate gyrus, the hippocampus proper consisting of CA3, CA2 and CA1 regions and the subiculum. The cortex that forms the HF is a three-layered structure. The first layer is a polymorph layer that contains interneurons and a mixture of afferent and efferent fibers. Superficial to this layer is the cell layer consisting of principal cells and interneurons. The most superficial layer (molecular layer) is referred to as the stratum moleculare in the DG and CA regions. The stratum moleculare is subdivided into three sublayers in CA3 and two sublayers in CA2 and CA1. In CA3, these sublayers are the stratum lucidum that receives input from DG, the stratum radiatum and the stratum lacunosum moleculare. Similar lamination is seen in CA2 and CA1 except that the stratum lucidum sublayer is absent (van Strien et al., 2009). The stratum lucidum is occupied by mossy fiber synaptic terminals that arise from all parts of the granule cell layer. Mossy fiber terminals extend through the hilar region of the dentate gyrus to the pyramidal cell layer (Figure 1.3A), some of which travel above and below the pyramidal cell layer to form the suprapyramidal bundle that is confined to the stratum lucidum. There are small varicosities (approx. 2 µm) found along the course of mossy fibers in hilus, which can form *en passant* contacts and filopodia-like extensions. These mossy fiber collaterals (which are approx. 200 in number) synapse onto the dendrites of inhibitory interneurons. Also, there are a group of larger varicosities (3-5 µm) similar to those seen in the CA3 field that terminate on complex spines or what are called 'thorny excrescences" on

proximal dendrites of mossy cells in hilus. The mossy fiber axons when enters the CA3 field, has few collaterals and form larger boutons that contact the CA3 pyramidal cells (Figure 1.3B) (Claiborne et al., 1986; Paxinos, 2004). The interval between the boutons increased significantly in the CA3c to CA3a direction, although the density of pyramidal cells is similar in these subregions (Acsády et al., 1998a).

The mossy fiber boutons that synapse onto the thorny excrescences of CA3 spines, is said to be 100 times larger in volume than a typical presynapse (Martin et al., 2017). Because of the large size, it harbors multiple release sites. It is estimated that large boutons can have up to 37 release sites (Bischofberger et al., 2006a). Due to the presence of multiple active zones and close proximity to the CA3 pyramidal cell body, release at a single bouton can have profound effects on the activity of connected CA3 neurons, making it as a detonator synapse (Martin et al., 2017). Compared with other hippocampal projections, the mossy fiber-CA3 (MF-CA3) projection is numerically and spatially limited. It is estimated that the boutons are found approximately at every 135 μm (modal value). With this estimation and considering the transverse dimension of the CA3 field to be ~2 mm, each mossy fiber will possess roughly 14 such boutons. If we take the approximate diameter of the soma of a pyramidal cell to be about 20 μm, then it would appear that mossy fibers will contact every sixth or seventh CA3 pyramidal cell along its transverse trajectory (Claiborne et al., 1986). Since single mossy fiber boutons contact spines from only one parent dendrite of CA3 pyramidal cells (or maximum two dendrites of adjacent pyramidal cells) (Chicurel and Harris, 1992; Acsády et al., 1998b), each granule cell is likely to impact 14-28 pyramidal cells.

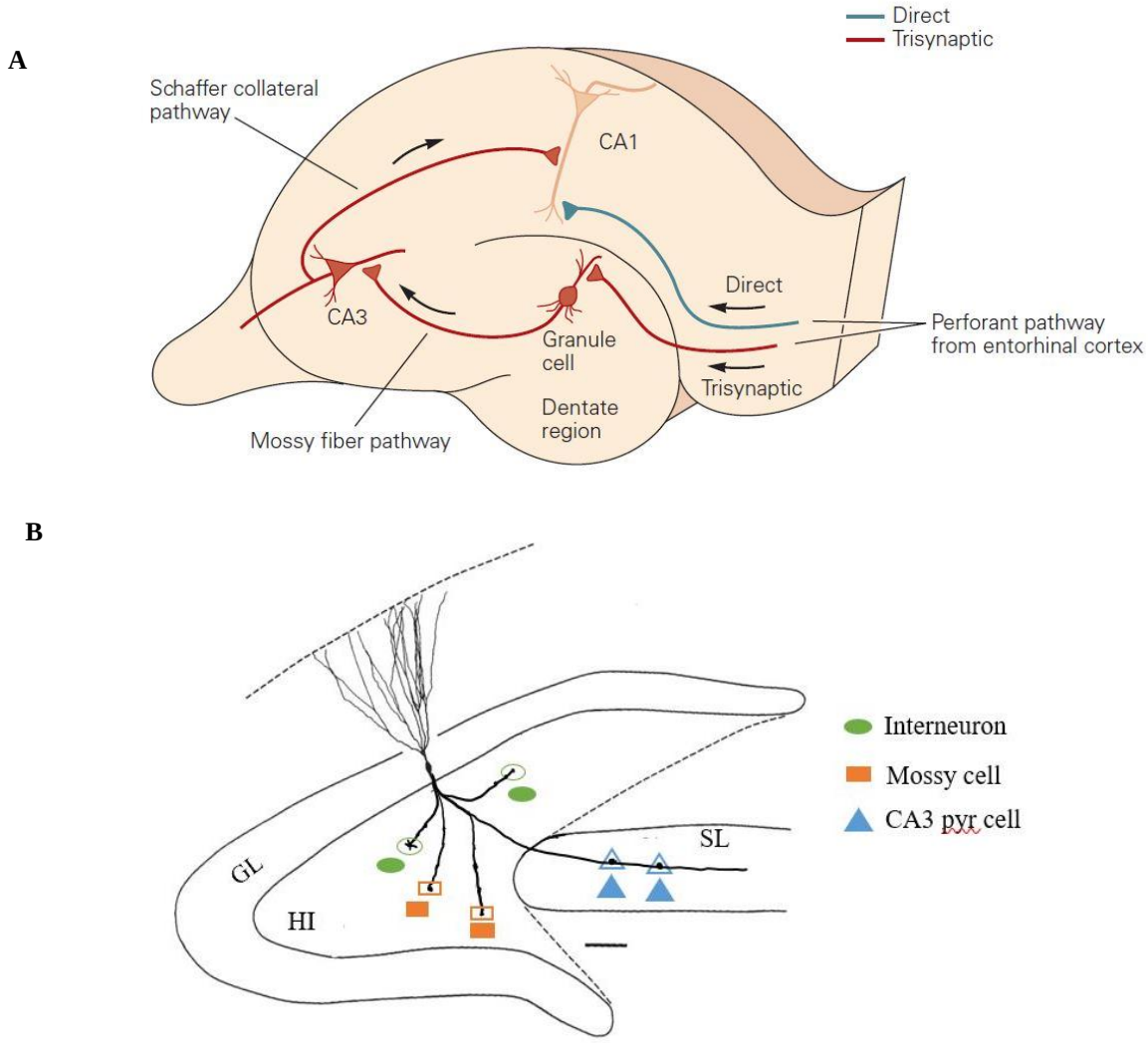

Figure 1.4. The hippocampal trisynaptic circuitry. (A) Afferent fibers enter the hippocampus from layer II of the entorhinal cortex (EC) through the perforant pathway, which projects to the CA1 pyramidal neurons both by direct and indirect (trisynaptic) pathway. Axons from the entorhinal cortex form excitatory synapses on the granule cells of the dentate gyrus, which then synapse on the proximal dendrites of CA3 pyramidal neurons through mossy fiber terminals. In the Schaffer collateral pathway, axons of the CA3 neurons project to the CA1 dendrites. In the direct pathway, fibers from layer III of the entorhinal cortex project to the distal dendrites of CA1 pyramidal neurons without any intervening synapses (Kandel, 2013). The figure is taken from the book, Principles of neural science, 5th edition, Kandel 2013. (B) Cartoon diagram showing a granule cell from the granule cell layer (GL) and its processes to summarize the major mossy fiber projections in hilus (HI) and stratum lucidum (SL). Mossy fiber collaterals in hilus form either filopodia-like extensions or *en passant* contacts (green open ovoid) on the hilar interneurons (green closed ovoid). A slightly larger collateral branches (orange open rectangle) that resemble the mossy fiber terminals found in CA3 contact the hilar mossy cells (orange closed rectangle). The mossy fiber axons ultimately enter the CA3 field where they form larger boutons (blue open triangle) that projects to the proximal dendrites of CA3 pyramidal cells (blue closed triangle). The cartoon is modified from Claiborne et al., 1986.

1.3.5. Overview of electrical and dye coupling in the hippocampus

Though evidence of Cx36 localization at mossy fibers in the stratum lucidum and hilar region by immunostaining indicates the presence of neuronal gap junctions, direct evidence to show the presence of electrical communication mediated via gap junction channels is limited. One line of evidence to establish the existence of electrical communication via gap junctions among neurons is the presence of electrical depolarizations in the form of spikelets. Spikelets are small, all-or-none fast depolarizing postsynaptic potentials resulting from presynaptic action potentials observed in electrically coupled networks (Parker et al., 2009). Dual whole-cell recording using patch-clamp electrodes that permitted recordings from neighbouring cells was an important technique that allowed the detection of spikelets. Another indication of electrical coupling via gap junctions is the observation of dye coupling between neurons following the injection of a low molecular weight dye that is permeable through gap junctions. Examples of gap junction permeable dyes include biocytin, neurobiotin, lucifer yellow, carboxyfluorescein and rhodamine 123. Apart from gap junction channel pore size, the conductance of each specific connexin that forms gap junction channels also determines dye permeability. Hence, Cx36-containing gap junction channels tend to not pass lucifer yellow, but Cx45 channels do (Traub et al., 2018). The transference of dye injected into one neuron to a neighbouring neuron suggests the presence of electrical synapses between the two neurons because chemical synapses do not allow such dye transfer.

In the hippocampus, electrical coupling between principal neurons or between interneurons has been demonstrated through paired recordings (Bennett and Pereda, 2006; Mercer et al., 2006). Dendro-dendritic gap junctions were shown to be present in GABAergic interneurons containing calcium binding protein parvalbumin (PV) in areas CA1 (Katsumaru et al., 1988), CA3 and dentate gyrus (Bennett and Zukin, 2004). Also, gap junction coupled interneurons were found between the inhibitory cells of the hilus and CA1 areas through paired-recordings of interneurons (Venance et al., 2000) and dye coupling (Michelson and Wong, 1994). The excitatory cells of the hippocampus also interact via electrical synapses. Evidence for axo-axonal electrical coupling via gap junctions was found in the rat CA1, CA3 and dentate gyrus where spikelets were observed in the somata when axons were activated. Dye coupling was observed between CA1 pyramidal neurons (43%) with the somata of the coupled cells clearly separated (Schmitz et al., 2001; Mercer et al., 2006). The spikelet amplitude observed through *in vitro* recordings was higher than the amplitude that was predicted through computer simulations performed to model electrical

interaction between two neurons. This suggests that the spikelets observed were a product of several neurons firing synchronously, which, as noted earlier, is a property conferred by electrical synapses (Vigmond et al., 1997). Studies of dye coupling between rat hippocampal CA1 pyramidal neurons suggested that dye coupling can be modified by neurotransmitters (Velazquez et al., 1997) and also is pH-dependent. Incidence of dye coupling was found to be increased with intracellular alkalinization of the CA1 pyramidal cells (Church and Baimbridge, 1991).

1.3.6. Synaptic plasticity at mossy fiber pathway

Synaptic plasticity at electrical synapses is important because it can impart dynamic changes in neural circuitry (Alcamí and Pereda, 2019) and can affect the degree of neuronal synchronization (Theoden et al., 2005). The Mauthner cell system, where the functional and physiological role of mixed synapses were well studied, exhibited activity-dependent plasticity. Repetitive stimulation (100 Hz protocol) of the posterior VIIIth nerve evoked persistent potentiation of both the chemical and electrical components of the postsynaptic EPSP responses (Pereda et al., 2013). Given that we observe mixed synapses at mossy fibers, there is a possibility of observing synaptic plasticity at both the chemical and electrical components at these synapses, which could contribute to maintaining transmission fidelity at mossy fiber terminals.

The storage of long-term memory in the hippocampus is dependent on long-lasting changes in connections between synapses. A brief stimulus, or sometimes called tetanus, given at any pathway in the hippocampus, often leads to an increase in the amplitude of excitatory postsynaptic potentials (EPSPs), a phenomenon known as long-term potentiation (LTP). LTP is a form of synaptic plasticity where the synapses are strengthened for neurotransmission through distinct molecular and cellular mechanisms. Stimulation in the Schaffer collateral pathway or the direct pathway from the entorhinal cortex to CA1 induces LTP that is dependent on the activation of NMDA receptors. Interestingly, LTP in the mossy fiber pathway does not require the activation of NMDA receptors but requires protein kinase A (PKA), which is a distinguishing feature of this pathway. Tetanus given at this pathway induces an influx of Ca^{2+} into the presynaptic terminal, which then activates the calcium/calmodulin-dependent adenylyl cyclase complex, and thereby increases cAMP production leading to activation of PKA (Kandel, 2013). Hippocampal mossy fiber synapses show several other unique transmission and plastic properties compared with other synapses. Mossy fiber synapses generate large postsynaptic currents and voltage in CA3 pyramidal neurons (Gianmaria et al., 1998; Henze et al., 2002), and have low basal release probability of

neurotransmitters (Kimberly et al., 2003). Because of the large number of release sites per bouton, mossy fiber synapses exhibit marked paired pulse and frequency facilitation (Nicoll and Schmitz, 2005). Also, the lower probability of neurotransmitter release at these synapses offers them a much greater range for increasing the release to have a higher frequency facilitation compared with the other non-mossy fiber synapses (Salin et al., 1996). The pyramidal cells now get excited robustly due to the massive facilitation at mossy fiber synapses, providing high fidelity to the synaptic transmission (McBain, 2008).

Synaptic plasticity at the trisynaptic circuit is important for hippocampal dependent learning and memory tasks. The degree of synaptic plasticity at these circuits in the hippocampus varies along the dorsal-ventral hippocampal axis. Studies have reported that LTP has a significantly higher amplitude in dorsal than the ventral hippocampus in the CA1 region of both rats and mice *in vivo* and *in vitro* (Papatheodoropoulos and Kostopoulos, 2000; Maruki et al., 2001; Milior et al., 2016). In the perforant pathway, it was found that LTP magnitude increased towards the ventral DG in mice (Schreurs et al., 2017). In agreement with these findings, there are molecular, anatomical and functional differences between the dorsal and ventral hippocampus. Gene expression studies reveal that there are specific genes expressed in the dorsal hippocampus that correlate with regions involved in information processing and specific genes in the ventral hippocampus that correlate with areas involved in emotion and stress. There is sufficient behavioral evidence indicating the functional segmentation (dorsal ventral) within the hippocampus. Both dorsal and ventral hippocampus receive inputs from and project to overlapping but also distinct brain regions, allowing them to have different functional capabilities. Dorsal hippocampus is associated with navigation, exploration and locomotion while the ventral hippocampus is involved in motivational and emotional behaviour (Fanselow and Dong, 2010). Given that we observe mixed synapses only within the ventral hippocampus, a region involved in emotional memory, it is possible that there may be differences in the magnitude of LTP at mossy fiber terminals in dorsal *vs.* ventral hippocampus if the electrical component of transmission at these terminals in the ventral hippocampus contributes to the development of LTP. More generally, the presence of Cx36-containing gap junctions at mossy fiber terminals in the ventral hippocampus raises the possibility that mixed synaptic neurotransmission at these terminals has a functional role in processing strong emotional memories.

1.3.7. Evidence for electrical transmission at mossy fiber terminals

To date, there are only two reports presenting electrophysiological evidence for electrical transmission from mossy fiber terminals to CA3 pyramidal cells (Vivar et al., 2012; Ixmatlahua et al., 2020). One of these reports appeared concomitantly with a publication demonstrating the presence of Cx36-containing gap junctions detected by immunofluorescence at mossy fiber terminals (Nagy, 2012) and another showing the association of ultrastructurally-identified gap junctions with hippocampal principal cells, some of which may have been localized to these terminals (Hamzei-Sichani et al., 2012). If the electrical synaptic component of the morphologically mixed synapses at these terminals is operational, then CA3 pyramidal cells might be expected to display the hallmark of electrical transmission, namely spikelet depolarizations, accompanied by a chemically mediated EPSP after stimulation of granule cells. Following such stimulation, spikelets were observed in about 35 pyramidal cells when stimulation was applied to greater than 700 granule cells, which represent a very low level of spikelet detection (~ 5%). These spikelets persisted after elimination of chemical synaptic transmission and were shown to be blocked by the gap junction blocker carbenoxolone (Vivar et al., 2012). An unfortunate aspect of this report is that the authors did not mention whether their data was derived from studies of the dorsal or ventral hippocampal regions, which is a critical issue, given their low incidence of spikelet detection, because it was noted in the report appearing concomitantly (Nagy, 2012) that Cx36-containing gap junctions were associated with mossy fiber terminals only in the ventral hippocampus of rat and not with those in the dorsal hippocampus. Also, the gap junction blocker carbenoxolone is known to have a variety of off-target actions, including reduction of excitatory synaptic currents, blockade of postsynaptic NMDA receptors, suppression of action potentials and blockade of calcium channels, and therefore cannot be considered a specific gap junction channel blocker (Kenneth et al., 2009; Connors, 2012). To control for the non-specific effects of the drug on chemical synaptic transmission, it is necessary to distinguish properties such as pronounced frequency facilitation and inhibition by a known metabotropic glutamate transporter mGluR2 agonist, DCG-IV at mossy fiber synapses after the application of carbenoxolone. Also, the percent inhibition by DCG-IV at mossy fiber synapses was reported as 65 ± 7 % (Vivar et al., 2012), while others report inhibition as high as 80% (Gianmaria et al., 1998; Yeckel et al., 1999). In an attempt for a broader detection of mixed synapses in the rat ventral hippocampus, a second study focused on recording from CA3 pyramidal cells after intracellular acidification, which, as noted earlier in the introduction could serve to open Cx36-containing gap junctional channels. Lowering

intracellular pH was attained by recording after intracellular injection of CA3 pyramidal cells with trimethylamine (TMA), although actions of TMA in addition to altering pH are not well understood. Application of TMA intracellularly in hippocampal slices revealed spikelets after 20-40 min of recording. Also, 2 - 5 dye coupled pyramidal cells were observed when recorded with intracellular TMA. However, no dye coupling was observed in between interneurons and the basis for selectivity of TMA-induced dye coupling solely of principal cells and not interneurons is unclear.

1.4.Thesis objectives and hypothesis

1. To further characterize the association of Cx36-containing gap junction with mossy fiber terminals at mixed synapses in the stratum lucidum of the ventral hippocampus in rat using immunofluorescence approaches.
2. To establish the spatial relationships between Cx36-containing gap junctions localized to mossy fiber terminals and adherens junctions linking these terminals to CA3 pyramidal cells, and to determine if similar relationships occur at mixed synapses in other CNS regions.
3. To determine whether Cx36-containing gap junctions at mossy fiber terminals contribute to the strength of synaptic plasticity and magnitude of LTP during transmission from these terminals to CA3 pyramidal cells by comparing these parameters in dorsal *vs.* ventral hippocampus.
4. To develop viral-mediated delivery of short hairpin RNA (shRNA) that specifically targets knockdown of Cx36 expression in rat hippocampal granule cells, which in the longer term can be used to explore electrophysiological deficits in mossy fiber synaptic transmission and behaviour impairments related to functions associated with the ventral hippocampus.

Hypothesis: Cx36-containing gap junctions are localized to selective specific subcellular sites at mossy fiber terminals and contribute to the fidelity of synaptic plasticity at these terminals within the ventral hippocampus.

1.5. References

Acsády L, Kamondi A, Sík A, Freund T, Buzsáki G (1998a) GABAergic Cells Are the Major Postsynaptic Targets of Mossy Fibers in the Rat Hippocampus. The Journal of neuroscience 18:3386-3403.

Acsády L, Kamondi A, Sík A, Freund T, Buzsáki G (1998b) GABAergic cells are the major postsynaptic targets of mossy fibers in the rat hippocampus. The Journal of neuroscience : the official journal of the Society for Neuroscience 18:3386-3403.

Alcamí P, Pereda AE (2019) Beyond plasticity: the dynamic impact of electrical synapses on neural circuits. Nature reviews Neuroscience 20:253-271.

Alle H (2006) Combined Analog and Action Potential Coding in Hippocampal Mossy Fibers. Science (American Association for the Advancement of Science) 311:1290-1293.

Apostolides PF, Trussell LO (2013) Regulation of interneuron excitability by gap junction coupling with principal cells. Nature neuroscience 16:1764-1772.

Bautista W, McCrea DA, Nagy JI (2014) Connexin36 identified at morphologically mixed chemical/electrical synapses on trigeminal motoneurons and at primary afferent terminals on spinal cord neurons in adult mouse and rat. Neuroscience 263:159-180.

Benjamin B, Eve-Ellen G, Justin C, Linda Van A (2000) The Junctional Multidomain Protein AF-6 Is a Binding Partner of the Rap1A GTPase and Associates with the Actin Cytoskeletal Regulator Profilin. Proceedings of the National Academy of Sciences - PNAS 97:9064-9069.

Bennett M (1997) Gap junctions as electrical synapses. Journal of Neurocytology 26:349-366.

Bennett MV, Aljure E, Nakajima Y, Pappas GD (1963) Electrotonic junctions between teleost spinal neurons: electrophysiology and ultrastructure. Science (New York, NY) 141:262-264.

Bennett MVL (2000) Electrical synapses, a personal perspective (or history). Brain Research Reviews 32:16-28.

Bennett MVL, Zukin RS (2004) Electrical Coupling and Neuronal Synchronization in the Mammalian Brain. Neuron 41:495-511.

Bennett MVL, Pereda A (2006) Pyramid power: Principal cells of the hippocampus unite. Brain Cell Biology 35:5-11.

Bischofberger J, Engel D, Frotscher M, Jonas P (2006a) Timing and efficacy of transmitter release at mossy fiber synapses in the hippocampal network. Pflügers Archiv 453:361-372.

Bischofberger J, Engel D, Li L, Geiger JRP, Jonas P (2006b) Patch-clamp recording from mossy fiber terminals in hippocampal slices. Nature protocols 1:2075-2081.

Boettner B, Herrmann C, Van Aelst L (2001) [11] Ras and Rap1 interaction with AF-6 effector target. Methods in enzymology 332:151-168.

Carmen EF, Xinbo L, Michael VLB, James IN, Alberto EP (2008) Interaction between connexin35 and zonula occludens-1 and its potential role in the regulation of electrical synapses. Proceedings of the National Academy of Sciences - PNAS 105:12545-12550.

Caron E (2003) Cellular functions of the Rap1 GTP-binding protein: A pattern emerges. Journal of cell science 116:435-440.

Chicurel ME, Harris KM (1992) Three-dimensional analysis of the structure and composition of CA3 branched dendritic spines and their synaptic relationships with mossy fiber boutons in the rat hippocampus. Journal of Comparative Neurology 325:169-182.

Church J, Baimbridge KG (1991) Exposure to high-pH medium increases the incidence and extent of dye coupling between rat hippocampal CA1 pyramidal neurons in vitro. Journal of Neuroscience 11:3289-3295.

Claiborne BJ, Amaral DG, Cowan WM (1986) A light and electron microscopic analysis of the mossy fibers of the rat dentate gyrus. Journal of comparative neurology (1911) 246:435-458.

Connors BW (2009) Electrical Signaling with Neuronal Gap Junctions. In: Connexins: A Guide (Harris AL, Locke D, eds), pp 143-164. Totowa, NJ: Humana Press.

Connors BW (2012) Tales of a Dirty Drug: Carbenoxolone, Gap Junctions, and Seizures: Carbenoxolone and Seizures. Epilepsy currents 12:66-68.

Connors BW, Long MA (2004) ELECTRICAL SYNAPSES IN THE MAMMALIAN BRAIN. Annual review of neuroscience 27:393-418.

Coulon P, Landisman CE (2017) The Potential Role of Gap Junctional Plasticity in the Regulation of State. Neuron (Cambridge, Mass) 93:1275-1295.

Curti S, O'Brien J (2016) Characteristics and plasticity of electrical synaptic transmission. BMC cell biology 17:13-13.

Daniel G-N, Juan MG-H, Belén L, Cristina G, María DM, Ilaria F, John OB, Agata Z, Federico C, Luis CB (2008) Regulation of neuronal connexin-36 channels by pH. Proceedings of the National Academy of Sciences 105:17169.

Del Corsso C, Iglesias R, Zoidl G, Dermietzel R, Spray DC (2012) Calmodulin dependent protein kinase increases conductance at gap junctions formed by the neuronal gap junction protein connexin36. Brain Research 1487:69-77.

Derangeon M, Spray DC, Bourmeyster N, Sarrouilhe D, Hervé J-C (2009) Reciprocal influence of connexins and apical junction proteins on their expressions and functions. Biochimica et biophysica acta Biomembranes 1788:768-778.

Evans WH (2015) Cell communication across gap junctions: a historical perspective and current developments. Biochem Soc Trans 43:450-459.

Fanselow MS, Dong H-W (2010) Are the Dorsal and Ventral Hippocampus Functionally Distinct Structures? Neuron (Cambridge, Mass) 65:7-19.

Flores CE, Nannapaneni S, Davidson KG, Yasumura T, Bennett MV, Rash JE, Pereda AE (2012) Trafficking of gap junction channels at a vertebrate electrical synapse in vivo. Proc Natl Acad Sci U S A 109:E573-582.

Fukuda T, Kosaka T (2000) Gap Junctions Linking the Dendritic Network of GABAergic Interneurons in the Hippocampus. Journal of Neuroscience 20:1519-1528.

Fukuda T, Kosaka T, Singer W, Galuske RAW (2006) Gap Junctions among Dendrites of Cortical GABAergic Neurons Establish a Dense and Widespread Intercolumnar Network. Journal of Neuroscience 26:3434-3443.

Furshpan EJ (1964) "Electrical Transmission" at an Excitatory Synapse in a Vertebrate Brain. Science (American Association for the Advancement of Science) 144:878-880.

Geiger JRP, Jonas P (2000) Dynamic Control of Presynaptic Ca2+ Inflow by Fast-Inactivating K+ Channels in Hippocampal Mossy Fiber Boutons. Neuron (Cambridge, Mass) 28:927-939.

Gianmaria M, Katalin T, Chris JM (1998) Target-Specific Expression of Presynaptic Mossy Fiber Plasticity. Science (American Association for the Advancement of Science) 279:1368-1370.

Goodenough DA, Paul DL (2009) Gap junctions. Cold Spring Harb Perspect Biol 1:a002576.

Haas JS, Greenwald CM, Pereda AE (2016) Activity-dependent plasticity of electrical synapses: Increasing evidence for its presence and functional roles in the mammalian brain. BMC cell biology 17:14-14.

Hamzei-Sichani F, Davidson KGV, Yasumura T, Janssen WGM, Wearne SL, Hof PR, Traub RD, Gutiérrez R, Ottersen OP, Rash JE (2012) Mixed Electrical-Chemical Synapses in Adult

Rat Hippocampus are Primarily Glutamatergic and Coupled by Connexin-36. Frontiers in neuroanatomy 6:13.

Harris TJC, Tepass U (2010) Adherens junctions: from molecules to morphogenesis. Nature reviews Molecular cell biology 11:502-514.

Henze DA, Wittner L, Buzsáki G (2002) Single granule cells reliably discharge targets in the hippocampal CA3 network in vivo. Nature neuroscience 5:790-795.

Ixmatlahua DJ, Vizcarra B, Gómez-Lira G, Romero-Maldonado I, Ortiz F, Rojas-Piloni G, Gutiérrez R (2020) Neuronal Glutamatergic Network Electrically Wired with Silent but Activatable Gap Junctions. The Journal of neuroscience 40:4661-4672.

Kandel E (2013) Principles of neural science. In, 5th ed. Edition (Kandel ER, ed). New York: McGraw-Hill Medical.

Katsumaru H, Kosaka T, Heizmann CW, Hama K (1988) Gap junctions on GABAergic neurons containing the calcium-binding protein parvalbumin in the rat hippocampus (CA1 region). Experimental brain research 72:363-370.

Kenneth RT, Brady JM, Gary LW (2009) Direct Actions of Carbenoxolone on Synaptic Transmission and Neuronal Membrane Properties. Journal of Neurophysiology 102:974-978.

Khan AK, Jagielnicki M, McIntire WE, Purdy MD, Dharmarajan V, Griffin PR, Yeager M (2020) A Steric "Ball-and-Chain" Mechanism for pH-Mediated Regulation of Gap Junction Channels. Cell Rep 31:107482.

Kimberly AM, Roger AN, Dietmar S (2003) Adenosine Gates Synaptic Plasticity at Hippocampal Mossy Fiber Synapses. Proceedings of the National Academy of Sciences - PNAS 100:14397-14402.

Komiyama NH, Watabe AM, Carlisle HJ, Porter K, Charlesworth P, Monti J, Strathdee DJC, O'Carroll CM, Martin SJ, Morris RGM, O'Dell TJ, Grant SGN (2002) SynGAP Regulates ERK/MAPK Signaling, Synaptic Plasticity, and Learning in the Complex with Postsynaptic Density 95 and NMDA Receptor. The Journal of neuroscience 22:9721-9732.

Kooistra MRH, Dube N, Bos JL (2006) Rap1: a key regulator in cell-cell junction formation. Journal of cell science 120:17-22.

Korn H, Sotelo C, Crepel F (1973) Electrotonic coupling between neurons in the rat lateral vestibular nucleus. Experimental Brain Research 16.

Krapivinsky G, Medina I, Krapivinsky L, Gapon S, Clapham DE (2004) SynGAP-MUPP1-CaMKII Synaptic Complexes Regulate p38 MAP Kinase Activity and NMDA Receptor-Dependent Synaptic AMPA Receptor Potentiation. Neuron (Cambridge, Mass) 43:563-574.

Lampl I, Yarom Y (1993) Subthreshold oscillations of the membrane potential: a functional synchronizing and timing device. Journal of neurophysiology 70:2181-2186.

Li X, Lynn BD, Nagy JI (2012) The effector and scaffolding proteins AF6 and MUPP1 interact with connexin36 and localize at gap junctions that form electrical synapses in rodent brain. The European journal of neuroscience 35:166-181.

Li X, Olson C, Lu S, Kamasawa N, Yasumura T, Rash JE, Nagy JI (2004) Neuronal connexin36 association with zonula occludens-1 protein (ZO-1) in mouse brain and interaction with the first PDZ domain of ZO-1. The European journal of neuroscience 19:2132-2146.

Long MA, Deans MR, Paul DL, Connors BW (2002) Rhythmicity without Synchrony in the Electrically Uncoupled Inferior Olive. Journal of Neuroscience 22:10898-10905.

Lynn BD, Li X, Nagy JI (2012) Under Construction: Building the Macromolecular Superstructure and Signaling Components of an Electrical Synapse. The Journal of Membrane Biology 245:303-317.

Lynn BD, Li X, Hormuzdi SG, Griffiths EK, McGlade CJ, Nagy JI (2018) E3 ubiquitin ligases LNX1 and LNX2 localize at neuronal gap junctions formed by connexin36 in rodent brain and molecularly interact with connexin36. The European journal of neuroscience 48:3062-3081.

Martin EA, Woodruff D, Rawson RL, Williams ME (2017) Examining hippocampal mossy fiber synapses by 3D electron microscopy in wildtype and kirrel3 knockout mice. eNeuro 4:ENEURO.0088-0017.2017.

Maruki K, Izaki Y, Nomura M, Yamauchi T (2001) Differences in paired-pulse facilitation and long-term potentiation between dorsal and ventral CA1 regions in anesthetized rats. Hippocampus 11:655-661.

McBain CJ (2008) Differential mechanisms of transmission and plasticity at mossy fiber synapses. Progress in brain research 169:225-240.

Mercer A, Bannister AP, Thomson AM (2006) Electrical coupling between pyramidal cells in adult cortical regions. Brain Cell Biol 35:13-27.

Michelson HB, Wong RK (1994) Synchronization of inhibitory neurones in the guinea-pig hippocampus in vitro. The Journal of Physiology 477:35-45.

Milior G, Di Castro MA, Sciarria LP, Garofalo S, Branchi I, Ragozzino D, Limatola C, Maggi L (2016) Electrophysiological Properties of CA1 Pyramidal Neurons along the Longitudinal Axis of the Mouse Hippocampus. Scientific reports 6:38242.

Miyahara M, Nakanishi H, Takahashi K, Satoh-Horikawa K, Tachibana K, Takai Y (2000) Interaction of nectin with afadin is necessary for its clustering at cell-cell contact sites but not for its cis dimerization or trans interaction. The Journal of biological chemistry 275:613-618.

Mori M, Rikitake Y, Mandai K, Takai Y (2013) Roles of Nectins and Nectin-Like Molecules in the Nervous System. Cell Adhesion Molecules 8:91-116.

Nagy JI (2012) Evidence for connexin36 localization at hippocampal mossy fiber terminals suggesting mixed chemical/electrical transmission by granule cells. Brain Res 1487:107-122.

Nagy JI, Lynn BD (2018) Structural and Intermolecular Associations Between Connexin36 and Protein Components of the Adherens Junction–Neuronal Gap Junction Complex. Neuroscience 384:241-261.

Nagy JI, Pereda AE, Rash JE (2018) Electrical synapses in mammalian CNS: Past eras, present focus and future directions. Biochim Biophys Acta Biomembr 1860:102-123.

Nagy JI, Pereda AE, Rash JE (2019) On the occurrence and enigmatic functions of mixed (chemical plus electrical) synapses in the mammalian CNS. Neurosci Lett 695:53-64.

Nagy JI, Bautista W, Blakley B, Rash JE (2013) Morphologically mixed chemical-electrical synapses formed by primary afferents in rodent vestibular nuclei as revealed by immunofluorescence detection of connexin36 and vesicular glutamate transporter-1. Neuroscience 252:468-488.

Nakajima Y (1974) Fine structure of the synaptic endings on the Mauthner cell of the goldfish. Journal of Comparative Neurology 156:375-402.

Nicoll RA (2017) A Brief History of Long-Term Potentiation. Neuron 93:281-290.

Nicoll RA, Schmitz D (2005) Synaptic plasticity at hippocampal mossy fibre synapses. Nat Rev Neurosci 6:863-876.

O'Brien J (2014) The ever-changing electrical synapse. Current opinion in neurobiology 29:64-72.

O'Brien J (2019) Design principles of electrical synaptic plasticity. Neuroscience letters 695:4-11.

Papatheodoropoulos C, Kostopoulos G (2000) Decreased ability of rat temporal hippocampal CA1 region to produce long-term potentiation. Neuroscience letters 279:177-180.

Parker PRL, Cruikshank SJ, Connors BW (2009) Stability of Electrical Coupling despite Massive Developmental Changes of Intrinsic Neuronal Physiology. The Journal of neuroscience 29:9761-9770.

Paxinos G (2004) The rat nervous system, 3rd ed. Edition. San Diego, CA: Elsevier Academic.

Pena V, Bonneau F, Hothorn M, Parret A, Gremer L, Scheffzek K, Kaschau N, Eberth A, Ahmadian MR (2008) The C2 domain of SynGAP is essential for stimulation of the Rap GTPase reaction. EMBO reports 9:350-355.

Pereda A, apos, Brien J, Nagy JI, Bukauskas F, Davidson KGV, Kamasawa N, Yasumura T, Rash JE (2003) Connexin35 Mediates Electrical Transmission at Mixed Synapses on Mauthner Cells. Journal of Neuroscience 23:7489-7503.

Pereda AE (2014) Electrical synapses and their functional interactions with chemical synapses. Nat Rev Neurosci 15:250-263.

Pereda AE, Bennett MVL (2017) Electrical Synapses in Fishes: Their Relevance to Synaptic Transmission. In: Network Functions and Plasticity: Perspectives from Studying Neuronal Electrical Coupling in Microcircuits, pp 161-181.

Pereda AE, Bell TD, Faber DS (1995) Retrograde synaptic communication via gap junctions coupling auditory afferents to the Mauthner cell. Journal of Neuroscience 15:5943-5955.

Pereda AE, Rash JE, Nagy JI, Bennett MVL (2004) Dynamics of electrical transmission at club endings on the Mauthner cells. In, pp 227-244: Elsevier B.V.

Pereda AE, Curti S, Hoge G, Cachope R, Flores CE, Rash JE (2013) Gap junction-mediated electrical transmission: Regulatory mechanisms and plasticity. Biochimica et biophysica acta Biomembranes 1828:134-146.

Peters A (1991) The fine structure of the nervous system : neurons and their supporting cells, 3rd ed. -- Edition. New York: Oxford University Press.

Rash JE, Dillman RK, Bilhartz BL, Duffy HS, Whalen LR, Yasumura T (1996) Mixed synapses discovered and mapped throughout mammalian spinal cord. Proceedings of the National Academy of Sciences - PNAS 93:4235-4239.

Rash JE, Staines WA, Yasumura T, Patel D, Furman CS, Stelmack GL, Nagy JI (2000) Immunogold evidence that neuronal gap junctions in adult rat brain and spinal cord contain

connexin-36 but not connexin-32 or connexin-43. Proceedings of the National Academy of Sciences of the United States of America 97:7573-7578.

Rash JE, Kamasawa N, Vanderpool KG, Yasumura T, O'Brien J, Nannapaneni S, Pereda AE, Nagy JI (2015) Heterotypic gap junctions at glutamatergic mixed synapses are abundant in goldfish brain. Neuroscience 285:166-193.

Restivo L, Vetere G, Bontempi B, Ammassari-Teule M (2009) The Formation of Recent and Remote Memory Is Associated with Time-Dependent Formation of Dendritic Spines in the Hippocampus and Anterior Cingulate Cortex. The Journal of neuroscience 29:8206-8214.

Ribak CE, Seress L, Leranth C (1993) Electron microscopic immunocytochemical study of the distribution of parvalbumin-containing neurons and axon terminals in the primate dentate Gyrus and Ammon's horn. Journal of comparative neurology (1911) 327:298-321.

Richmond MA, Yee BK, Pouzet B, Veenman L, Rawlins JNP, Feldon J, Bannerman DM (1999) Dissociating Context and Space Within the Hippocampus: Effects of Complete, Dorsal, and Ventral Excitotoxic Hippocampal Lesions on Conditioned Freezing and Spatial Learning. Behavioral neuroscience 113:1189-1203.

Rimkute L, Kraujalis T, Snipas M, Palacios-Prado N, Jotautis V, Skeberdis VA, Bukauskas FF (2018) Modulation of Connexin-36 Gap Junction Channels by Intracellular pH and Magnesium Ions. Frontiers in physiology 9:362.

Robert WK, Parmender PM, Birgit R, Lawrence SH, Werner RL, Urs R (1988) Neural Differentiation, NCAM-Mediated Adhesion, and Gap Junctional Communication in Neuroectoderm. A Study in Vitro. The Journal of cell biology 106:1307-1319.

Rubio ME, Nagy JI (2015) Connexin36 expression in major centers of the auditory system in the CNS of mouse and rat: Evidence for neurons forming purely electrical synapses and morphologically mixed synapses. Neuroscience 303:604-629.

Salin PA, Scanziani M, Malenka RC, Nicoll RA (1996) Distinct short-term plasticity at two excitatory synapses in the hippocampus. Proceedings of the National Academy of Sciences - PNAS 93:13304-13309.

Schmitz D, Schuchmann S, Fisahn A, Draguhn A, Buhl E, Petrasch-Parwez E, Dermietzel R, Traub R (2001) Axo-Axonal Coupling: A Novel Mechanism for Ultrafast Neuronal Communication. Neuron 31:831-840.

Schreurs A, Sabanov V, Balschun D (2017) Distinct Properties of Long-Term Potentiation in the Dentate Gyrus along the Dorsoventral Axis: Influence of Age and Inhibition. Scientific reports 7:5157-5110.

Sik A, Hajos N, Gulacsi A, Mody I, Freund TF (1998) The absence of a major Ca2+ signaling pathway in GABAergic neurons of the hippocampus. Proceedings of the National Academy of Sciences - PNAS 95:3245-3250.

Söhl G, Degen J, Teubner B, Willecke K (1998) The murine gap junction gene connexin36 is highly expressed in mouse retina and regulated during brain development. FEBS letters 428:27-31.

Somekawa S, Fukuhara S, Nakaoka Y, Fujita H, Saito Y, Mochizuki N (2005) Enhanced Functional Gap Junction Neoformation by Protein Kinase A–Dependent and Epac-Dependent Signals Downstream of cAMP in Cardiac Myocytes. Circulation research 97:655-662.

Sotelo C, Palay SL (1970) The fine structure of the lateral vestibular nucleus in the rat. II. synaptic organization. Brain research 18:93-115.

Srinivas M, Rozental R, Kojima T, Dermietzel R, Mehler M, Condorelli D, Kessler J, Spray D (1999) Functional Properties of Channels Formed by the Neuronal Gap Junction Protein Connexin36. Journal of Neuroscience 19:9848-9855.

Takai Y (2003) Nectin and afadin: novel organizers of intercellular junctions. Journal of cell science 116:17-27.

Tanaka H, Shan W, Phillips GR, Arndt K, Bozdagi O, Shapiro L, Huntley GW, Benson DL, Colman DR (2000) Molecular modification of N-cadherin in response to synaptic activity. Neuron (Cambridge, Mass) 25:93-107.

Theoden IN, Matthew IB, Alan DD, Corey DA, Julie SH, Nancy K, John AW (2005) Synchronization in Hybrid Neuronal Networks of the Hippocampal Formation. Journal of Neurophysiology 93:1197-1208.

Thomas L, Matthias G, Birgit KJ, Christoph B, Hans Robert K, Alfred W, Christian H (1999) Thermodynamic and Kinetic Characterization of the Interaction between the Ras Binding Domain of AF6 and Members of the Ras Subfamily. Journal of Biological Chemistry 274:13556-13562.

Traub RD, Whittington MA, Gutierrez R, Draguhn A (2018) Electrical coupling between hippocampal neurons: contrasting roles of principal cell gap junctions and interneuron gap junctions. Cell Tissue Res 373:671-691.

Tuttle R, Masuko S, Nakajima Y (1986) Freeze-fracture study of the large myelinated club ending synapse on the goldfish Mauthner cell: Special reference to the quantitative analysis of gap junctions. Journal of Comparative Neurology 246:202-211.

van Strien NM, Cappaert NLM, Witter MP (2009) The anatomy of memory: an interactive overview of the parahippocampal–hippocampal network. Nature reviews Neuroscience 10:272-282.

Velazquez JLP, Han D, Carlen PL (1997) Neurotransmitter Modulation of Gap Junctional Communication in the Rat Hippocampus. European Journal of Neuroscience 9:2522-2531.

Venance L, Rozov A, Blatow M, Burnashev N, Feldmeyer D, Monyer H (2000) Connexin expression in electrically coupled postnatal rat brain neurons. Proc Natl Acad Sci U S A 97:10260-10265.

Vigmond EJ, Velazquez JLP, Valiante TA, Bardakjian BL, Carlen PL (1997) Mechanisms of Electrical Coupling Between Pyramidal Cells. Journal of neurophysiology 78:3107-3116.

Vivar C, Traub RD, Gutierrez R (2012) Mixed electrical-chemical transmission between hippocampal mossy fibers and pyramidal cells. Eur J Neurosci 35:76-82.

Willecke K, Eiberger J, Degen J, Eckardt D, Romualdi A, Güldenagel M, Deutsch U, Söhl G (2002) Structural and functional diversity of connexin genes in the mouse and human genome. Biological chemistry 383:725-737.

Yamasaki N et al. (2008) Alpha-CaMKII deficiency causes immature dentate gyrus, a novel candidate endophenotype of psychiatric disorders. Molecular brain 1:6-6.

Yeckel MF, Johnston D, Kapur A (1999) Multiple forms of LTP in hippocampal CA3 neurons use a common postsynaptic mechanism. Nature Neuroscience 2:625-633.

Zhang W-N, Bast T, Feldon J (2001) The ventral hippocampus and fear conditioning in rats: different anterograde amnesias of fear after infusion of N-methyl- d-aspartate or its noncompetitive antagonist MK-801 into the ventral hippocampus. Behavioural brain research 126:159-174.

Zsiros V, Maccaferri G (2005) Electrical Coupling between Interneurons with Different Excitable Properties in the Stratum Lacunosum-Moleculare of the Juvenile CA1 Rat Hippocampus. Journal of Neuroscience 25:8686-8695.

Chapter 2:

Characterization of connexin36 at mixed chemical/electrical synapses formed by mossy fiber terminals in rat ventral hippocampus

D. Thomas, A. Recabal-Beyer, J.M.M. Senecal, B.D. Lynn, M.F. Jackson, J. I. Nagy*

Department of Physiology and Pathophysiology, Max Rady College of Medicine, Rady Faculty of Health Sciences, University of Manitoba, Winnipeg, Canada

Running title: mixed synapses in rat ventral hippocampus

No. of pages: 62

No. of figures: 14

No. of Tables: 3

No. of words: Abstract, 252; Introduction, 865; Discussion, 2212

Address for correspondence:

Dr. James I. Nagy

Department of Physiology and Pathophysiology

Max Rady College of Medicine

Rady Faculty of Health Sciences

University of Manitoba

745 Bannatyne Ave, Winnipeg, Manitoba

Canada R3E 0J9

Email: James.Nagy@umanitoba.ca

Tel. (204) 789-3767

Fax (204) 789-3934

Highlights

Immunolabelling of Cx36 is selectively localized to hippocampal mossy fiber terminals

Adherens junction proteins are closely associated with gap junctions at mixed synapses

Gap junctions are localized at mossy fiber terminal contacts with pyramidal cell dendritic shafts

Long-term potentiation at mossy fiber terminals is greater in the ventral *vs.* dorsal hippocampus

The electrical transmission component at these terminals may contribute to this enhanced LTP

Abstract – Granule cells in the hippocampus project axons to hippocampal CA3 pyramidal cells where they form large mossy fiber terminals. We have reported the presence of gap junction protein connexin36 (Cx36) specifically in the stratum lucidum of rat ventral hippocampus, thus creating morphologically mixed synapses that have the potential for dual chemical/electrical transmission capabilities. There is some electrophysiological evidence that these terminals have a gap junction-mediated electrical transmission component under some conditions. Here, we used various approaches to further characterize molecular and electrophysiological relationships between the Cx36-containing gap junctions at mossy fiber terminals and their postsynaptic elements. In the CA3b and CA3c hippocampal regions, the vast majority of these terminals, identified by their selective expression of vesicular zinc transporter-3 (ZnT3), displayed multiple, fine immunofluorescent Cx36-puncta representing gap junctions, which were absent at mossy fiber terminals in the dorsal hippocampus. These puncta were invariably found in close proximity to the protein constituents of adherens junctions (i.e., N-cadherin and nectin-1) that are a structural hallmark of mossy fiber terminals that contact dendritic shafts of CA3 pyramidal cells, thus indicating the loci of gap junctions at these contacts. Cx36-puncta were also associated with adherens junctions at mixed synapses in other regions of the CNS. Electrophysiologically induced long-term potentiation of field responses evoked by mossy fiber stimulation was greater in the ventral than dorsal hippocampus, and it remains to be determined whether the electrical component of transmission at mossy fiber terminals contributes to the enhancement of these responses.

Keywords: mixed electrical synapses, electrical coupling, rat hippocampus, electrical/chemical neurotransmission, immunofluorescence.

Introduction

Electrical synapses are now well accepted to be widespread functionally operative components that contribute to neuronal communication in circuitry of most major structures in the mammalian central nervous system (CNS) (Connors et al., 2004; Connors, 2009; Pereda et al., 2013; Pereda, 2014; Nagy et al., 2018; Alcami and Pereda, 2019). These synapses are formed by gap junctions composed of connexins that form hexamers (connexons) in plasma membranes (Evans and Martin, 2002; Goodenough and Paul 2009). Clusters of connexons in apposing membranes dock to create intercellular pores that allow cell-to-cell passage of ions and small molecules, thus creating pathways for current flow between neurons (Bennet, 1997). Among the family of twenty connexins, several are known to form electrical synapses in restricted CNS areas, but connexin36 (Cx36) is the most widely expressed in neurons of adult as well as developing brain and spinal cord (Condorelli et al., 2000; Nagy et al., 2018) and is the constituent of the vast majority of neuronal gap junctions (nGJs) that have been identified ultrastructurally (Rash et al., 2000, 2001, 2004, 2007a,b; Nagy et al., 2004) or by other means (Bennett and Zukin, 2004; Hormuzdi et al., 2004). Similar to the structural and functional diversity of chemical synapses, electrical synapses also have a variety of distinguishing features reflected by their multiplicity of subcellular localizations and occurrence often between inhibitory neurons, less frequently between excitatory neurons and more rarely between excitatory and inhibitory neurons (Nagy et al., 2018). Electrical synapses also share in common with chemical synapses their now recognized highly dynamic nature, such that they exhibit plasticity of their synaptic strength (Hass et al., 2011; Hass and Landisman, 2012; Pereda et al., 2013; Mathy et al., 2014; Turecek et al., 2014; O'Brien, 2014, 2019), which is imparted by various well understood and some yet to be defined modes of regulation (Hass et al., 2011; Hass and Landisman, 2012; Pereda et al., 2013; Mathy et al., 2014; Turecek et al., 2014; O'Brien, 2014, 2019). And finally, just as chemical synaptic transmission is supported by complex molecular machinery, so too electrical synapses are composed not just of connexins aggregates, but are emerging to consist of a composite of structural, scaffolding and regulatory proteins, some of which appear to be linked with intracellular signalling pathways while others are components of adherens junctions, which all form what we have referred to as the adherens junction-neuronal gap junction complex (AJ-nGJ complex) (Li et al., 2004, 2012; Lynn et al., 2012, 2018; Nagy and Lynn, 2018; Nagy et al., 2018). All of these properties of electrical synapses could potentially impact on the qualitative and quantitative influence they have on information flow in circuits in which they are embedded and, more generally on CNS network

activity (Connors, 2009; O'Brien, 2014; Pereda, 2014; Nagy et al., 2018; Alcami and Pereda, 2019).

One brain area that best exemplifies the diverse cellular and subcellular deployment of nGJs and their contribution to electrical synaptic transmission is the hippocampus. Among the best characterized electrical synapses are those between various classes of hippocampal interneurons, where they contribute to the generation of high frequency oscillations, among other functions (Connors and Long, 2004; Kosaka and Hama, 1985; Posluszny, 2014). An equally long history surrounds evidence of coupling between presumably the somata and/or dendrites of CA1 and between those of CA3 hippocampal principal cells (Dudek et al., 1983; Mercer et al., 2006), although Cx36 mRNA expression was found only in CA3 pyramidal cells (Condorelli et al., 2000) and ultrastructurally-identified gap junctions between dendritic arbours or somata of principal cells have yet to be definitively found. Yet another site of electrical coupling between pyramidal cells that has been inferred from results of various approaches suggested the occurrence of gap junctions between their initial axons segments (Schmitz et al., 2001; reviewed in Traub and Whittington, 2010). However, gap junctions between pyramidal cell axons have not yet been detected. More recently, we have shown immunofluorescence labelling of Cx36 localized to glutamatergic mossy fiber terminals in the stratum lucidum of rat ventral hippocampus, rendering these terminals morphologically mixed synapses with potential for dual chemical electrical transmission (Nagy, 2012). This observation is consistent with ultrastructural detection of Cx36 at gap junctions along mossy fiber axons and at excitatory nerve terminals in rat hippocampus by freeze-fracture replica immunogold labelling (FRIL) (Hamzei-Sichani et al., 2007, 2012), notwithstanding that those terminals could not be definitively identified as belonging to mossy fiber terminals (Hamzei-Sichani et al., 2012). In addition, electrophysiological studies have also provided some support for functionally operative electrical transmission at these terminals (Vivar et al., 2012; Ixmatlahua et al., 2020). Though provocative, some of the above findings clearly warrant further investigation to better define the degree to which electrical synapses are extant in hippocampal neuronal circuitry and ultimately to understand their functional contributions to network activity. In particular, knowledge surrounding the mixed synapses of rat hippocampal mossy fiber terminals remains rudimentary. Here, we use immunofluorescence approaches to examine distinguishing molecular features of those synapses and Cx36 knockdown approaches in combination with electrophysiological measures to probe functional consequences of Cx36 ablation.

EXPERIMENTAL PROCEDURES

Animals and antibodies

Animals used in this study included a total of forty-five adult male Sprague-Dawley rats greater than two months of age and weighing 200 to 275 g, and eight adult male wild-type C57 BL/6-129SvEv mice greater than six weeks of age and weighing 25 to 30 g. Both rats and mice were used because data from early literature related to the present work were derived from rat tissues, and more recent similarly related studies involved the use of mice. Animals were obtained from the Central Animal Care Services at the University of Manitoba and utilized according to approved protocols by the Central Animal Care Committee of University of Manitoba. Rats and mice were housed with exposure to a twelve hr light/dark cycle, with food and water freely available, and all efforts were made to minimize animal suffering and the number of animals used. Tissues from some animals were taken for use in other studies, thereby contributing to reduction of the total number of rats and mice used by laboratory personnel in various unrelated studies.

Immunofluorescence studies were conducted with the list of monoclonal and polyclonal primary antibodies given in Table 1, with western blotting and/or immunolabelling validation of antibody specificity for target proteins provided by the commercial supplier. A monoclonal anti-Cx36 antibody (ThermoFisher, Rockford, Il, USA; formerly Life Technologies Corporation, and originally Invitrogen/Zymed Laboratories) has been previously characterized for specificity of Cx36, which was confirmed using wild-type *vs*. Cx36 null mice (Li et al., 2004; Rash et al., 2007a,b; Curti et al., 2012). Secondary antibodies all produced in donkey included Cy5-conjugated anti-guinea pig diluted 1:500 (Jackson ImmunoResearch Laboratories, West Grove, PA, USA). Cy3-conjugated anti-mouse diluted 1:600 (Jackson ImmunoResearch Laboratories), and AlexaFlour 488-conjugated anti-chicken, anti-guinea pig, anti-sheep and anti-rabbit each diluted 1:600 (Molecular Probes, Eugene, OR, USA). All primary and secondary antibodies were diluted in 50 mM Tris-HCl, pH 7.4, containing 1.5% sodium chloride (TBS) and 0.3% Triton X-100 (TBSTr), which additionally contained 10% normal donkey serum.

Tissue preparation

Two tissue fixation methods were used. In the first, rats and mice were deeply anaesthetized and euthanized with an overdose of equithesin (3 ml/kg), placed on a bed of ice, and perfused transcardially with cold (4 ^{o}C) pre-fixative containing 50 mM sodium phosphate buffer (pH 7.4), 0.1% sodium nitrite, 0.9% NaCl, and 1 unit/ml heparin, using a total volume of 3 ml for mice and

25 ml for rats. This was followed by perfusion with cold (4 ^{o}C) fixative containing 0.16 mM sodium phosphate buffer (pH 7.4), 0.2% picric acid, and either 1%, 2% or 4% formaldehyde that was prepared by diluting a stock 20% solution of formaldehyde stored in sealed ampules (Electron Microscopy Sciences, Hatfield, PA, USA). Mice were perfused with a fixative volume of 40 ml, and rats with a volume of 100 to 150 ml. In the final step, animals were perfused with a cold (4 ^{o}C) solution containing 10% sucrose in 25 mM sodium phosphate buffer (pH 7.4) to reduce excessive fixation. Brains were removed and stored at 4 ^{o}C for 24 to 48 hr in cryoprotectant containing 25 mM sodium phosphate buffer (pH 7.4), 10% sucrose and 0.04% sodium azide. In the second fixation method which was used primarily for fixing slices after electrophysiology recordings, rats were anesthetized with isoflurane, decapitated, and brains were removed and placed into ice-cold oxygenated (5% CO_2, 95% O_2) standard artificial cerebrospinal fluid (aCSF) (in mmol/l: 124 NaCl, 3 KCl, 1.3 MgCl2, 2.6 CaCl2, 1.25 NaH2PO4, 26 NaHCO3, and 10 D-glucose; osmolarity adjusted to 300-310 mOsM). Hippocampi were then dissected and transverse slices of 350 µm were cut using a vibratome (Campden 7000smz2). The slices were stored in aCSF for 30 min at 32°C and then transferred to aCSF at room temperature for 1 hr. Free-floating slices were then immersion fixed for 8 min in fixative solution containing 1% formaldehyde. The slices were then stored in the cryoprotectant solution as above. Both perfusion fixed and immersion fixed tissues were flash-frozen, and sections of 14 to 16 µm thickness were cut using a cryostat, and sections were collected on gelatinized slides and stored at -40°C.

Immunofluorescence procedures

For immunofluorescence labelling, slide-mounted sections removed from storage were dried at room temperature for 10 min, and washed for 20 min in TBSTr. For double and triple immunofluorescence, sections were incubated simultaneously with two or three primary antibodies diluted in TBSTr containing 10% normal donkey serum for 18 to 24 h at 4 °C, then washed for 1 h in TBSTr and incubated with appropriate secondary antibodies at room temperature for 1.5 hr. The sections were then washed in TBSTr for 20 min, and then in 50 mM Tris, pH 7.4, for 30 min. Some sections processed for immunolabelling were counterstained with deep red Nissl NeuroTrace (stain N21479) (Molecular Probes, Eugene, OR, USA). All sections were coverslipped with the antifade medium Fluoromount-G (SouthernBiotech, Birmingham, AB, USA) and air-dried for 1 hr before transferring them to -20 ^{o}C for long-term storage.

Immunofluorescence microscopy

Immunofluorescence in tissue sections was examined and photographed by widefield microscopy using either on a Zeiss Imager Z2 microscope and at higher resolution using a Zeiss LSM 710 laser scanning confocal microscope. Images were collected as CZI files using Zeiss Zen Black or Zen blue software (Carl Zeiss Canada, Toronto, Ontario, Canada). Widefield or confocal images were collected either as single scans or as z-stack images with 10 to 24 scans capturing a thickness of 4 to 8 µm of tissue at z scanning intervals of typically 0.4 using a 40x objective lens. Final images were assembled using CorelDraw Graphics (Corel Corp., Ottawa, Canada) and Adobe Photoshop CS software (Adobe Systems, San Jose, CA, USA). Images with Cy5 immunolabelling or deep red counterstaining were pseudocoloured either blue or white. In all figures displaying double and triple immunofluorescence labelling, panels identified by the same letters show the same fields. Proteins named in each panel are colour coded according to the fluorophore used to label the protein. Overlap of the red and green fluorophores is seen as yellow, and overlap of red, green and blue or white appears white.

Several procedures were used as search strategies for localization and quantification of the number and size of Cx36-puncta in stratum lucidum and stratum radiatum. In each region examined, numerous randomly selected fields were photographed. Each z-stack image was first viewed as a maximum intensity projection to obtain an overview of Cx36-puncta. A total of 2,593 Cx36-positive puncta taken from 8 images photographed from stratum lucidum and 2,701 puncta from a total of 50 images taken from the stratum radiatum region was used to examine the size difference between Cx36-puncta seen in these regions. Using Zeiss Zen software tools and raw (*i.e.,* unadjusted for displayed intensity) single scan images, the diameter of each puncta was calculated. To determine the number of Cx36-puncta associated with mossy fiber terminals immunolabelled for ZnT3, confocal images captured with a 40x objective lens were used. A total of 86 terminals with diameters ranging for 3-5 µm were examined in 4 images to count the number of Cx36-puncta per terminal. The overlap of labels for ZnT3 and Cx36 was examined in z-stack images by 3D rendering in transparency mode, with image rotation in x, y and z-axes to exclude cases where labels for ZnT3 and Cx36 overlapped but were separated in the z-axis, and to confirm cases where labels were found that overlapped in standard 2D views of the x and y axes, but not separated in the z-axis. Single, consecutive scan images within the compiled z-stack were then visually scrutinized at high digital image magnification to further confirm qualitatively the association of labels for ZnT3 and Cx36 in all three axes. The puncta per terminal were then

counted manually twice from the 4 fields. To establish significance, data were subject to unpaired two-tailed Student's t-test for samples with unequal variance. Unequal sample variance was first determined using the F-test for variance. Criterion for significance was set at $p < 0.05$. All data were expressed as means ± s.e.m. Statistical analysis was conducted using Microsoft Excel 2010 software.

Brain slice electrophysiology

Hippocampal slices were prepared from 3-4 weeks old Sprague-Dawley rats as previously described (Xie et al., 2011; Yang et al., 2012, 2014; Sun et al., 2017) with modifications. Hippocampi dissection and slicing were performed in NMDG containing aCSF: (in mmol/L) 93 N-Methyl- D –glucamine, 3 KCl, 5 $MgCl_2$, 0.5 $CaCl_2$, 1.25 NaH_2PO_4, 30 $NaHCO_3$, 20 HEPES buffer, 25 glucose, 5 Na ascorbate, 3 Na pyruvate; pH adjusted to 7.4 with HCl, osmolarity adjusted to 300-310 mOsM. Prior to recording, slices were stored in HEPES containing aCSF: (in mmol/L) 95 NaCl, 3 KCl, 1.3 $MgCl_2$, 2.6 $CaCl_2$, 1.25 NaH_2PO_4, 30 $NaHCO_3$, 20 HEPES, 25 glucose, 5 Na ascorbate, 3 Na pyruvate; pH adjusted to 7.4 with NaOH, osmolarity adjusted to 300-310 mOsM) for 30 min at 32°C and then at room temperature for 1 hr.

For extracellular field recordings, slices were transferred to a submersion recording chamber perfused with oxygenated aCSF at a flow rate of 3 ml/min and maintained at 30-32°C. Patch pipettes were pulled from borosilicate glass (World Precision Instruments, Inc., Sarasota, FL). fEPSPs were evoked by giving stimuli with a concentric bipolar stimulating electrode positioned beneath the cell layer of the dentate gyrus where mossy fibers from this region travel as a thick band to synapse onto CA3 pyramidal cells. The recording electrode with a pipette resistance of 2-5 MΩ was filled with aCSF and positioned at the CA3 pyramidal cell layer. One of the distinguishing features of the mossy fiber-CA3 response is that they show pronounced frequency facilitation (FF). The FF was measured by recording the baseline response for 2 min at 0.05 Hz, then switching to 1 Hz stimulation for 40 sec, and switching back to 0.05 Hz stimulation. A minimum of 300% increase in the field response amplitude compared with the baseline was set as a criterion for confirming that the response originated from mossy fiber stimulation. The recording and stimulating electrodes were repositioned until this minimum criterion was met. One challenge for studying the electrophysiological properties of the mossy fiber pathway is that the bulk stimulation of the dentate gyrus, hilus or stratum lucidum can evoke at least two different synaptic inputs to CA3 pyramidal cells besides the intended activation of the MF-CA3 pathway. One

contamination arising from strong stimulation is activation of hilar axons of associational collaterals of CA3 pyramidal cells. Stimulation in the cell layer of the dentate gyrus or hilus can activate these collaterals, which antidromically activate CA3 pyramidal cells. A second contamination results from the CA3 associational recurrent collaterals where CA3 pyramidal cells form synapses with one another. Stimulation in the DG or hilus can lead to firing of CA3 pyramidal neurons via the mossy fiber pathway, and firing of these neurons can activate responses on the CA3 pyramidal cells that are being recorded. To avoid these contaminations, the stimulus intensity was set to a single value that gave the field response of amplitude 0.2 – 0.3 mV. Also, to confirm the recorded events were generated from mossy fibers, a metabotropic glutamate transporter mGluR2 agonist, dicarboxycyclopropyl) glycine (DCG-IV) (1 µM), was applied at the end of the recordings. A 75-80% reduction in the fEPSP response amplitude is considered as validation for mossy fiber response. For experiments involving long-term potentiation (LTP), 2-amino-5-phosphonopentanoic acid (APV) (50 µM) was added to the perfusion medium, and baseline fEPSPs were recorded for 20 min in current-clamp mode. A high-frequency stimulation (HFS) consisting of two consecutive 100 Hz stimulation trains lasting 1 sec each, with an inter-train interval of 20 sec were given. Responses were then recorded for 60 min, and DCG-IV was applied for 5 min at the end of the recordings. Amplitudes of the fEPSPs were normalized to the baseline and analyzed. The field potentials were amplified using Molecular Devices 200B amplifier and digitized with Digidata 1322A. The data were sampled at 10 kHz and filtered at 2 kHz. Traces were obtained by pClamp 9.2 and analyzed using Clampfit 10.7.

Intracellular dye filling

Acute hippocampal slices of 350 µm thickness were prepared from 3-4 weeks old rats as described above following brain dissection in NMDG containing aCSF. Patch pipettes had a resistance of 4–5 MΩ when filled with intracellular fluid (ICF) containing (in mmol/L) 142 potassium gluconate, 2 $MgCl_2$ and 10 HEPES adjusted to pH 7.2 with KOH and osmolarity adjusted to 300 mOsM/litre. A 1 ml volume of the ICF was supplemented with 0.2% biocytin and dextran (10,000 MW) conjugated with Alexa488 (1 mg/ml). The stimulation electrode was placed near the hilus to activate the mossy fiber-CA3 pathway. Under infrared differential interference contrast optics (DIC), an appropriate CA3 pyramidal neuron was selected for patching. The pipette was lowered carefully to minimize any disruption of adjacent cells or their processes. Neurons were voltage clamped at -60 mV, and stimulation for intracellular dye injection was given every 20 sec for a period of 20 min. The pipette was then very slowly pulled away from the patched neuron. Since

dextran fills the soma and the processes of the dye injected neuron, visualization of Alexa488 fluorescence in the soma of the recorded neuron indicated successful disengagement of the pipette. Slice were retained in the recording chamber for 3-5 min before transferring them into 12 or 24 well plates containing 1% PFA. Slices were fixed overnight, transferred to cryoprotectant solution for 24 hr, and then washed three times for 15 min each in 0.1 M sodium phosphate buffer, pH 7.4, containing 0.9% saline (PBS) with continuous shaking. Slices were then incubated in PBS and 0.3% Triton X-100 containing Cy3-conjugated streptavidin (2 µl/ml) at 4°C for 16 hr in the dark, then washed for 30 min three times in 0.1 M PBS, and mounted onto glass slides with DAPI-containing mounting medium. The slices were visualized by widefield and confocal microscopy to reveal the neurons filled with biocytin labelled red and Alexa488-dextran labelled green.

Validation of shRNA *in vitro*

Six novel short hairpin RNAs (shRNAs) targeting rat Cx36 were designed based on 19 mer siRNA target predictions from multiple websites (Table 2). Sequences were examined in silico for specificity and all six selected targeting sequences showed no significant hybridization to known sequences. Control non-targeting shRNA was similarly designed using a scrambled targeting sequence. Sequences were cloned into the pLB vector for expression of shRNA under the direction of the U6 promoter and co-expression of the marker protein enhanced green fluorescence protein (eGFP) under direction of the CMV promoter. Both targeting and non-targeting shRNA plasmids were tested for silencing of Cx36 *in vitro* by transient co-transfection with an expression plasmid encoding rat Cx36 in N2A cells using Lipofectamine LTX transfection reagent. Following cell transfection (18-20 hr), proteins were isolated and subject to western blotting.

For western blotting, N2A cell cultures were rinsed in PBS and cells were lysed in RIPA buffer (20 mM Tris-HCl, pH 7.5, 150 mM NaCl, 1 mM Na_2EDTA, 1 mM EGTA, 1% NP-40, 1% sodium deoxycholate, 2.5 mM sodium pyrophosphate, 1 mM β-glycerophosphate, 1 mM Na_3VO_4, 1 µg/ml leupeptin). Following a brief sonication, cell lysates were centrifuged at 20,000 g for 20 min at 4°C, and supernatants were taken for protein determination using Bradford reagent (Bio-Rad Laboratories, Hercules, CA, USA). Proteins (15 µg of protein per lane) were separated by SDS-PAGE using 10% gels followed by transblotting to polyvinylidene difluoride membranes (Bio-Rad Laboratories) in standard Tris-glycine transfer buffer, pH 8.3, containing 0.5% SDS. Membranes were blocked for 1 hr at room temperature in 10 mM Tris-HCl, pH 8.0, 150 mM NaCl, and 0.2% Tween 20 (TBT) containing 5% nonfat milk powder, rinsed briefly in in TBT, and

incubated overnight at 4°C with anti-Cx36 antibody in TBT containing 1% nonfat milk powder. Membranes were washed in TBT three times for 10 min each, incubated with horseradish peroxidase-conjugated donkey anti-rabbit IgG diluted to 1:5000 (Sigma-Aldrich) in TBT containing 1% nonfat milk powder for 1 hr at room temperature, washed in TBST three time s for 10 min each, and resolved by ECL chemiluminescence.

Cloning and virus production

To maximize gene silencing *in vivo*, two targeting sequences were chosen that demonstrated the most efficient silencing of Cx36 *in vitro.* A microRNA miR-30-based targeting construct was then designed that encoded both of these sequences within a chimeric intron (chI) upstream of the open reading frame (ORF). Advantages of this strategy are that shRNAmir expression has no impact on the protein expressed from the ORF (Boudreau et al., 2009; Casanotto et al., 2007; McBride et al., 2008) and multiple gene specific shRNAmir hairpins can be expressed from a single construct, greatly enhancing knockdown efficiency (Chung, 2006; Zhu et al., 2007). Additionally, in this construct, the expression of both eGFP and shRNAmir are contained in an expression cassette driven by the same excitatory-cell-specific CaMKIIα promoter (Fig. 1A). Thus, knockdown of Cx36 by shRNA is confined to excitatory neurons, and the identification of cells expressing shRNA is confidently monitored by virtue of their eGFP fluorescence. In brief, the targeting sequences were modified to a miR-30-based shRNA sequence (Chang et al., 2013). This modified shRNA sequence was then cloned in silico into the optimized MIR-E backbone (Fellmann et al., 2013) and subsequently linked together, separated by a spacer region. This shRNAmir-e multimer was then inserted within a chimeric intron (chI) sequence between the splice donor and branch point sites. The resulting chI-[2X(shRNAmir-e)] cassette along with overhanging restriction sites (SmaI) was synthesized by the ThermoFisher GeneArt Gene Synthesis service. The cassette was excised from the GeneArt construct and then ligated into an ssAAV backbone, which contained the mCaMKIIα promoter, the chI, and an eGFP open reading frame (Fig. 1B). This final construct was transformed into MDS42 bacterial cells by heat-shock. Using plasmid DNA from individual colonies, the integrity of these SmaI sites was determined using SmaI digestion to confirm ITR integrity and to allow selection of correct clones following cloning of the shRNA cassette (Fig. 1C), with correct sequence of the region encompassing the cassette confirmed by DNA sequencing (Robarts Research Institute, London ON). Correct clones were inoculated into TB media containing ampicillin. Plasmids were purified from overnight bacterial cultures (Thermo Fisher Maxiprep). A scrambled non-silencing construct, consisting of 2 hairpins targeting the sequence

5’-CAATTCTCCGAACGTGTCACGT-3’, was similarly constructed and confirmed (Fig. 1C). These plasmids were sent to the Neurophotonics Molecular Tools Center (University of Laval) for production of silencing and non-silencing AAV serotype 8 particles.

RESULTS

Our previous demonstration of the association of Cx36 with hippocampal mossy fiber terminals was based on the localization of immunofluorescence labelling for Cx36 at nerve terminals immunolabelled for the excitatory transmitter marker vesicular glutamate transporter1 (vglut1) in the stratum lucidum of the hippocampal CA3 region, where the axons of granule cells in the dentate gyrus terminate as mossy fiber terminals (Nagy, 2012). In the stratum lucidum and many other CNS regions we have examined (Li et al., 2004a; Kamasawa et al., 2006; Curti et al., 2012; Bautista and Nagy, 2014; Bautista et al., 2014; Rubio and Nagy; 2015; Nagy et al., 2017, 2018), immunofluorescence labelling of Cx36 has an exclusively punctate appearance (*i.e.*, Cx36-puncta) and is invariably localized to the surface of neuronal elements. Intracellular labelling for Cx36 remains largely undetectable at least *in vivo*, perhaps due to rapid trafficking of Cx36 to plasma membranes leaving low levels within cells, or due to masking of Cx36 epitopes at intracellular compartments rendering them undetectable by currently available antibodies. Throughout the CNS, the localization of Cx36-puncta is well correlated with sites of ultrastructurally-defined Cx36-containing nGJs (Rash et al., 2000, 2001, 2004, 2007a,b; Fukuda, 2009; Shigematsu et al., 2018), and those puncta therefore serve as markers for such junctions *in vivo*. The localization of Cx36-puncta at vglut1-positive (vglut1+) terminals in the stratum lucidum thus represents strong evidence for the presence of nGJs at these terminals. However, vglut1 is a marker not only of mossy fiber terminals, but also other excitatory terminals within and surrounding the stratum lucidum, and nGJs have been found ultrastructurally at various types of excitatory nerve terminals in the different strata of the hippocampus (Hamzei-Sichani et al., 2012). Thus, to examine Cx36 localization more selectively to mossy fiber terminals, we used a marker expressed at exceptionally high levels in these terminals, namely vesicular zinc transporter3 (ZnT3) (Palmiter et al., 1996; Wenzel et al., 1997).

An overview of immunolabelling for ZnT3 in the hippocampal hilus and stratum lucidum is shown in Figure 2A, and its high expression in mossy fiber terminals is shown magnified in Figure 2B. The typical appearance of Cx36-puncta in the stratum lucidum of the rat ventral hippocampus is shown in Figure 2C1, and the co-distribution of those puncta among ZnT3+ mossy fiber terminals is shown in Figure 2C2. Higher magnification confocal imaging revealed a remarkable

degree of co-distribution of clusters of Cx36-puncta (Fig. 2D1) with ZnT3+ terminals (Fig. 2D2). With reference to hippocampal nomenclature (Scharman, 1993; Ishizuka et al., 1995), where the proximal-distal regions of the CA3 subfields have been designated as CA3c, CA3b and CA3a, we described the highest density of Cx36-puncta associated with mossy fiber terminals in the CA3b and *distal* CA3c subfields and an absence in the CA3a subfield in the rat ventral hippocampus, and a total absence of those puncta in all three of these subfields in the dorsal hippocampus of rat (Nagy, 2012). Conversely, many ZnT3 terminals in the CA3b and CA3c regions of the stratum lucidum displayed Cx36-puncta. From counts of the proportion of those terminals containing puncta these fields, we found that 62 ± 6 % harboured Cx36-puncta, with the remainder devoid of puncta.

To the extent that individual isolated ZnT3+ structures could be designated as single mossy fiber terminals in images such as shown in Fig. 2D2, many of those structures contained at least one Cx36-punctum, but most contained several puncta. Among those ZnT3+ terminals displaying Cx36-puncta, analysis of numerous terminals showed that they contained an average of 2.4 ± 0.2 puncta per terminals. This is likely an underestimate because while z-stack images may have captured the entirety of some mossy fiber terminals, the upper and lower extremities of those stacks could exclude out-of-field portions of terminals where Cx36-puncta may be localized, though this may be mitigated somewhat by our examination only of terminals that were 3-5 um in diameter.

Consistent with the identification of ultrastructually-identified nGJs in virtually all areas of the hippocampus (Kosaka and Hama, 1985; Hamzei-Sichani et al., 2012), Cx36-puncta at various densities occupied all regions of the hippocampal formation. A comparison of the appearance of those in the stratum lucidum *vs.* radiatum in the ventral hippocampus is shown in Figure 3A and 3B. Puncta in the stratum lucidum (Fig. 3A) were present at high density, organized in clusters as expected given their localization to mossy fiber terminals, and displayed a wide range of sizes. In contrast, Cx36-puncta in the stratum radiatum in the CA3 region (Fig. 3B) and the CA1 region (Fig. 3B, inset) were often arranged in linear arrays reflecting their localization along dendritic shafts such as those of parvalbumin+ interneuronal dendrites (Fig. 3C), and tended to be of larger size than Cx36-puncta in the stratum lucidum. Measures of Cx36-puncta diameters in the two strata (Fig. 3D) showed an average of 450 ± 0.004 nm for those in the stratum lucidum, which was significantly different from the average of 683 ± 0.005 nm for those in the stratum radiatum. This is consistent with observations by FRIL that gap junctions formed by interneurons were larger than those at excitatory mixed synapses (Hamzei-Sichani et al., 2012). It should be noted that these are

relative measures and, due to halation incurred by immunofluorescence imaging, are not reflective of the actual much smaller sizes of nGJs as seen by both thin-section electron microscopy (EM) and FRIL (Kosaka and Hama, 1985; Hamzei-Sichani et al., 2012).

It has been recognized that unlike other cortical principle neurons, granule cells are unique in that they have more than one terminal type associated with their axons (Ramon y Cajal, 1911; Amaral, 1979; Acsady et al., 1998). Thus, in addition to mossy fiber terminals, there are filopodial extensions and *en passant* contacts (approximately 2 µm) along mossy fibers, which synapse with inhibitory interneurons in the hippocampal hilus. Also, there are other mossy fiber expansions (3-5 µm diameter) similar to the boutons seen at CA3 which contact the dendrites and somata of excitatory mossy cells in this region (Amaral, 1979; Acsady et al., 1998; Scharfman et al., 1990; see also Fig. 1.4B in the introduction). We sought to determine whether the filopodial extensions, *en passant* terminals and the larger expansions that contact mossy cells in hilus also formed mixed synapses similar to those at mossy fiber terminals in CA3. Immunofluorescence labelling for ZnT3 was detected at very high density in the hilus of the ventral hippocampus (Fig. 4A1; dotted boxed square in Fig. 2A), where this labelling was presumably associated with the endings of mossy fiber collaterals that terminate on hilar mossy cells. In contrast, Cx36-puncta were very sparsely distributed in the ventral hilus (Fig. 4A2), and none of the Cx36-puncta were associated with ZnT3+ terminals (Fig. 4A3), which was confirmed by rotation of z-stacked 3D images captured from 15 to 24 confocal scans. We were confident that the paucity of Cx36-puncta in the ventral hilar region was not due to ineffective labelling by examining Cx36 in a nearby region of the stratum lucidum of the same tissue section, where the density of Cx36-puncta and the association of these with mossy fiber terminals was typical of that usually seen (Fig. 4B). Presumptive mossy cells visualized by intensely labelled ZnT3+ terminal contacts on their somata located at the border between the hilus and granule cell layer (Fig. 4C1) and having previously described morphologies (Amaral, 1978) were also found in fields with very few Cx36-puncta (Fig. 4C2) and these terminals were also devoid of Cx36-puncta (Fig. 4C3). It thus appears that mossy fiber collaterals do not form mixed synapses with their postsynaptic targets.

Cx36 association with adherens junctions at mixed synapses in hippocampus

We previously reported that nGJs referred at “purely electrical synapses” are frequently immediately adjacent to or intimately surrounded by adherens junctions linking plasma membranes, forming what we termed the AJ-nGJ complex (Nagy and Lynn, 2018). Here, we

examined whether the same is true at mixed synapses, because a similar association at these synapses could shed some light on the organization of their gap junction component based on known deployment of synaptic adherens junctions. Adherens junctions at individual mossy fiber terminals consist of rows of multiple punctate junctions, with cumulative lengths of up to 2-3 µm when viewed on-edge and corresponding diameters when viewed *en-face*, consistent with thin-section EM measures of the span encompassed by these junctional arrays (Amaral, 1979; Chicurel and Harris, 1992). These adherens junctions have been the subject of intensive study and they have served as a model system to define the molecular constituents of these junctions, including the closely linked proteins N-cadherin and nectin-1 (Inagaki et al., 2003; Irie et al., 2004; Majima et al., 2009). The distribution of immunofluorescence labelling for N-cadherin in various layers of the hippocampus is shown in Figure 5A, with a magnified region showing intense labelling for N-cadherin in the stratum lucidum (Fig. 5B). Triple immunofluorescence labelling of ZnT3, Cx36 and N-cadherin in the stratum lucidum is shown in Figure 5C. Labelling of N-cadherin appeared as long slender structures in on-edge views and ovoid or irregular shapes when viewed *en-face* or at oblique angles (Fig. 5C1). Cx36-puncta localized to mossy fiber terminals (Fig. 5C2) and labelling for N-cadherin localized to these terminals (Fig. 5C3) were seen to be highly co-distributed, with Cx36-puncta of much smaller size than the adherens junctions associated with mossy fiber terminals often overlapping, immediately adjacent to or straddling N-cadherin+ junctions (Fig. 5C4). Similarly, triple labelling for Cx36, nectin-1 and ZnT3 showed a high density of labelling for nectin-1 in the stratum lucidum (Fig. 6A1), with the vast majority of Cx36-puncta overlapping or straddling nectin-1+ adherens junctions (Fig. 6A2) that were localized to mossy fiber terminals (Fig. 6A3), which is shown at higher confocal magnification in Figure 6B. The above results thus indicate that maintenance of an AJ-nGJ complex is a characteristic feature of a subpopulation of mossy fiber terminals restricted to the CA3b and CA3C regions. Some of the larger Cx36-puncta in these fields lacked association with nectin-1 and ZnT3 and therefore may represent gap junctions localized on dendrites of interneurons as shown in Figure 3C, which may be devoid of or have less distinctive adherens junctions, or likely express different cadherin and nectin proteins at such junctions.

We next examined the localization of Cx36-puncta and N-cadherin at the AJ-nGJ complex of mossy fiber terminals in relation to CA3 pyramidal cell dendrites labelled for the microtubule marker microtubule-associated protein2 (MAP2). Triple immunofluorescence labelling for Cx36, N-cadherin and MAP2 in the CA3b and CA3C regions of the stratum lucidum revealed numerous

sites where Cx36-puncta associated with N-cadherin+ adherens junctions (i.e., the AJ-nGJ complex) were localized to MAP2+ dendrites (Fig. 7A) that could often be followed back to their parent CA3 pyramidal cell bodies of origin (not shown). In images of the AJ-nGJ complex viewed on-edge, the complex was typically seen extending along one peripheral border of dendrites (Fig. 7B) and occasionally along both peripheral border (Fig. 7C). With the AJ-nGJ complex viewed *en-face*, clusters of Cx36-puncta localized among patches of labelling for N-cadherin were seen along large MAP2+ dendrites (Fig. 7D). In the case of AJ-nGJ complexes viewed on-edge, some Cx36-puncta and their associated adherens junctions were displaced by usually less than 0.2 µm slightly outside of labelling for MAP2, which is likely due to the sparse distribution and hence low level of labelling for MAP2-associated microtubules near the plasma membranes of dendritic shafts (Amaral, 1979; Pivovarova et al., 2002). Because adherens junctions between mossy fiber terminals and CA3 pyramidal cells link these terminals directly to dendritic shafts (Amaral, 1979; Amaral and Dent, 1981; Chicurel and Harris, 1992; Rollenhagen et al., 2007), the above results taken together suggest that Cx36-containing gap junctions also occur at terminal/shaft contracts, as depicted in Figure 8.

Cx36 association with adherens junctions at mixed synapses in brainstem and spinal cord

To determine the generality with which Cx36 co-distributes with adherens junctions at mixed synapses, we examined several CNS locations in mouse and rat at which we have described Cx36-containing mixed synapses, including the lateral vestibular nucleus (LVN), the medial nucleus of the trapezoid body (MNTB), posteroventral cochlear nucleus (PVCN), ventral horn of the spinal cord and the red nucleus (Nagy et al., 2013, 2019; Bautista et al., 2014; Rubio and Nagy, 2015). In the LVN, the somata and proximal dendrites of large neurons are contacted by primary afferent terminals that form mixed synapses (Korn et al., 1973; Nagy et al., 2013). A low magnification image of three such neurons is shown in Figure 9A, which is triple labelled for Cx36, N-cadherin and the additional marker zonula occluden-1 (ZO-1) that is a protein component of both nGJs and adherens junctions (Li et al., 2004), thus providing confirmatory support for structural associations between these junctions. The LVN neurons are not counterstained, but a high density of immunolabelling for these three proteins delineated their soma and proximal dendrites. Higher confocal magnification of a single neuronal soma showed labelling of Cx36, N-cadherin and ZO-1 to be concentrated around the periphery of the soma in a typical punctate fashion (Fig. 9B1, B2 and B3). Total co-localization was seen between Cx36 and ZO-1 (Fig. 9B4), as also seen in other brain regions (Li et al., 2004), while labelling of N-cadherin together with either ZO-1 (Fig. 9B5)

or Cx36 (Fig. 9B6) showed substantial overlap or were found in very close proximity. In the MNTB, large neuronal somata receive dense coverage and envelopment by calyx of Held terminals that originate from globular bushy cells in the anterior ventral cochlear nucleus. We previously reported that these calyceform terminals that harbour Cx36-puncta, thus indicating the presence of Cx36-containing gap junctions at these terminals and their formation of mixed synapses on MNTB neuronal somata (Rubio and Nagy, 2015). Labelling of Cx36 and N-cadherin on these somata showed that Cx36-puncta either partially overlapped with or were nestled immediately adjacent to punctate labelling of N-cadherin (Fig. 9C,D). However, N-cadherin puncta outnumbered Cx36-puncta leaving some of those devoid of association with Cx36. Double labelling of these two proteins on large somata and dendrites in the PVCN showed their similar close association (Fig. 9E) at what we previously described to be Cx36-containing mixed synapses (Rubio and Nagy, 2015). In the lumbar spinal cord, it is well known that individual Ia muscle spindle afferents form multiple monosynaptic terminals on motoneurons throughout the motor pools (Brown and Fyffe 1978), and we have reported that these terminals form Cx36-containing mixed synapses (Bautista et al., 2014). Similarly, we have found that large neuronal somata in the brainstem red nucleus were laden with mixed synapses formed by nerve terminals of unknown origin (Nagy et al., 2019). Here, we show close Cx36-puncta association with N-cadherin at mixed synapses on both spinal cord motoneurons (Fig. 10A) and red nucleus neurons (Fig. 10B,C). Thus, just as the AJ-nGJ complex is a widespread feature of purely electrical synapses (Nagy and Lynn, 2019), it appears that this complex is also a consistent structural component at mixed synapses.

Electrophysiological properties of the mossy fiber-CA3 pathway

For the purposes of subsequent experiments to be performed, we first established electrical stimulation and recording parameters of the mossy fiber-CA3 pathway by first characterizing a few distinct properties of hippocampal mossy fiber synapses. One of those properties is the frequency facilitation that these synapses undergo, where increasing the frequency of mossy fiber stimulation causes a huge increase in postsynaptic responses of CA3 cells. A minimum of 300% facilitation criteria was set for a recording to be included for the analysis and for determining the position of both recording and stimulating electrodes, as shown in Figure 11A. The percent increase in facilitation of mossy fiber fEPSP synaptic response during mossy fiber stimulation was ~500% when recorded extracellularly from 23 hippocampal slices obtained from 13 rats (Fig. 11B). The stimulation intensity given at the mossy fibers was set so that a field response of amplitude 0.2 to 0.3 mV was obtained. This criterion minimizes stimulation of non-mossy fiber

inputs to CA3 pyramidal cells that could be activated at higher intensity stimulation. Next, we analyzed LTP induced by high frequency stimulation (100 Hz for 1 sec, repeated twice at 20 sec intervals) at mossy fiber pathway. Since this LTP does not require the activation of NMDA receptors, APV (50 µM), an NMDA blocker was added to the solution. We observed potentiation, represented as the average fEPSP taken from measurements gathered in the 5 min interval prior to addition of DCG-IV, of 183.65 ± 13.26 % (n=13; with baseline set at 100%) (Fig. 11C). This confirmed that LTP at mossy fiber synapses does not require the activation of NMDA receptors and is not blocked by APV. The mossy fiber response was seen to be inhibited by DCG-IV application at the end of the recording (Fig 11C). A 75-80% reduction in fEPSP amplitude was considered to reliably indicate recording of CA3 responses to mossy fiber stimulation.

Dorsal *vs.* ventral differences in electrophysiological properties

We next examined whether any differences in frequency facilitation or LTP in the mossy fiber-CA3 pathway could be observed in the dorsal *vs.* ventral rat hippocampal slices, with the subsequent aim of determining whether any differences found in these parameter could be attributed to the presence of mixed synapses in the ventral but not dorsal hippocampus. Slices from each hippocampus were placed in a 6-well chamber with 2 to 3 slices per chamber .The first six and last six hippocampal slices (300 µm each) were used for recording, which corresponded to the most dorsal or ventral portion of the hippocampus, respectively. In addition, the shape of the dentate gyrus cell layer was used to confirm that slices were taken from dorsal (Fig. 12A1) or ventral (Fig. 12A2) hippocampus where the gyrus exhibits a 'V' shape vs. a 'U' shape, respectively. Field responses from ventral hippocampal slice exhibited a large positivity (Fig 12A4, black trace), which was not observed in dorsal slices (Fig 12A3, green trace). The observed positivity remained even after the frequency facilitation (Fig. 12A5, blue trace) and LTP (Fig 12A5, green trace) protocols were applied to the ventral hippocampal slices. Apparently, we are not clear about the source of this positivity, but we know the origin of this positivity is not inhibitory interneurons as bicuculline, a GABA receptor antagonist had no effect on the positivity (Fig.12A6). Frequency facilitation reflecting short-term plasticity was not significantly different between dorsal and ventral hippocampal slices (Fig 12B). Subsequent LTP experiments showed a difference in potentiation in ventral *vs.* dorsal slices (Fig 12C). The ventral slices had a higher potentiation (218 ± 24) compared with dorsal slices (160 ± 10, n=11; $p < 0.05$, unpaired t-test) by the last 5 min of the recording (Fig 12D).

AAV vector mediated knockdown of Cx36

The electrophysiological results presented above provided the motivation to develop AAV-mediated knockdown of Cx36 to test whether the presence of mixed synapses at mossy fiber terminals in the ventral but not dorsal hippocampus contributed to the greater levels of LTP observed in the ventral hippocampal region. The shRNA approach for Cx36 knockdown was first tested in N2A cells (see Experimental Procedures), where three of the six shRNA sequence examined showed substantial reductions in Cx36 expression (Fig. 13), of which two were chosen to implement AAV-mediated knockdown. The two sequence have been inserted downstream of the promoter for CaMKIIa, which is highly expressed and enriched in DG neurons (Sik et al., 1998; Yamasaki et al., 2008). Work on the effectiveness of those vectors for *in vivo* Cx36 knockdown in the hippocampus remains in progress.

It should be noted that this AAV-mediated knockdown approach in rats, besides offering the advantage of selectivity for Cx36 knockdown in hippocampal principle cells *vs.* electrically coupled inhibitory interneurons, was necessary in lieu of the use transgenic mice, because as discussed earlier mossy fiber terminals lack mixed synapses in both dorsal and ventral regions of the hippocampus of mice and are only present in the ventral hippocampus of rat (Nagy, 2012). In this context, it is instructive to summarize what is known concerning Cx36 expression in hippocampal principle cells of the two rodent species, to the extent that this has been determined by various approaches including in situ hybridization for Cx36 mRNA, fluorescent protein expression (eGFP and CFP) driven by the Cx36 promoter and immunofluorescence detection of Cx36 (Table 3). Unfortunately, while a clear species difference is seen between patterns of Cx36 expression in dorsal *vs.* ventral hippocampus, most studies cited in Table 3 appeared to have examined the dorsal hippocampus, and therefore Cx36 expression patterns in the ventral hippocampus of the two species remains to be determined by approaches in addition to our use of immunofluorescence labelling for Cx36.

Biocytin tracer injections into hippocampal pyramidal and granule cells

A previous study reported that intracellular injection of individual CA3 pyramidal cells with the fluorescent dye lucifer yellow resulted in transfer of dye from the injected cell to what were putative mossy fibers contacting or in the vicinity of the injected cell (Hamzei-Sichani et al., 2012), suggesting that dye-transfer occurred from the cell to the fiber presumably via gap junctions linking these two structures. However, there continues to be several interpretational difficulties

with that work. First, the authors failed to indicate whether they examined dye coupling in dorsal *vs.* ventral hippocampus, where mossy fibers terminals lack or contain Cx36-containing gap junctions, respectively, as we have noted. Second, the dye-coupling studies were undertaken in formaldehyde-fixed hippocampal sections, which may have resulted in artifactual dye-coupling. And third, the dye used (i.e., lucifer yellow) is known to be very poorly permeable across Cx36-containing gap junctional channels, and we have not detected any other connexin than Cx36 at mossy fiber terminals among many candidate connexins tested that do form channels permeable to this dye. Thus, we performed intracellular biocytin injections into ventral hippocampal CA3 pyramidal cells in an attempt to reproduce the results of Hamzei-Sichani et al. (2012). In addition, we performed similar injections into granule cells to determine if gap junction-mediated biocytin transfer occurred from mossy fiber terminals to CA3 pyramidal cells and then back to other mossy fiber terminals not arising from the injected granule cell. A total of twenty-five pyramidal cells and seven granule cells were successfully injected, and these displayed somata, dendrites and mossy fibers together with their terminals that were well labelled for biocytin (supplementary fig. 1). No transfer of biocytin from pyramidal cells to mossy fibers was seen and only one example of a biocytin labelled mossy fiber terminal was observed lacking Alexa488-dextran, suggesting transfer of the smaller biocytin tracer, but not the larger MW dextran tracer despite the parent granule cell axon having displayed both tracer. These experimental approaches were abandoned due to their time-consuming nature, shortage of time for thesis completion and uncertainty of positive outcomes.

DISCUSSION

The present results extend our initial work demonstrating the association of Cx36-containing gap junctions with vglut1+ mossy fiber terminals in the CA3b and CA3c subregions of the stratum lucidum in ventral hippocampus in adult rat (Nagy, 2012). In contrast to the localization of vglut1 in many different types of excitatory nerve terminals, the very high levels of vesicular ZnT3 in mossy fiber terminals (Palmiter et al., 1996; Wenzel et al., 1997) in conjunctions with our present use of immunofluorescence labelling for this protein afforded more specific visualization of these structures and confirmed localization of multiple Cx36-puncta with a large percentage of those in the above hippocampal subregions. These Cx36-puncta were significantly smaller than those belonging to dendrites of parvalbumin+ interneurons in the vicinity of the stratum lucidum, consistent with findings that ultrastructurally-defined gap junctions examined by FRIL within this hippocampal layer generally had fewer connexon channels than those linking the dendrites of

interneurons (Hamzei-Sichani et al., 2012). In relation to this, although we found that the majority of diminutive Cx36-puncta within the stratum lucidum were associated with large ZnT3+ mossy fiber terminals, some gap junctions of even smaller size have been identified by FRIL at other types of what were designated excitatory mixed synapses within this structure (Hamzei-Sichani et., 2012), and their small size may have rendered them below the detection limit of our immunofluorescence procedures. In any case, the present results are consistent with the ultrastructural detection of gap junctions by FRIL at what appear to be mixed synapses at a number of locations in the hippocampus, including stratum lucidum, though as noted earlier most of those gap junctions could not be definitively identified to be associated specifically with mossy fiber terminals (Hamzei-Sichani et al., 2012). Putative gap junctional contacts between mossy fiber axons and at mossy fiber terminals have been reported on the basis of observations by thin-section EM, but these failed to meet the heptalaminar criterion at plasma membrane contacts for designation as gap junctions (Hamzei-Sichani et al., 2007, 2012). Although it is curious that bonafide heptalaminar gap junctional structures at mossy fiber terminals have not been reported despite extensive examination of these terminals by thin-section EM over the span of decades, it should be noted that exceptional ultrastructural preservation would be required to identify these structures and at much greater magnification than is typically used to visualize synaptic elements, particularly so given their very short lengths along plasma membranes.

Mixed synapses at only one of the three types of mossy fiber axon terminals

In contrast to the occurrence of mixed synapses at mossy fiber terminals, our finding that the collaterals of these fibers forming filopodial extensions and *en passant* terminals lack association with Cx36-puncta and therefore do not form mixed synapses raises questions pertaining to how this can occur. Here, we consider four possibilities. First, it may be that only subpopulations of granule cells form mixed synapses at their mossy fiber terminals and these specifically lack collateral projections to the hilus and to mossy cells. This is unlikely based on quantitative analyses of the axonal ramifications of individual granule cells (Acsady et al., 1998). Second, Cx36 may be selectively transported to mossy fiber terminals but not to mossy fiber collateral branches. This also is unlikely because it would require selectivity of protein transport at axonal branch points, where transport occurs along one branch but not another, for which we know of no precedent. Third, production of Cx36 protein from Cx36 mRNA may take place exclusively in mossy fiber terminals and mossy fiber collateral terminals may lack this capacity. This possibility suffers from the same problem as point two above. And fourth, as discussed below, adherens junctions may

serve as structural determinants of subcellular sites at which nGJs are deployed. This possibility is supported by the formation of numerous adherens junctions by mossy fiber terminals and the absence of these junctions between the postsynaptic targets of filopodial extensions or *en passant* terminals (Acsady et al., 1998). Cx36 may be transported along mossy fiber axon collaterals, but it may be rapidly recirculated in the absence of molecular machinery for its incorporation into gap junction within the plasma membrane.

It is interesting to consider this mixed synaptic feature that distinguishes the terminal types of mossy fibers in the context of Dale's principle (Dale, 1934), which as reformulated by Eccles et al. (1954) states "In conformity with Dale's principle (1934, 1952) that the same chemical transmitter is released from all the synaptic terminals of a neuron…". Although this principle applies to chemical synaptic transmission and was formulated before electrical synapses were identified, it seems reasonable to consider that all terminals of a neuron should have that same transmission capabilities regardless of the nature of that transmission (i.e., chemical or electrical). If this is a legitimate tenet, then it would appear that the electrical component of mixed synapses violates Dale's principle, at least in the case of hippocampal granule cells and their projections.

The AJ-nGJ complex at mixed synapses

Adherens junctions and gap junctions composed of various connexins have intimate structural and functional interactions in peripheral tissues (Derangeon et al., 2009), where it has been established that cell adhesion mediated via N-cadherin or E-cadherin is required for the formation of gap junctions (Keane et al., 1988), including those composed of connexin40 and connexin43 (Meyer et al., 1992; Hertig et al., 1996; Li et al., 2005; Segretain and Falk, 2004). Similarly, in ultrastructural studies of the CNS, nGJs were frequently noted to be in continuity with adherens junctions in a variety of brain regions (Gwyn et al., 1977; Sloper and Powell, 1978; Kosaka, 1983; Katsumaru et al., 1988; Peters et al., 1991; Kosaka and Kosaka, 2003), and our previous report using the more global view afforded by immunofluorescence labelling of adherens junctions in combination with labelling of Cx36-containing gap junctions showed that the AJ-nGJ complex is a general feature of at least purely electrical synapses formed between many types of neurons in the CNS, notwithstanding that this complex may contain some cadherin other than N-cadherin at electrical synapses formed by GABAergic inhibitory neurons (Nagy and Lynn, 2018). Of course, adherens junctions independent of nGJs are a critical structural component that link a wide variety of neuronal subcellular elements, including nerve terminals to their postsynaptic elements (Basuy

et al., 2015; Friedman et al., 2015; Stocker and Chenn, 2015). Here, we show that the AJ-nGJ complex is also a prominent and characteristic feature at mixed synapses that have been identified in several mammalian CNS areas. Among the best characterized adherens junctions (aka, puncta adherentia) ultrastructurally are those joining large mossy fiber terminals to exclusively the dendritic shafts of CA3 pyramidal cells in the stratum lucidum of the hippocampus, where these junctions consist of a series of multiple (2-13), closely spaced contacts per terminal (Amaral, 1979; Amaral and Dent, 1981; Chicurel and Harris, 1992; Rollenhagen et al., 2007). The protein constituents of these junctions, including N-cadherin, nectins and ZO-1, have also been extensively studied and their visualization by immunolabelling at the resolution of immunofluorescence shows the series of contacts they form to be merged as distinctive linear strands (Nishioka et al., 2000; Mizoguchi et al., 2002; Inagaki et al., 2003; Honda et al., 2006; Toyoshima et al., 2014). This is of note because it could then be presumed that the Cx36-puncta we observe associated with adherens junctions at mixed synapses represent gap junctions interdigitated between and among these intermittently localized and closely spaced adherens junctions, which was evident here in some on-edge and en-face views of the AJ-nGJ complex. This is consistent with the reported close proximity between adherens junctions and gap junctions at some mixed synapses examined ultrastructurally in other regions of mammalian brain (Sotelo and Palay, 1970).

In addition to N-cadherin, nectins and ZO-1, other key proteins found at adherens junctions of mossy fiber terminals include AF6 (aka, afadin), α-catenin and β-catenin (Nishioka et al., 2000; Mizoguchi et al., 2002; Inagaki et al., 2003; Majima et al., 2009; Nagy, 2012), all of which are found either co-localized with or in close association with nGJs at purely electrical synapses (Nagy and Lynn, 2018). Based on an assortment of known direct molecular interactions between these proteins, we have previously proposed a model whereby these interactions may physically tether nGJs to their adjacent adherens junctions at these synapses (Nagy and Lynn, 2018). Specifically, it is known that nectin-1 interacts with AF6 linked to ZO-1, that cadherins bind α-catenin and β-catenin, and that the nectin-AF6 and cadherin-catenin systems associate through AF6-α-catenin interaction (Shapiro and Weis, 2009; Harris and Tepass, 2010) to co-operatively organize adherens junctions (Miyahara et al., 2000; Takai and Nakanishi, 2003, 2008; Mori et al., 2014). The reported association of ZO-1 and AF6 with both adherens junctions and nGJs (Itoh et al., 1993; Mandai et al., 1997; Takahashi et al., 1999; Li et al., 2004; 2012), together with the known direct molecular interaction of the carboxy-terminus motif of Cx36 with PDZ (PSD-95, DlgA, ZO-1) domains contained in each of ZO-1 and AF6, provide a mechanism for molecular links involving AF6/ZO-

1/Cx36 and/or AF6/Cx36 interactions between these two types of intercellular junctions (see Fig. 13 in Nagy and Lynn, 2018). We have previously discussed the possible organization of such links in relation to structural configurations in which AJs and nGJs subdomains occur in plasma membranes (Nagy and Lynn, 2018; see also Segretain and Falk, 2004; Kamasawa et al., 2006). The present results suggest that a similar set of molecular interactions mediate tethering nGJ to adherens junctions at the AJ-nGJ complex now identified at mixed synapses, but these possibilities remain to be directly tested by molecular manipulations of these proteins in appropriate model systems. Further, in Cx36 null mice, we found a persistence of the adherens junction components of the AJ-nGJ complex at subcellular sites (Nagy and Lynn, 2018) that normally harbour nGJs (Curti et al., 2012), suggesting that various components of the AJ-nGJ complex serve as pre-existing nucleation sites for assembly of Cx36-containing gap junctions. Such a scenario is consistent with targeting of other connexins to adherens junctions in various cell types (Meyer et al., 1992; Shaw et al., 2007), and may also occur at mixed synapses.

Beyond the above structural considerations, identification of the AJ-nGJ complex at mixed synapses raises possible relationships between regulation of the activities of this complex and intracellular signalling systems at nerve terminals harbouring this complex. In particular, the GTP-binding protein Rap1 serves as a major regulator of neurotransmission at chemical synapses (Kennedy, 2013) and is an activator of one of its effector targets, namely AF6 (Linnemann et al., 1999; Boettner et al., 2000, 2001; Kooistra et al., 2006). In peripheral tissues, Rap1 promotes the formation and maintenance of adherens junctions (Caron, 2003; Kooistra et al., 2006; Birukova et al., 2011), and it may perform a similar function via its AF6 effector at the AJ-nGJ complex at mixed synapses. Moreover, electrical synapses formed by Cx36 are well known to be regulated by cAMP via protein kinase A (Urschel et al., 2006; Kothmann et al., 2009; O'Brien, 2014), but cAMP can also activate Epac (exchange protein directly activated by cAMP, which is a guanine nucleotide exchange factor (GEF) that activates Rap1. Thus, cAMP/Epac/Rap1 signalling to AF6 at the adherens junction component and/or the nGJ component of the AJ-nGJ complex at mixed synapses may contribute to the assembly of this complex and regulation of electrical transmission at these synapses.

Functional considerations of AJ-nGJ complex loci at mossy fiber terminals

The close association between Cx36-containing gap junctions and adherens junction we found at mossy fiber terminals, together with the known localization of these adherens junctions exclusively

at plasma membrane of these terminals that contact the dendritic shafts of CA3 pyramidal cells (Amaral, 1979; Amaral and Dent, 1981; Chicurel and Harris, 1992; Rollenhagen et al., 2007), strongly suggest that gap junctions are highly restricted to compartments directly linking mossy fiber terminals to dendritic shafts (Fig. 8). In contrast, chemical transmission at these terminals occurs at active zones distributed around thorny excrescences emanating from CA3 pyramidal cell dendrites, but not at direct terminal-dendritic shaft contacts where there is a paucity of synaptic vesicles and an absence of active zones (ibid, above). It thus appears that mossy fiber terminals exhibit spatial separation of subcellular loci that mediate the chemical *vs.* electrical components of their mixed synaptic transmission. This configuration could have important consequences for functional interaction between the two forms of communication and thus properties imparted onto mixed MF synapses at thorny excrescences of CA3 pyramidal cells (Spruston, 2008), for which there are several possibilities. First, the electrical component could produce subthreshold dendritic depolarizations that summate with the chemical transmission component at spines to facilitate dendrite activation. Second, pyramidal cell spike or burst activity could be propagated antidromically via the electrical component into multiple spine heads to enhance chemical synaptic activation of spines. And third, at neuronal microcompartments such as the dendritic spine head/neck assembly, electrical field effects have been considered to have an impact on electrical current flow between this assembly and the dendritic shaft following synaptic activation of spine heads (Holcman and Yuste, 2015). We speculate that the strategic placement of gap junctional channels could influence those field effects by modulating the voltage drop between spine head and dendritic shaft, which may serve to modify synaptic transmission efficacy.

Acknowledgements

This work was supported by grants from the Canadian Institutes of Health Research, the Canadian Natural Sciences and Engineering Research Council to J.I.N., and the University of Manitoba Rady Innovation Fund to JIN and MFJ. These funding sources had no involvement in the design or any other facet of this report. We thank B McLean for excellent technical assistance related to immunofluorescence work, and Dr. M Stobart and N Lavine for help with the design and construction of the shRNA and AAV vectors. We also thank Drs. BW Connors (Brown University, Providence), J O'Brien (University of Texas, Houston) and A. Pereda (Albert Einstein College of Medicine, New York) for helpful discussions concerning the potential functional impact of electrical synapses specifically localized at contacts between mossy fiber terminals and the dendritic shafts of CA3 pyramidal cells.

Conflict of interest

The authors have no conflict of interest to declare.

Author contributions

Work concerning immunofluorescence and related quantification was conducted by DT, AR-B and JMMS; work surrounding shRNA analyses was conducted by DT and BDL; figure preparation was conducted by DT, JMMS, BDL and JIN; electrophysiological approaches and related data collection were undertaken by DT and MFJ; and stereotaxic surgical procedures were conducted by DT and AR-B. All authors contributed to data interpretation and the manuscript was written with input from DT, BDL, MFJ and JIN.

Data statement

The raw data will not be deposited in a public repository due to the complexity of its assembly, but it can be obtained upon request to the corresponding author.

Abbreviations

AJ-nGJ, adherens junction-neuronal gap junction complex; CNS, central nervous system; Cx36, connexin36; E-cadherin, epithelial cadherin; fEPSP, field excitatory postsynaptic potential; LTP, Long term potentiation. MUPP1, multi-PDZ protein-1; N-cadherin, neural cadherin; nGJs, neuronal gap junctions; PBS, phosphate buffer containing 0.9% saline; PDZ, PSD-95, DlgA, ZO-1 domains; TBS, 50 mM Tris-HCl containing 1.5% sodium chloride; TBSTr, 50 mM Tris-HCl containing 1.5% sodium chloride and 0.3% Triton X-100;. ZO-1, zonula occludens-1.

REFERENCES

Acsady L, Kamondi A, Sik A, Freund T, Buzsaki G (1998) GABAergic cells are the major postsynaptic targets of mossy fibers in the rat hippocampus. J Neurosci 18:3386-3403.

Alcami P, Pereda AE (2019) Beyond plastcity: the dynamic impact of electrical synapses on neural circuits. Nature Rev Neurosci 20:253-271.

Amaral DG (1978) A Golgi study of cell types in the hilar region of the hippocampus in the rat. J Comp Neural 182:851-914.

Amaral DG (1979) Synaptic extensions from the mossy fibers of the fascia dentata. Anat Embrol 155:241-251.

Amaral DG and Dent JA (198) Development of the mossy fibers of the dentate gyrus: I. A light and electron microscopic study of the mossy fibers and their expansions. J Comp Neurol 195:51-86.

Basuy R, Taylory MR, Williams ME (2015) The classic cadherins in synaptic specificity. Cell Adhes Migrat 9:193—201.

Bautista W, McCrea DA, Nagy JI (2014) Connexin36 identified at morphologically mixed chemical/electrical synapses on trigeminal motoneurons and at primary afferent terminals on spinal cord neurons in adult mouse and rat. Neuroscience 263:159-180.

Belluardo N, Mud G, Trovato-Salinaro A, Gurun SL, Charollais A, Serre-Beinier V, Amato G, Haefliger JA, Meda P, Condorelli DF (2000) Expression of connexin36 in the adult and developing rat brain. Brain Res 865:121-138.

Bennett MVL (1997) Gap junctions as electrical synapses. J Neurocytol 26:349-366.

Bennett MVL, Zukin SR (2004) Electrical coupling and neuronal synchronization in the mammalian brain. Neuron 41:495-511.

Birukova AA, Zebda N, Fu P, Poroyko V, Cokic I, Birukov KG (2011) Association between adherens junctions and tight junctions via Rap1 promotes barrier protective effects of oxidized phospholipids. J Cell Physiol 226:2052-2062.

Boettner B, Govek EE, Cross J, Van Aelst L (2000) The junctional multidomain protein AF-6 is a binding partner of the Rap1A GTPase and associates with the actin cytoskeletal regulator profilin. Proc Natl Acad Sci (USA) 97:9064-9069.

Boettner B, Herrmann C, Van Aelst L (2001) Ras and Rap1 interaction with AF-6 effector target. Methods Enzymol 332:151-168.

Boudreau RL, Martins I, Davidson BL (2009) Artificial MicroRNAs as siRNA Shuttles: Improved Safety as Compared to shRNAs In vitro and In vivo. Mol thera 17:169-175.

Brown AG, Fyffe RE (1978) The morphology of group Ia afferent fibre collaterals in the spinal cord of the cat. J Physiol 274:111-127.

Caron E (2003) Cellular functions of the Rap1 GTP-binding protein: a pattern emerges. J Cell Sci 116:435-440.

Castanotto D, Sakurai K, Lingeman R, Li H, Shively L, Aagaard L, Soifer H, Gatignol A, Riggs A, Rossi JJ (2007) Combinatorial delivery of small interfering RNAs reduces RNAi efficacy by selective incorporation into RISC. Nuc Acids Res 35:5154-5164.

Chang K, Marran K, Valentine A, Hannon GJ (2013) Creating an miR30-based shRNA vector. Cold Spr Harb Prot 2013:631-635.

Chicurel ME, Harris KM (1992) Three-dimensional analysis of the structure and composition of CA3 branched dendritic spines and their synaptic relationships with mossy fiber boutons in the rat hippocampus. J Comp Neurol 325:169-82.

Chung KH (2006) Polycistronic RNA polymerase II expression vectors for RNA interference based on BIC/miR-155. Nuc acids Res 34:53-53.

Condorelli DF, Belluardo, N, Trovato-Salinaro A, Mudo, G (2000) Expression of Cx36 in mammalian neurons. Brain Res Rev 32:72-85.

Condorelli DF, Trovato-Salinaro A, Mudò G, Mirone MB, Belluardo N (2003) Cellular expression of connexins in the rat brain: neuronal localization, effects of kainate-induced seizures and expression in apoptotic neuronal cells. Eur J Neurosci 18:1807-27.

Connors BW, Long MA (2004) Electrical synapses in the mammalian brain. Annu Rev Neurosci 27:393-418.

Connors, B.W. (2009) Electrical signaling with neuronal gap junctions. In: A.Harris, D.Locke (Eds.), Connexins: A Guide, Humana Press/Springer, pp. 143-164.

Curti S, Hoge G, Nagy JI, and Pereda AE (2012) Synergy between electrical coupling and membrane properties promotes strong synchronization of neurons of the mesencephalic trigeminal nucleus. J. Neurosci 32:4341-4359.

Dale HH (1934) Pharmacology and nerve-ending. Proc Royal Soc Med 28:319–30.

Degen J, Meier C, van der Giessen RS, Sohl G, Petrasch-Parwez E, Urschel S, Dermietzel R, Schilling K, de Zeeuw CI, Willecke K (2004) Expression pattern of lacZ reporter gene representing connexin36 in transgenic mice. J Comp Neurol 473:511-525.

Derangeon M, Spray DC, Bourmeyster N, Sarrouilhe D, Herve J-C (2009) Reciprical influence of connexins and apical junction proteins on their expression and functions. Biochim Biophys Acta 1788:768-778.

Eccles JC, Fatt P, Koketsu K (1954) Cholinergic and inhibitory synapses in a pathway from motor-axon collaterals to motoneurons. J Physiol 126: 524–62.

Evans WH, Martin EM (2002) Gap junctions: structure and function (review). Mol Membr Biol 19:121-136.

Dudek FE, Andrew RD, MacVicar BA, Snow RW, Taylor CP (1983) Recent evidence for and possible significance of gap junctions and electrotonic synapses in the mammalian brain. In: H.H. Jasper, N.M. van Gelder (Eds.), Basic Mechanisms of Neuronal Hyperexcitability, Alan R. Liss, New York, pp. 31– 73.

Fellmann C, Hoffmann T, Sridhar V, Hopfgartner B, Muhar M, Roth M, Lai Dan Y, Barbosa-Inês AM, Kwon Jung S, Guan Y, Sinha N, Zuber J (2013) An Optimized microRNA Backbone for Effective Single-Copy RNAi. Cell Rep 5:1704-1713.

Friedman LG, Benson DL, Huntley GW (2015) Cadherin-based transsynaptic networks in establishing and modifying neural connectivity. Curr Top Dev Biol 112:415–465.

Fukuda J (2009) Network architecture of gap junction-coupled neuronal linkage in the striatum. J Neurosci 29:1235-1243.

Goodenough, D.A. & Paul, D.L. (2009) Gap junctions. Cold Spring Harb Perspect Biol.

Gwyn DG, Nicholson GP, Flumerfelt BA (1977) The inferior olivary nucleus of the rat: A light and electron microscopic study. J Comp Neurol 174:489-520.

Haas JS, Zavala B, Landisman CE (2011) Activity-dependent long-term depression of electrical synapses. Science 334:389-393.

Haas JS, Landisman CE (2012) Bursts modify electrical synaptic strength. Brain Res 1487:140-149.

Hamzei-Sichani F, Kamasawa N, Janssen WGM, Yasumura T, Davidson KGV, Hof PR, Wearne SL, Stewart MG, Young SR, Whittington MA, Rash JE, Roger D. Traub RD (2007) Gap junctions

on hippocampal mossy fiber axons demonstrated by thin-section electron microscopy and freeze–fracture replica immunogold labeling. Proc Natl Acad Sci 104:12548–12553.

Hamzei-Sichani F, Davidson KGV, Yasumura T, Janssen WGM, Wearne SL, Hof PR, Traub RD, Gutierrez R, Ottersen OP, Rash JE (2012) Mixed electrical-chemical synapses in adult rat hippocampus are primarily glutamatergic and coupled by connexin36. Front Neuroant 6:1-26.

Harris TJC, Tepass U (2010) Adherens junctions: from molecules to morphogenesis. Nat Rev Mol Cell Biol 11:502-514.

Helbig I , Sammler E, Eliava M, Bolshakov AP, Rozov A, Bruzzone R, Monyer H, Hormuzdi SG (2010) In vivo evidence for the involvement of the carboxy terminal domain in assembling connexin 36 at the electrical synapse. Mol Cell Neurosci 45:47-58.

Hertig CM, Eppenberger-Eberhardt M, Koch S, Eppenberger HM (1996) N-cadherin in adult rat cardiomyocytes in culture. I. Functional role of N-cadherin and impairment of cell-cell contact by a truncated N-cadherin mutant. J Cell Sci 109:1-10.

Holcman D, Yuste R (2015) The new nanophysiology: regulation of ionic flow in neuronal subcompartments. Nat Rev Neurosci 16:685-692.

Honda T, Sakisaka T, Yamada T, Kumazawa N, Hoshino T, Kajita M, Kayahara T, Ishizaki H, Tanaka-Okamoto M, Mizoguchi A, Manabe T, Miyoshi J, Takai Y (2006) Involvement of nectins in the formation of puncta adherentia junctions and the mossy fiber trajectory in the mouse hippocampus. Mol Cell Neurosci 31:315-325.

Hormuzdi SG, Pais I, LeBeau FEN, Towers SK, Rozov A, Buhl EH, Whittington MA, Monyer H (2001) Impaired electrical signaling disrupts gamma frequency oscillations in connexin36-deficient mice. Neuron 31:487-495.

Hormuzdi SG, Filippov MA, Mitropoulon G, Monyer H, Bruzzone R (2004) Electrical synapses: a dynamic signaling system that shapes the activity of neuronal networks. Biochem Biophys Acta 1662:113-137.

Inagaki M, Irie K, Deguchi-Tawarada M, Ikeda W, Ohtsuka T, Takeuchi M, Takai Y (2003) Nectin-dependent localization of ZO-1 at puncta adhaerentia junctions between the mossy fiber terminals and the dendrites of the pyramidal cells in the CA3 area of adult mouse hippocampus. J Comp Neurol 460:514-524.

Irie K, Shimizu K, Sakisaka T, Ikeda W, Takai Y (2004) Roles and modes of action of nectins in cell-cell adhesion. Semin Cell Dev Biol 15:643-656.

Itoh M, Nagafuchi A, Yonemura S, Kitani-Yasuda T, Tsukita S, Tsukita S (1993) The 220-kD protein colocalizing with cadherins in non-epithelial cells is identical to ZO-1, a tight junction-associated protein in epithelial cells: cDNA cloning and immunoelectron microscopy. J Cell Biol 121:491-502.

Ishizuka N, Cowan WM, Amaral DB (1995) A quantitative analysis of the dendritic organization of pyramidal cells in the rat hippocampus. J Comp Neurol 362:17-45.

Irie K, Shimizu K, Sakisaka T, Ikeda W, Takai Y (2004) Roles and modes of action of nectins in cell-cell adhesion. Semin Cell Dev Biol 15:643-656.

Ixmatlahua DJ, Vizcarra B, Gómez-Lira G, Romero-Maldonado I, Ortiz F, Rojas-Piloni G, Gutiérrez R (2020) Neuronal glutamatergic network electrically wired with silent but activatable gap junctions. J Neurosci 40:4661-4672.

Kamasawa N, Furman CS, Davidson KGV, Sampson JA, Magnie AR, Gebhardt BR, Kamasawa M, Yasumura T, Zumbrunnen JR, Pickard GE, Nagy JI, Rash JE (2006) Abundance and ultrastructural diversity of neuronal gap junctions in the OFF and ON sublaminae of the inner plexiform layer of rat and mouse retina. Neuroscience 142:1093-1117.

Katsumaru H, Kosaka T, Heizmann CW, Hama K (1988) Gap junctions on GABAergic neurons containing the calcium-binding protein parvalbumin in the rat hippocampus (CA1 region). Exp Brain Res 72:363-370.

Keane RW, Mehta P, Rose B, Honig LS, Loewenstein WR, Rutishauser U (1988) Neural differentiation, NCAM-mediated adhesion, and gap junctional communication in neuroectoderm: A study in vitro. J Cell Biol 106:1307-1319.

Kennedy MB (2013) Synaptic signaling in learning and memory. Cold Spring Harb Perspect Biol 8:1-16.

Kooistra MRH, Bube N, Bos JL (2006) Rap1: a key regulator in cell-cell junction formation. J Cell Sci 120:17-22.

Korn H, Sotelo C, Crepel F (1973) Electrotonic coupling between neurons in the lateral vestibular nucleus. Exp Brain Res 16:255-275.

Kosaka T (1983) Gap junctions between non-pyramidal cell dendrites in the rat hippocampus (CA1 and CA3 regions) Brain Res 271:157-161.

Kosaka T, Hama K (1985) Gap junctions between non-pyramidal cell dendrites in the rat hippocampus (CA1 and CA3 regions): a combined Golgi-electron microsc opy study. J Comp Neurol 231:150–161.

Kothmann WW, Massey SC, O'Brien J (2009) Dopamine-stimulated dephosphorylation of Connexin36 mediates AII amacrine cell uncoupling. J Neurosci 29:14903-14911.

Li X, Olson C, Lu S, Kamasawa N, Yasumura T, Rash JE, Nagy JI (2004) Neuronal connexin36 association with zonula occludens-1 protein (ZO-1) in mouse brain and interaction with the first PDZ domain of ZO-1. Eur J Neurosci 19:2132-2146.

Li J, Patel VV, Kostetskii I, Xiong Y, Chu AF, Jacobson JT, Yu C, Morley GE, Molkentin JD, Radice GL (2005) Cardiac-specific loss of N-cadherin leads to alteration in connexins with conduction slowing and arrhythmogenesis. Circ Res 97:474-481.

Li X, Lynn BD, Nagy JI (2012) The effector and scaffolding proteins AF6 and MUPP1 interact with connexin36 and localize at gap junctions that form electrical synapses in rodent brain. Eur J Neurosci 35:166-181.

Linnemann T, Geyer M, Jaitner BK, Block C, Kalbitzer HR, Wittinghofer A, Herrmann C (1999) Thermodynamic and kinetic characterization of the interaction between the Ras binding domain of AF-6 and members of the Ras subfamily. J Biol Chem 274:13556-13562.

Lynn BD, Li X, Nagy JI (2012) Under construction: Building the macromolecular superstructure and signaling components of an electrical synapse. J Membr Biol 245:303-317.

Lynn BD, Li X, Hormuzdi SG, Griffiths, EK, McGlade CJ, Nagy JI (2018) E3 ubiquitin ligases LNX1 and LNX2 localize at neuronal gap junctions formed by connexin36 in rodent brain and molecularly interact with connexin36. Eur J Neurosi 48:3062-3081.

Majima T, Ogita H, Yamada T, Amano H, Togashi H, Sakisaka T, Tanaka-Okamoto M, Ishizaki H, Miyoshi J, Takai Y (2009) Involvement of afadin in the formation and remodeling of synapses in the hippocampus. Biochem Biophys Res Commun 385:539-544.

Mandai K, Nakanishi H, Satoh A, Obaishi H, Wada M, Nishioka H, Itoh M, Mizoguchi A, Aoki T, Fujimoto T, Matsuda Y, Tsukita S, Takai Y (1997) Afadin: A novel actin filament-binding protein with one PDZ domain localized at cadherin-based cell-to-cell adherens junction. J Cell Biol 139:517-528.

Mathy A, Clark BA, Hausser M (2014) Synaptically induced long-term modulation of electrical coupling in the inferior olive. Neuron 81:1290-1296.

McBride JL, Boudreau RL, Harper SQ, Staber PD, Monteys AM, Martins I, Gilmore BL, Burstein H, Peluso RW, Polisky B, Carter BJ, Davidson BL (2008) Artificial miRNAs mitigate shRNA-mediated toxicity in the brain: Implications for the therapeutic development of RNAi. Proc Natl Acad Sci 105:5868-5873.

Mercer A, Bannister P, Thomson AM (2006) Electrical coupling between pyramidal cells in adult cortical regions. Brain Cell Biol 35:13-27.

Meyer RA, Laird DW, Revel J-P, Johnson RG (1992) Inhibition of gap junction and adherens junction assembly by connexin and A-CAM antibodies. J Cell Biol 119:179-189.

Miyahara M, Nakanishi H, Takahashi K, Satoh-Horikawa K, Tachibana K, Takai Y (2000) Interaction of nectin with afadin is necessary for its clustering at cell-cell contact sites but not for its cis dimerization or trans interaction. J Biol Chem 275:613-618.

Mizoguchi A, Nakanishi H, Kimura K, Matsubara K, Ozaki-Kuroda K, Katata T, Honda T, Kiyohara Y, Heo K, Higashi M, Tsutsumi T, Sonoda S, Ide C, Takai Y (2002) Nectin: an adhesion molecule involved in formation of synapses. J Cell Biol 156:555-565.

Mori M, Rikitake Y, Mandai K, Takai Y (2014) Roles of nectins and nectin-like molecules in the nervous system. Adv Neurobiol 8:91-116.

Nagy JI, Dudek FE, Rash JE (2004) Update on connexins and gap junctions in neurons and glia in the mammalian nervous system. Brain Res Rev 47:191-215.

Nagy JI (2012) Evidence for connexin36 localization at hippocampal mossy fiber terminals suggesting mixed chemical/electrical transmission by granule cells. Brain Res 1487:107-122.

Nagy JI, Bautista W, Blakley B, Rash JE (2013) Morphologically mixed chemical-electrical synapses formed by primary afferents in rodent vetibular nuclei as revealed by immunofluorescence detection of connexin36 and vesicular glutamate transporter-1. Neuroscience 252:468-488.

Nagy JI, Pereda AE, Rash JE (2018) Electrical synapses in mammalian CNS: Past eras, present focus and future directions. Biochim Biophys Acta 1860:102-123.

Nagy JI, Lynn BD (2018) Structural and intermolecular associations between connexin36 and protein components of the adherens junction-neuronal gap junction complex. Neuroscience 384:241-261.

Nagy JI, Pereda AE, Rash JE (2019) On the occurrence and enigmatic functions of mixed (chemical plus electrical) synapses in the mammalian CNS. Neurosci Lett 695:53-64.

Nishioka H, Mizoguchi A, Nakanishi H, Mandai K, Takahashi K, Kimura K, Satoh-Moriya A, Takai Y (2000) Localization of l-afadin at puncata adhaerentia-like junctions between the mossy fiber terminals and the dendritic trunks of pyramidal cells in the adult mouse hippocampus. J Comp Neurol 424:297-306.

O'Brien J (2014) The ever-changing electrical synapse. Curr Opin Neurobiol 29:64-72.

O'Brien J (2019) Design principles of electrical synaptic plasticity. Neurosci Lett 4-11.

Palmiter RD, Cole TB, Quaife CJ, Findley SD (1999) ZnT3, a putative transporter of zinc into synaptic vesicles. Proc Natl Acad Sci 93:14934-14939.

Pereda AE, Curti S, Hoge G, Cachope R, Flores CE, Rash JE (2013) Gap junction-mediated electrical transmission: Regulatory mechanisms and plasticity. Biochim Biophys Acta 1828:134-146.

Pereda AE (2014) Electrical synapses and their functional interactions with chemical synapses. Nat Rev Neurosci 15:250-263.

Peters A, Palay SL, Webster HD (1991) The fine structure of the nervous system: Neurons and their supporting cells. Third Edition. Oxford University Press.

Pivovarova NB, Pozzo-Miller LD, Hongpaisan J, Brian Andrews (2002) Correlated calcium uptake and release by mitochondria and endoplasmic reticulum of CA3 hippocampal dendrites after afferent synaptic stimulation. J Neurosci 22:10653-10661.

Posluszny A (2014) The contribution of electrical synapses to field potential oscillations in the hippocampal formation. Front Nerual Cir 8:1-13.

Rash JE, Staines WA, Yasumura T, Pate, D, Hudson CS, Stelmack GL, Nagy J. (2000) Immunogold evidence that neuronal gap junctions in adult rat brain and spinal cord contain connexin36 (Cx36) but not Cx32 or Cx43. Proc Natl Acad Sci 97:7573-7578.

Rash JE, Yasumura T, Dudek FE, Nagy JI (2001) Cell-specific expression of connexins, and evidence for restricted gap junctional coupling between glial cells and between neurons. J Neurosci 21:1983-2000.

Rash JE, Pereda A, Kamasawa N, Furman CS, Yasumura T, Davidson KGV, Dudek FE, Olson C, Li X, Nagy JI (2004) High-resolution proteomic mapping in the vertebrate central nervous system: Close proximity of connexin35 to NMDA glutamate receptor clusters and co-localization of connexin36 with immunoreactivity for zonula occludens protein-1 (ZO-1). J Neurocytol 33:131-151.

Rash JE, Olson CO, Pouliot WA, Davidson KGV, Yasumura T, Furman CS, Royer S, Kamasawa N, Nagy JI, Dudek FE (2007a) Connexin36, miniature neuronal gap junctions, and limited electrotonic coupling in rodent suprachiasmatic nucleus (SCN). Neuroscience 149:350-371.

Rash JE, Olson CO, Davidson KGV, Yasumura T, Kamasawa N, Nagy JI (2007b) Identification of connexin36 in gap junctions between neurons in rodent locus coeruleus. Neuroscience 147:938-956.

Rollenhagen A, Satzler K, Rodriguez EP, Jonas P, Frotscher M, Lubke JHR (2007) Structural determinants of transmission at large hippocampal mossy fiber synapses. J Neursci 27:10434-10444.

Ramon y Cajal S (1911) Histologie de systeme nerveux de l'homme et des vertebres tomme II.Paris; Maloine.

Rubio ME, Nagy JI (2015) Connexin36 expression in major centers of the auditory system in the CNS of mouse and rat: evidence for neurons forming purely electrical synapses and morphologically mixed synapses. Neuroscience. 303:604-629.

Scharfman HE, Kunkel DD, Schwarzkroin PA (1990) Synaptic connections of dentate granule cells and hilar neurons: Results of paired intracellular recordings and intracellular horseradish peroxidase injections. Neuroscience 37:693-707.

Schmitz, D., Schuchmann, S., Fisahan, A., Draguhn, A., Buhl, E.H., Petrasch-Parwez, E., Dermietzel, R., Heinemann, U., & Traub, R.D. (2001) Axo-axonal coupling: A novel mechanism for ultrafast neuronal communication. *Neuron*, **31,** 831-840.

Segretain D, Falk MM (2004) Regulation of connexin biosynthesis, assembly, gap junction formation and removal. Biochim Biophys Acta 1662:3-21.

Shapiro L, Weis WI (2009) Structure and biochemistry of cadherins and catenins. Cold Spring Harb Perspect Biol 1:a003053.

Shaw RM, Fay AJ, Puthenveedu MA, von Zastrow, M, Jan YN, Jan LY (2007) Microtubule plus-end-tracking proteins target gap junctions directly from the cell interior to adherens junctions. Cell 126:547-560.

Shigematsu N, Nishi A, Fukuda T (2019) Gap junctions interconnect different subtypes of parvalbumin-positive interneurons in barrels and septa with connectivity unique to each subtype. Cereb Cortex 29:1414-1429.

Sloper JJ, Powell TPS. (1978) Gap junctions between dendrites and somata of neurons in the primate sensori-motor cortex. Proc R Soc Lond B 203:39-47.

Somekawa S, Fukuhura S, Nakaoka Y, Fujita H, Saito Y, Mochizuki N (2005) Enhanced functional gap junction neoformation by protein kinase A-dependent and Epac-dependent signals downstream of cAMP in cardiac myocytes. Circ Res 97:655-662.

Sotelo C, Palay SL (1970) The fine structure of the lateral vestibular nucleus in the rat. II. Synaptic organization. Brain Res 18:93-115.

Spruston N (2008) Pyramidal neurons: dendritic structure and synaptic integration. Nat Rev Neurosci 9:206-221.

Stocker AM, Chenn A (2015) The role of adherens junctions in the developing neocortex. Cell Adhes Migra 9:167-174.

Sun HS, Jackson MF, Martin LJ, Jansen K, Teves L, Cui H, Kiyonaka S, Mori Y, Jones M, Forder JP, Golde TE, Orser BA, MacDonald JF, Tymianski M (2009) Suppression of hippocampal TRPM7 protein prevents delayed neuronal death in brain ischemia. Nat Neurosci 12:1300–1307.

Takahashi K, Nakanishi H, Miyahara M, Mandai K, Satoh K, Satoh A, Nishioka H, Aoki J, Nomoto A, Mizoguchi A, Takai Y (1999) Nectin/PRR: an immunoglobulin-like cell adhesion molecule recruited to cadherin-based adherens junctions through interaction with Afadin, a PDZ domain-containing protein. J Cell Biol 145:539-549.

Takai Y, Nakanishi H (2003) Nectin and afadin: novel organizers of intercellular junctions. J Cell Sci 116:17-27.

Takai Y, Ikeda W, Ogita H, Rikitake Y (2008) The immunoglobulin-like cell adhesion molecule nectin and its associated protein afadin. Annu Rev Cell Dev Biol 24:309-342.

Traub RD, Whittington MA (2010) Cortical Oscillations in Health and Disease. Oxford University Press, New York.

Turecek J, Yuen GS, Han VZ, Zeng X-H, Bayer U, Welsh JP (2014) NMDA receptor activation strengthens weak electrical coupling in mammalian brain. Neuron 81:1375-1388.

Urschel S, Hoher T, Schubert T, Alev C, Sohl G, Worsdorfer P, Asahara T, Dermietzel R, Weiler R, Willecke K (2006) Protein kinase A-mediated phosphorylation of connexin36 in mouse retina results in decreased gap junctional communication between AII amacrine cells. J Biol Chem 281: 33163-33171.

Wellershaus A, Degen J, Deuchars J, Theis M, Charollaisd A, Cailled D, Gauthierd B, Janssen-Bienholde U, Sonntaga S, Herrera H, Meda P, Willecke K (2008) A new conditional mouse mutant reveals specific expression and functions of connexin36 in neurons and pancreatic beta-cells. Exp Cell Res 314:997-1012

Wenzel HJ, Cole TB, Born DE, Schwartzkroin PA, Palmiter RD (1997) Ultrastructural localization of zinc transporter-3 (ZnT-3) to synaptic vesicle membranes within mossy fiber boutons in the hippocampus of mouse and monkey. Proc Natl Acad Sci 94:12676-12681.

Vivar C, Traub RD, Gutiérrez R (2012) Mixed electrical-chemical transmission between hippocampal mossy fibers and pyramidal cells. Eur J Neurosci 35:76–82.

Xie YF, Belrose JC, Lei G, Tymianski M, Mori Y, MacDonald JF, Jackson MF (2011) Dependence of NMDA/GSK-3b mediated metaplasticity on TRPM2 channels at hippocampal CA3-CA1 synapses. Mol Brain 4:1-9.

Yang K, Lei G, Xie Y-F, MacDonald JF, Jackson MF (2014) Differential regulation of NMDAR and NMDARGÇÉmediated metaplasticity by anandamide and 2-AG in the hippocampus. Hippocampus 24:1601-1614.

Yang K, Trepanier C, Sidhu B, Xie Y-F, Li H, Lei G, Salter MW, Orser BA, Nakazawa T, Yamamoto T, Jackson MF, MacDonald JF (2012) Metaplasticity gated through differential regulation of GluN2A versus GluN2B receptors by Src family kinases. EMBO Journal 31:805-816.

Zhu X, Santat LA, Chang M, Liu J, Zavzavadjian JR, Wall EA, Kivork C, Simon MI, Fraser IDC (2007) A versatile approach to multiple gene RNA interference using microRNA-based short hairpin RNAs. BMC Mol Biol 8:98-98.

Table 1. **Primary antibodies used for immunofluorescence labelling, with type, species in which they were produced, designated catalogue number by supplier, dilution employed in this study and commercial source**

Antibody	Type	Species	Designation	Dilution	Source*
Cx36	monoclonal	mouse	39-4200	2-4 μg/ml	ThermoFisher
ZnT3	polyclonal	guinea pig	197 004	1:200	Synaptic Systems
parvalbumin	polyclonal	guinea pig	195 004	1:100	Synaptic Systems
N-cadherin	polyclonal	sheep	AF6426	2 μg/ml	R & D Systems
nectin-1	polyclonal	rabbit	SC-28639	1:50	Santa Cruz
MAP2	polyclonal	chicken	AB2138173	1:600	EnCor Biotech
ZO-1	polyclonal	rabbit	61-7300	4 μg/ml	ThermoFisher

*Addresses of commercial sources are as follows: ThermoFisher, Rockford, IL, USA; Synaptic Systems, , Goettingen, Germany; R & D Systems, Minneapolis, MN, USA; Santa Cruz, Dallas, TX, USA; EnCor Bioechnology Inc, Gainesville, FL, USA.

Table 2. List of shRNA sequences tested for targeting rat Cx36

shRNA	Target sequence (5’ – 3’)
1	GTTAAC-GGAGACGGTGTACGATGATGA-TCAAGAG-TCATCATCGTACACCGTCTCC-TTTTTT-CTCGAG
2	GTTAAC-GCATTTGTGTGGTGCTCAATC-TCAAGAG-GATTGAGCACCACACAAATGC-TTTTTT-CTCGAG
3	GTTAAC-GCCTTTCCCATCTCCCATATA-TCAAGAG-TATATGGGAGATGGGAAAGGC-TTTTTT-CTCGAG
4	GTTAAC-AGAGACCCTGCTGAGTCTATA-TCAAGAG-TATAGACTCAGCAGGGTCTCT-TTTTTT-CTCGAG
5	GTTAAC-CAGATTGCTTAGAGGTTAAAG-TCAAGAG-CTTTAACCTCTAAGCAATCTG-TTTTTT-CTCGAG
6	GTTAAC-GGTGGGCCAGTACTTTCTATA-TCAAGAG-TATAGAAAGTACTGGCCCACC-TTTTTT-CTCGAG
Scrambled	GTTAAC-AATTCTCCGAACGTGTCACGT-TCAAGAG-ACGTGACACGTTCGGAGAATT-TTTTTT-CTCGAG

Table 3. Expression of Cx36 in principal cells of the hippocampus as determined by various methods

	CA3 pyramidal cells		dentate gyrus granule cells		
species, method	dorsal hippocampus	ventral hippocampus	dorsal hippocampus	ventral hippocampus	references
rat ISH	positive	????	negative	????	Belluardo et al., 2000 Condorelli et al., 2000 Condorelli et al., 2003
mouse lacZ reporter	negative	????	negative	????	Degen et al., 2004
mouse ISH	negative	????	negative	????	Hormuzdi et al., 2001
mouse Cx36-eGFP	negative	????	negative	????	Helbig et al., 2010
Mouse, Cx36-CFP	negative	????	negative	????	Wellershaus et al., 2008
IF, Cx36	negative	positive	negative	negative	Nagy, 2012

ISH, in situ hybridization for Cx36 mRNA. IF, immunofluorescence labelling of Cx36. Cx36-eGFP and Cx36-CFP refer to reporter expression of enhanced green fluorescent protein and cyan fluorescent protein driven by the Cx36 promoter. The question marks indicate that the cited references showed images of dorsal hippocampus, and do not indicate whether the ventral hippocampus was also examined.

Figure legends

Fig. 1. Simplified depiction of the miR-30 based targeting constructs used for production of scrambled and Cx36-specific shRNA viral particles. **(A)** Molecular elements contained in the miR-30 based Cx36 targeting construct cassette used for AAV mediated shRNA expression. This cassette contains AAV8 ITRs (pink) at both 5' and 3' ends, a CaMKIIa promoter (yellow) located upstream of the two shRNA encoding sequences (red) that are followed by an expression construct encoding eGFP (green), a Woodchuck hepatitis virus post transcriptional regulatory element (WPRE; gray) and a human growth hormone polyadenylation signal (hGHpA; aqua). In this cassette, the expression of both eGFP and shRNAmir are driven by the same excitatory-cell-specific CaMKIIa promoter. **(B)** Image of plasmid pJN3 containing the targeting cassette of the Cx36-specific shRNA sequence. **(C)** Blots confirming the integrity of the SmaI sites as determined by SmaI digestion to confirm ITR integrity and selection of correct clones following cloning of the shRNA cassette.

Fig. 2. Association of Cx36 with ZnT3+ mossy fiber terminals in adult rat hippocampus. **(A)** Transverse section of the adult rat posterior hippocampus showing low magnification overview of immunofluorescence labelling for ZnT3 in the hippocampal stratum lucidum (arrows) and hilus (arrowheads) regions. **(B)** Higher magnification of the boxed area in A, showing a high density of ZnT3+ mossy fiber terminals (arrows) in the stratum lucidum. **(C)** Double immunofluorescence labelling showing a moderate density of Cx36-puncta in the stratum lucidum of the posterior hippocampus (C1) and their association with mossy fiber terminals in this region (C2, arrows). **(D)** Confocal magnification of double labelling in the posterior stratum lucidum showing clusters of Cx36-puncta (D1, arrows) co-localized with labelling for ZnT3+ mossy fiber terminals (D2, arrows).

Fig. 3. Cx36-puncta size distribution in regions of adult rat ventral hippocampus. (**A-C**) Comparison of density and configurations of Cx36-puncta in the ventral stratum lucidum where puncta are of moderate density and often appear in clusters (A, arrows) and in the ventral stratum radiatum of the CA1 region (B) and CA3 region (B, inset) where puncta are of generally large size, appear in linear arrays (B, arrows) and are localized to parvalbumin+ dendrites (C, arrows). (D) Frequency of Cx36-puncta diameters in the stratum lucidum (SL) *vs.* the stratum radiatum (SR), showing a shift to a larger diameter of those in the stratum radiatum.

Fig. 4. Paucity of Cx36-puncta among axon collaterals of mossy fibers in the ventral hippocampal hilus. **(A)** Double immunofluorescence labelling in a central region of the hilus in the ventral hippocampus showing a high concentration of ZnT3+ terminals formed by axon collaterals of mossy fibers in this region (A1, arrows) and the same field showing sparse Cx36-puncta (A2, arrows), with an absence of Cx36-puncta association with ZnT3+ terminals (A3). **(B)** A field in the same section as imaged in A and serving as positive control for labelling of Cx36 by showing the typically high density of Cx36-puncta (B1, arrows) in the CA3c region of the stratum lucidum and the typical localization of these puncta to ZnT3+ mossy fiber terminals (B2, arrows). **(C)** Image of a presumptive mossy cell (C1, asterisk) lying at the border between the ventral blade of the granule cell layer and the hilus, showing ZnT3+ terminals on the mossy cell soma (C1, arrows) and very sparse labelling for Cx36 in the same field (C2, arrows). ZnT3+ terminals on the mossy cell lack association with Cx36-puncta (C3, arrows).

Fig. 5. Association of Cx36 with N-cadherin+ adherens junctions at mossy fiber terminals in adult rat posterior hippocampus. **(A,B)** Low magnification overview of N-cadherin distribution in the posterior hippocampus (A), and magnification of the boxed area in A showing a high density of N-cadherin+ adherens junctions in the stratum lucidum (arrows). (C1-C4) The same field showing confocal magnification of labelling for N-cadherin, seen as linear strands in on edge views (C1, arrows) and as discs in *en face* views (C1, arrowheads), in a field containing Cx36-puncta localized to ZnT3+ mossy fiber terminals (C2, arrows). N-cadherin+ adherens junctions are localized to ZnT3+ mossy fiber terminals (C3, arrows) and Cx36-puncta are seen localized at or adjacent to these junctions (C4, arrows).

Fig. 6. Association of Cx36 with nectin-1+ adherens junctions at mossy fiber terminals in adult rat posterior hippocampus. **(A)** Low magnification overview of nectin-1 distribution in the posterior hippocampus, showing immunofluorescence labelling of nectin-1 highly concentrated in the stratum lucidum (A1, arrows) and co-distributed with Cx36-puncta and ZnT3+ mossy fiber terminals in this region (A3, arrows). **(B)** Higher confocal magnification of a region in stratum lucidum similar to that in A, showing the vast majority of Cx36-puncta overlapping with or immediately adjacent to nectin+ adherens junctions (B1, arrows) that are localized to ZnT3+ mossy fiber terminals (B2, arrows).

Fig. 7. Configuration of Cx36-puncta and adherens junction in relation to CA3 pyramidal cell dendrites. **(A)** Triple immunofluorescence labelling in the CA3b region of the stratum lucidum

showing numerous Cx36-puncta associated with N-cadherin+ adherens junctions that are localized to CA3 pyramidal cell dendrites labelled for the microtubule marker MAP2 (arrows). **(B)** Higher magnification of the boxed area in A, showing large MAP2+ pyramidal cell dendrites (arrowheads) with an N-cadherin+ adherens junction viewed on-edge along its upper border and several Cx36-puncta localized to the junction (B1, arrows), where the Cx36-puncta are shown in overlay with only the red/green channels (B2, arrows). **(C)** Triple labelling in the CA3c region of the stratum lucidum showing multiple Cx36-puncta co-distributed with N-cadherin+ adherens junctions localized to both the upper and lower edges of a large MAP2+ pyramidal cell dendrite (C1, arrows). The same image is shown with overlay of only the red/green channels and overlay of only the red/white channels to visualize Cx36-puncta association with the dendrite (C2, arrows) and with N-cadherin (C3 arrows). **(D)** Triple labelling in the CA3c stratum lucidum showing a N-cadherin+ adherens junction viewed *en-face* and overlaying a MAP2+ dendrite (C1, arrows), with clusters of Cx36-puncta (D2, arrows) closely associated with the N-cadherin+ junction (D3, arrows).

Fig. 8. Schematic diagram illustrating locations of the mixed synaptic components for neurotransmission from mossy fiber terminals to CA3 pyramidal cell dendrites. The chemical synapse component is localized on the spine head and the electrical component consisting of Cx36-containing gap junctions closed associated with adherens junctions at the AJ-nGJ complex is localized at contacts between the mossy fiber terminal and dendritic shaft of the CA3 pyramidal cell.

Fig. 9. Relationships of Cx36, N-cadherin and ZO-1 at morphologically mixed synapses in the LVN, MNTB and PVCN of adult mouse. **(A)** Low magnification of the LVN, showing immunofluorescence labelling associated with three neuronal somata (not counterstained, but marked by asterisks) and their initial dendrites (arrowheads) decorated with Cx36-puncta co-localized with N-cadherin and ZO-1, seen as white in overlay of triple labelling (arrows). **(B)** Higher magnification of the boxed area at a neuronal somata in A, showing individual labelling of Cx36-puncta (B1, arrows), N-cadherin (B2, arrows) and ZO-1 (B3, arrows), and with overlays showing near total co-localization of Cx36-puncta with ZO-1 (B4, arrows), substantial co-localization of N-cadherin with ZO-1 (B5, arrows) and Cx36-puncta partially overlapping with or adjacent to labelling of N-cadherin (B6, arrows). **(C,D)** Overlay image of double labelling for Cx36 and N-cadherin with blue fluorescence counterstain in the MNTB, showing neuronal somata (C, large arrows; boxed area in C magnified in D) displaying Cx36-puncta associated with N-

cadherin (small arrows) and patches of labelling for N-cadherin lacking association with Cx36-puncta (double arrowheads). **(E)** Overlay image showing Cx36-puncta association with N-cadherin on the somata (arrows) and initial dendrites (arrowheads) of a blue fluorescence counterstained octopus neuron in the PVCN, with the boxed area shown at higher magnification in the inset.

Fig. 10. Relationships of Cx36 and N-cadherin at morphologically mixed synapses in the spinal cord and red nucleus. **(A)** Double immunofluorescence labelling of Cx36 and N-cadherin with blue fluorescence Nissl counterstain in the lumbar spinal cord ventral horn of adult rat, showing overlay image of Cx36-puncta associated with labelling of N-cadherin on the somata (arrows) and initial dendrites (arrowheads) of a large motoneuron (asterisk), with inset of boxed area showing individual labelling for Cx36 (red) and N-cadherin (green) (arrows) that is magnified in overlay (arrow). **(B)** Double immunofluorescence labelling of Cx36 and N-cadherin with blue fluorescence Nissl counterstain in the red nucleus of adult mouse, with overlay image showing widespread association of Cx36-puncta with N-cadherin on the surface of large neuronal somata (large arrows). **(C)** Magnification of the single neuronal somata (asterisk) in the boxed area of B (rotated clockwise by 90 degrees), showing nearly all somal Cx36-puncta (C1, arrows) associated with labelling of N-cadherin (C2, arrows), as seen in overlay (C3, arrows), and separate labelling of N-cadherin devoid of association with Cx36 (arrowhead).

Fig. 11. Properties of mossy fiber field synaptic responses in transverse slices randomly selected along the dorsal-ventral long axis. **(A)** Schematic of a hippocampal slice showing the positioning of stimulating (stim) and recording (rec) electrodes. **(B)** Plot showing frequency facilitation at mossy fiber synapses, where increased stimulation frequency from low (0.05 Hz) to moderate (1 Hz) stimulation produced a pronounced increase in fEPSP amplitude. Traces represent averaged response (of last 10 sweeps) when stimulated at 0.05 Hz (black) and at 1 Hz (green). **(C)** Induction of LTP at mossy fiber synapses is independent of NMDAR activation, as shown by the persistence of mossy fiber LTP induction after blockade of NMDARs with the antagonist APV. At the end of the LTP induction protocol, the large degree of inhibition (75-80%) of the mossy fiber response by the mGluR2 agonist DCG-IV verified that stimulation evoked responses originated from activation of mossy fiber synapse. Traces represent average of the last 10 sweeps of baseline response recorded in aCSF (black) and post-application of DCG-IV (red).

Fig 12. Short-term and long-term synaptic plasticity in dorsal *vs.* ventral rat hippocampal slices. **(A)** DIC images of hippocampus sectioned perpendicular to its long axis, showing dorsal (A1) and ventral (A2) hippocampal slices, with the recording electrode appearing black. Traces show field responses recorded from dorsal (A3, green) and ventral (A4, black) hippocampal slices during the stimulation parameters described in Figure 11. Responses evoked in slices display a comparatively large positivity in ventral *vs.* dorsal hippocampal slices. This positivity in the baseline response (A5, black) remained after frequency facilitation (A5, blue) and LTP (A5, green) tetanus was given. Application of bicuculline (0.5μM) had no effect in the positivity observed in the baseline (A6, black) as well as the frequency facilitation (A6, blue) responses in the ventral hippocampal slices. **(B)** Frequency facilitation in dorsal and ventral hippocampal slices, showing a similar degree of facilitation in the two regions. **(C)** LTP in dorsal and ventral hippocampal slices, showing a higher degree of potentiation in the ventral *vs.* dorsal hippocampus. Arrows indicate onset of high frequency stimulation (2 trains of 100 Hz at 1 sec duration separated by 20 sec) given after recording baseline for 20 min. **(D)** Averaged fEPSP amplitude measured from the last 5 min of LTP in dorsal and ventral hippocampal slices, showing significantly greater potentiation in the ventral slices. * $p < 0.05$, unpaired Student's t test with Welch's correction and error bars representing standard error of the mean. Frequency facilitation was measured in dorsal hippocampus using 12 slices taken from 10 animals and in ventral hippocampus using 13 slices taken from 9 animals. LTP was measured in dorsal hippocampus using 11 slices taken from 9 animals and in ventral hippocampus using 11 slices taken from 9 animals.

Fig. 13. Immunoblot showing shRNA mediated knockdown of Cx36 in N2A cells. **(A)** Detection of Cx36 with Cx36 antibody 51-6300 in blots of cell lysates taken from cultures of N2A cells transfected with plasmid expressing Cx36 and separate cultures each co-transfected with one of the Cx36 targeted shRNAs indicated (lanes 4-9). Comparatively similar intensities of the Cx36 band is detected in lysates of control cultures transfected with Cx36 alone (lane 1) or co-transfected with Cx36 and either empty pLB vector (lane 2) or scrambled non-targeting shRNA (lane 3), indicating that empty vector or the scrambled shRNA had little effect on Cx36 expression. The shRNAs targeting Cx36 showed varying Cx36 band intensities, with lanes 4, 5 and 8 displaying the largest reductions of Cx36. The two shRNA sequences chosen for production of miR-30 based Cx36 knockdown construct are indicated by asterisks. **(B)** The blot depicted in A was stripped and probed with antibody against β-actin, and indicates equal protein loading among the lanes.

Supplementary fig.1. Whole-cell dye injections in rat hippocampal slices. **(A)** Images of mossy fiber collaterals when a granule cell (not shown) is injected with biocytin dye. The injected cell and its dye-filled processes are visualized after immunolabelling with streptavidin Cy3 (red). Images A1,A2,A3 are taken from adjacent fields. The dye injected in this particular granule cell was seen to be labelling small and larger varicosities along the parent axon. The larger varicosities had a diameter of 5-6 µm, resembling that of a mossy fiber bouton. **(B)** Higher magnification of a presumed mossy fiber bouton when a CA3 pyramidal neuron was injected with neurobiotin. The injected pyramidal neuron cell body was not recovered after the injection. Also, the CA3 neuron was not injected with dextran 10,000 (negative control), which constrained the confirmation of dye-coupling. Images B1,B2 are adjacent mossy fiber boutons that got filled when CA3 pyr neuron was injected. **(C)** Low magnification of a biocytin injected CA3 pyramidal cell body and its processes in a 300µm hippocampal slice. **(D)** A purkinje neuron in the cerebellum and its processes when filled with neurobiotin dye and visualized under confocal microscope. The cell soma and all its dendritic trees were seen to be labelled with dye.

A

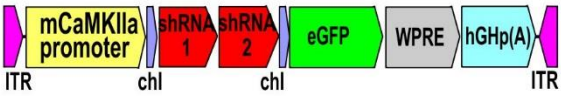
mCaMKIIa promoter
shRNA 1
shRNA 2
eGFP
WPRE
hGHp(A)
ITR
chI
chI
ITR

B

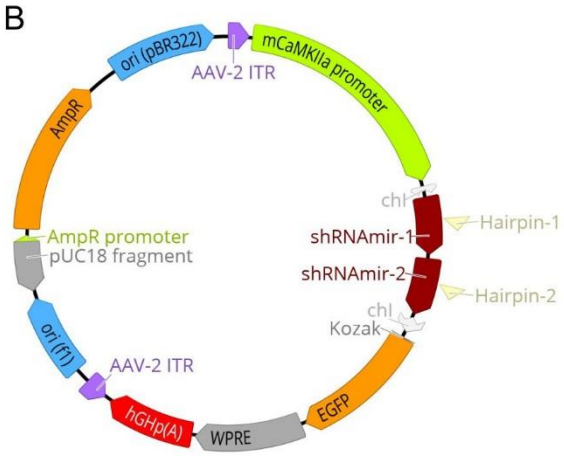
ori (pBR322)
AAV-2 ITR
mCaMKIIa promoter
AmpR
chI
Hairpin-1
shRNAmir-1
AmpR promoter
pUC18 fragment
shRNAmir-2
Hairpin-2
chI
Kozak
ori (f1)
AAV-2 ITR
EGFP
hGHp(A)
WPRE

C

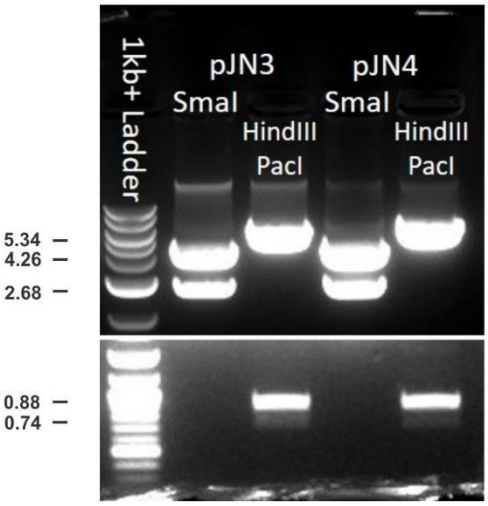
1kb+ Ladder
pJN3
SmaI
HindIII
PacI
pJN4
SmaI
HindIII
PacI
5.34
4.26
2.68
0.88
0.74

Fig. 1

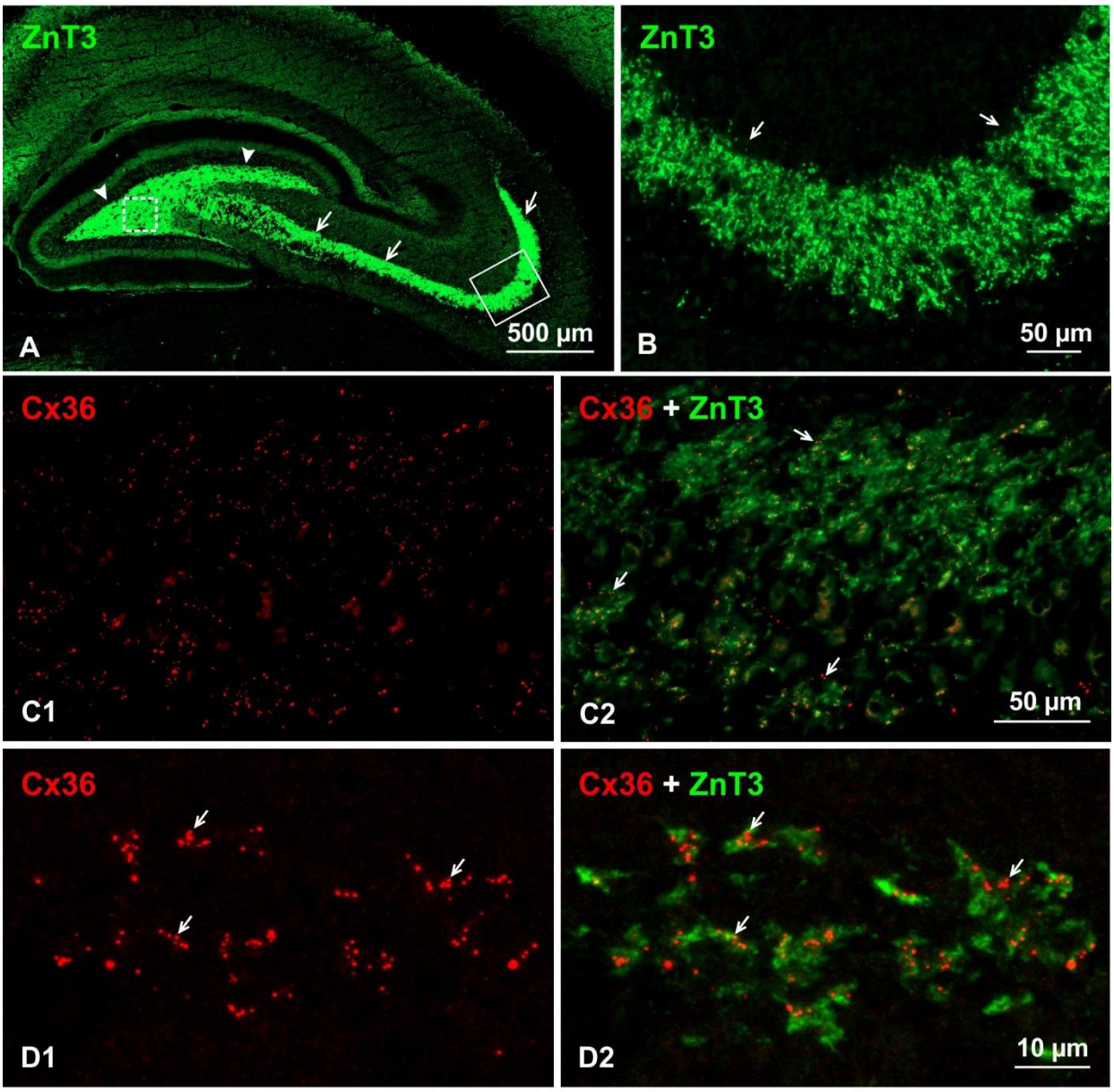
ZnT3
A
500 µm
ZnT3
B
50 µm
Cx36
C1
Cx36 + ZnT3
C2
50 µm
Cx36
D1
Cx36 + ZnT3
D2
10 µm

Fig 2

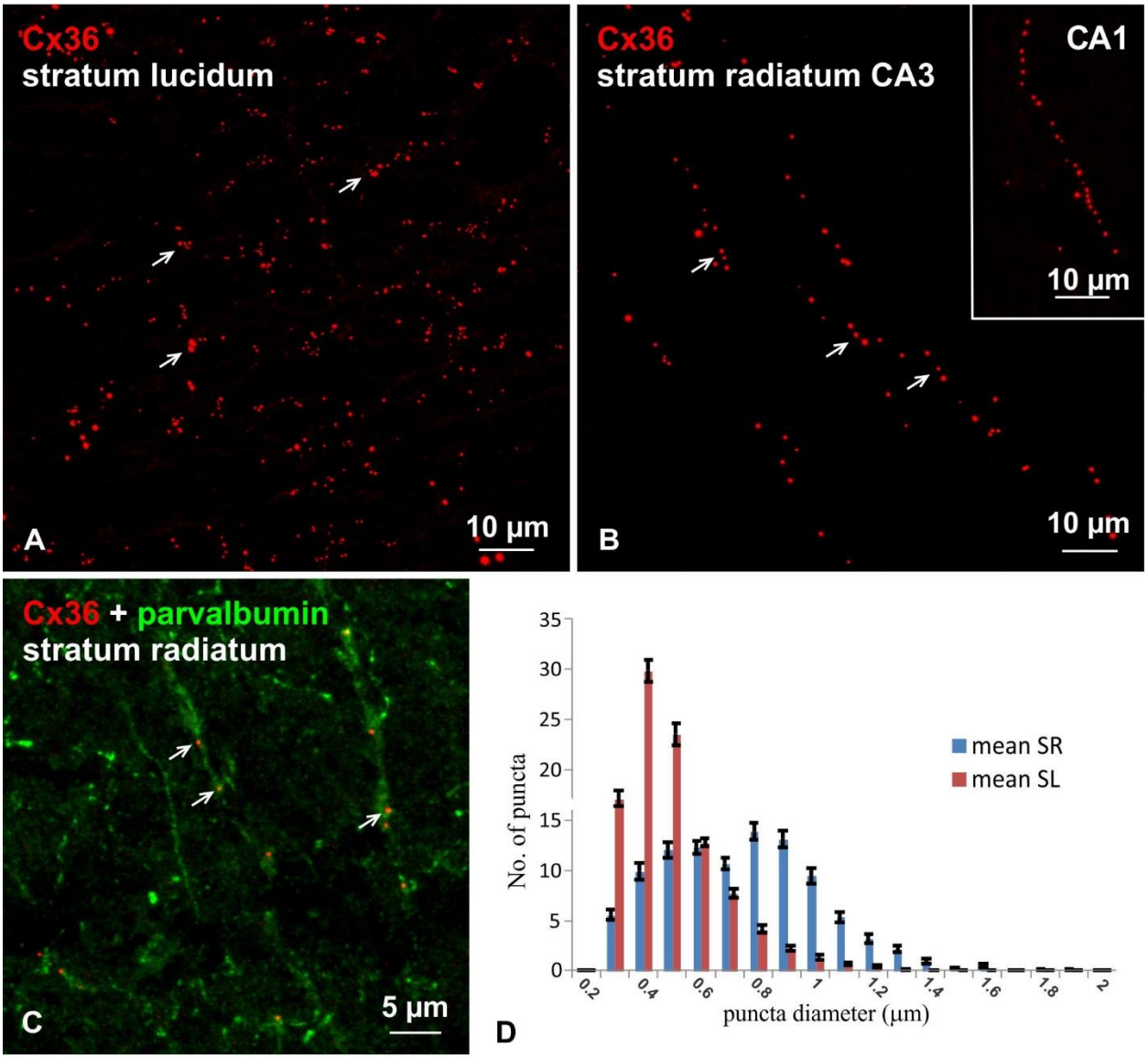
Cx36
stratum lucidum
A
10 µm
Cx36
stratum radiatum CA3
CA1
10 µm
B
10 µm
Cx36 + parvalbumin
stratum radiatum
C
5 µm
D
No. of puncta
puncta diameter (µm)
mean SR
mean SL
0
5
10
15
20
25
30
35
0.2
0.4
0.6
0.8
1
1.2
1.4
1.6
1.8
2

Fig. 3

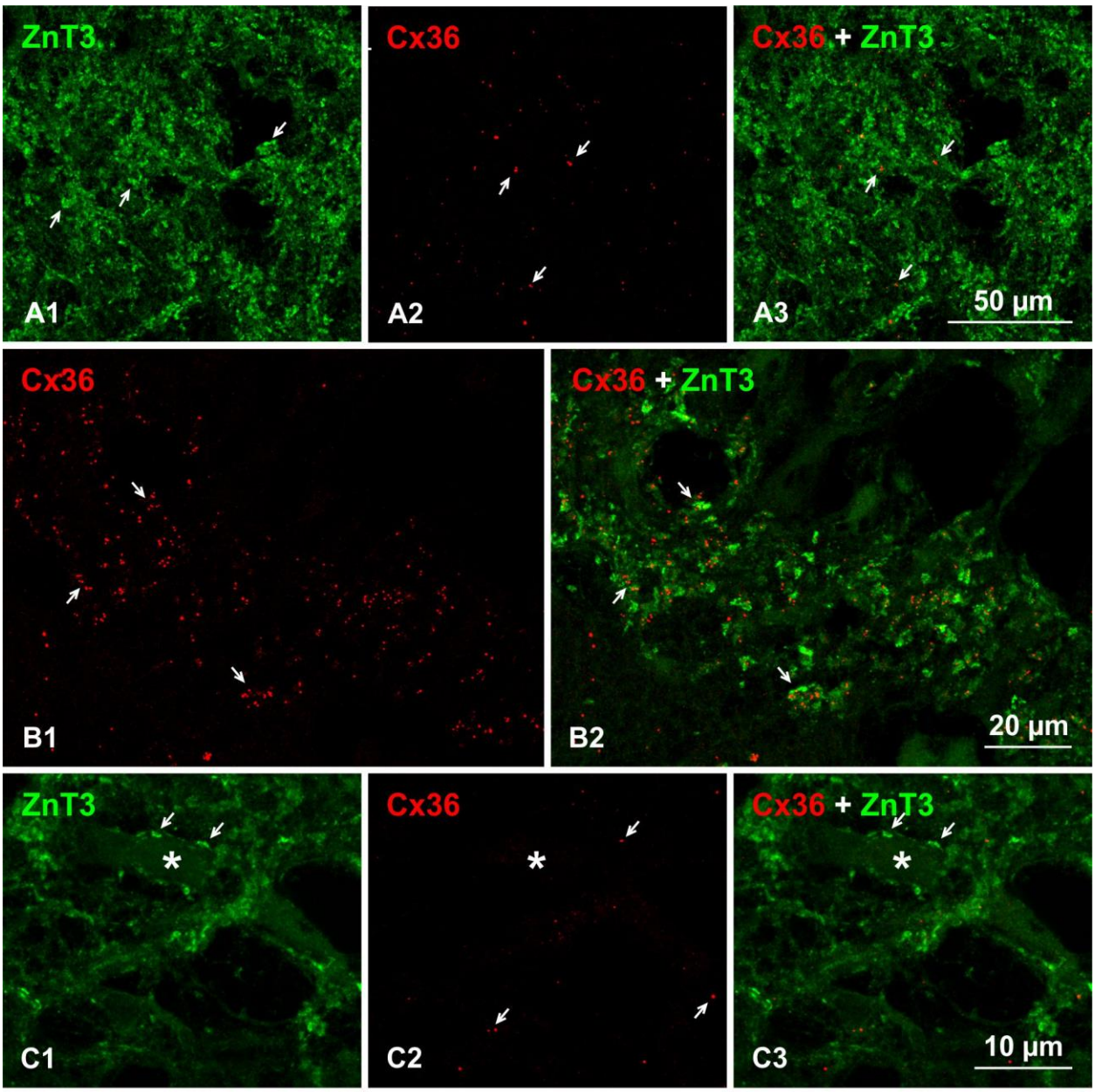
ZnT3
A1
Cx36
A2
Cx36 + ZnT3
A3
50 µm
Cx36
B1
Cx36 + ZnT3
B2
20 µm
ZnT3
C1
Cx36
C2
Cx36 + ZnT3
C3
10 µm

Fig. 4

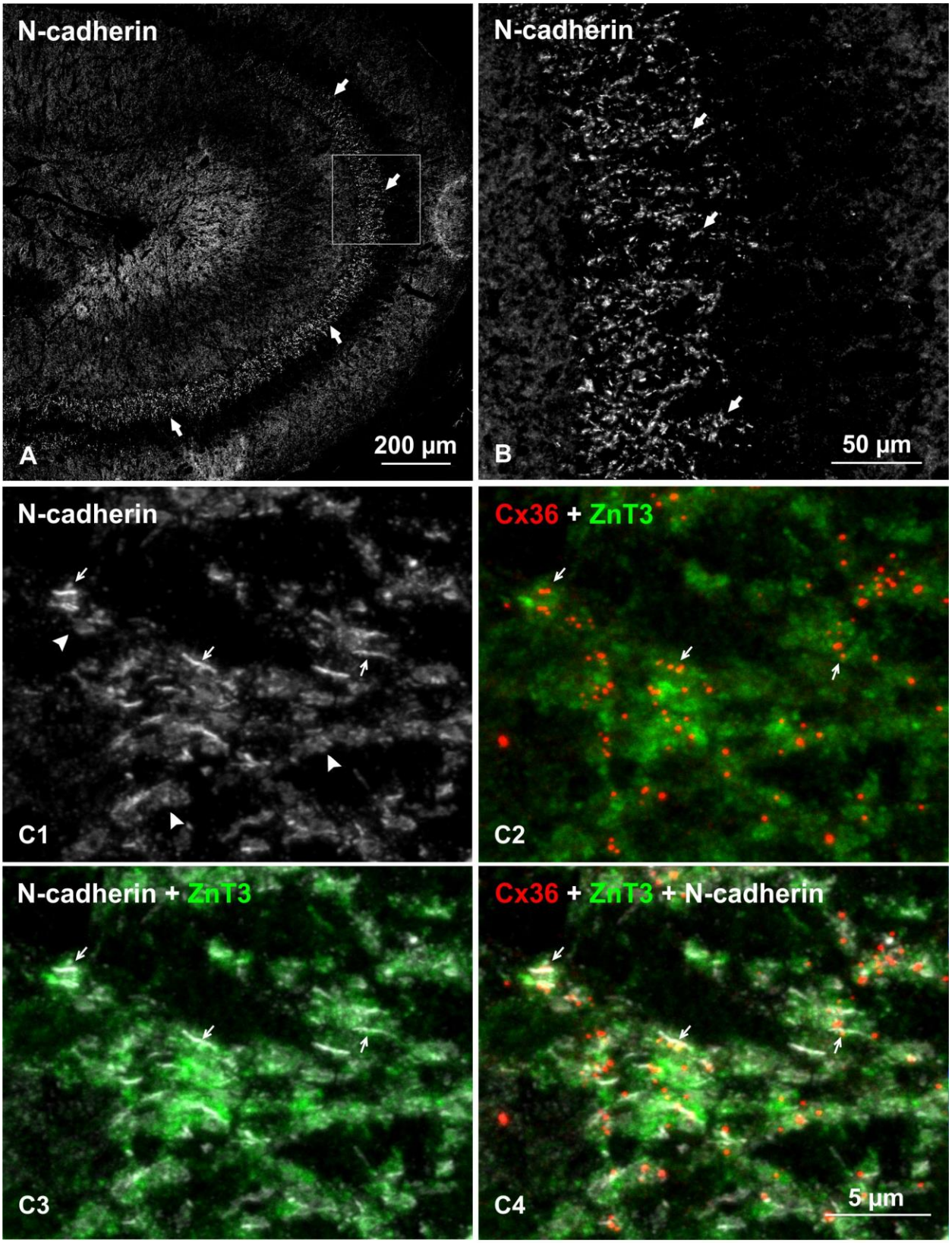
N-cadherin
A
200 µm
N-cadherin
B
50 µm
N-cadherin
C1
Cx36 + ZnT3
C2
N-cadherin + ZnT3
C3
Cx36 + ZnT3 + N-cadherin
C4
5 µm

Fig. 5

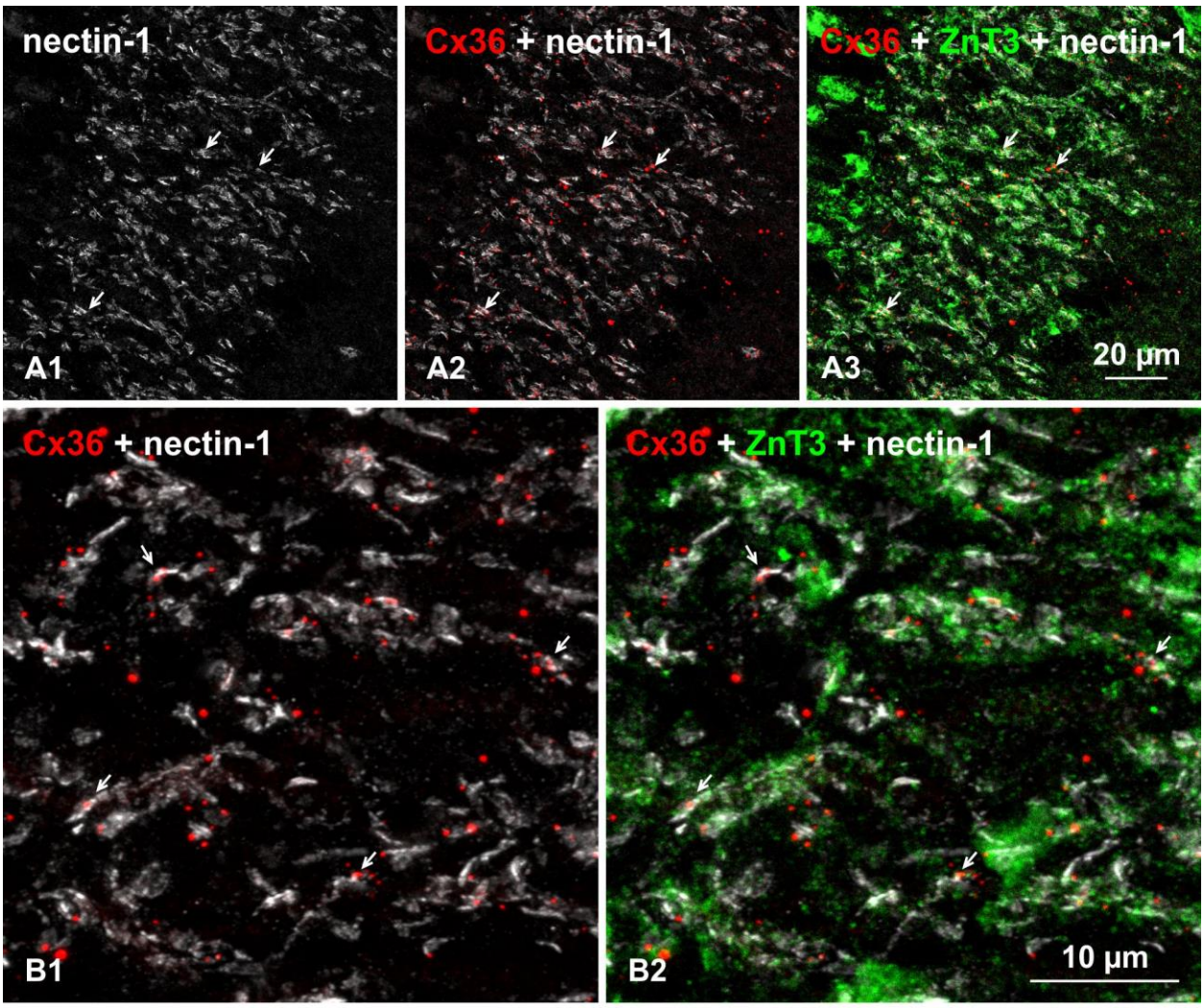
nectin-1
A1
Cx36 + nectin-1
A2
Cx36 + ZnT3 + nectin-1
A3
20 µm
Cx36 + nectin-1
B1
Cx36 + ZnT3 + nectin-1
B2
10 µm

Fig. 6

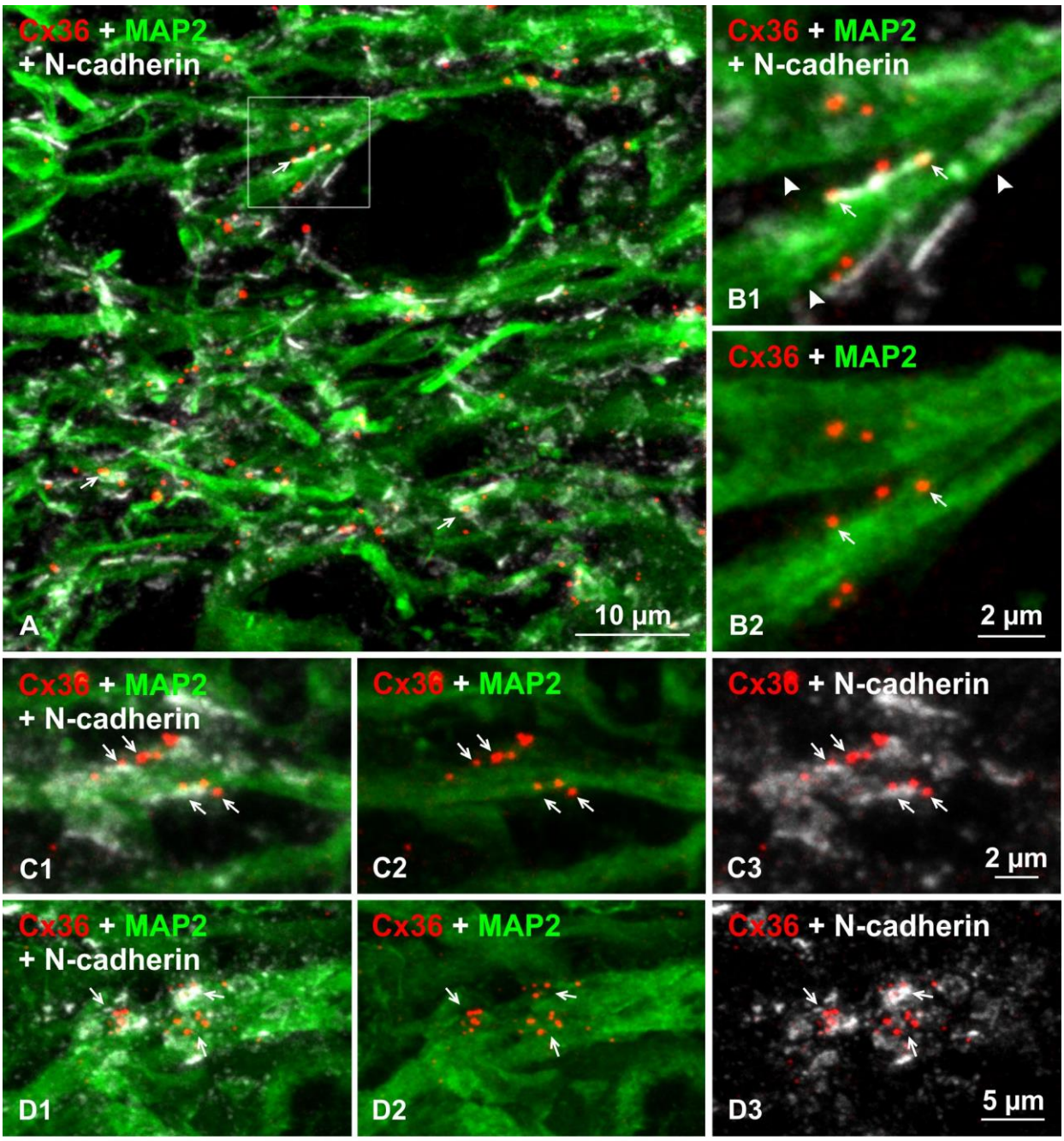
Cx36 + MAP2
+ N-cadherin
A
10 µm
Cx36 + MAP2
+ N-cadherin
B1
Cx36 + MAP2
B2
2 µm
Cx36 + MAP2
+ N-cadherin
C1
Cx36 + MAP2
C2
Cx36 + N-cadherin
C3
2 µm
Cx36 + MAP2
+ N-cadherin
D1
Cx36 + MAP2
D2
Cx36 + N-cadherin
D3
5 µm

Fig 7

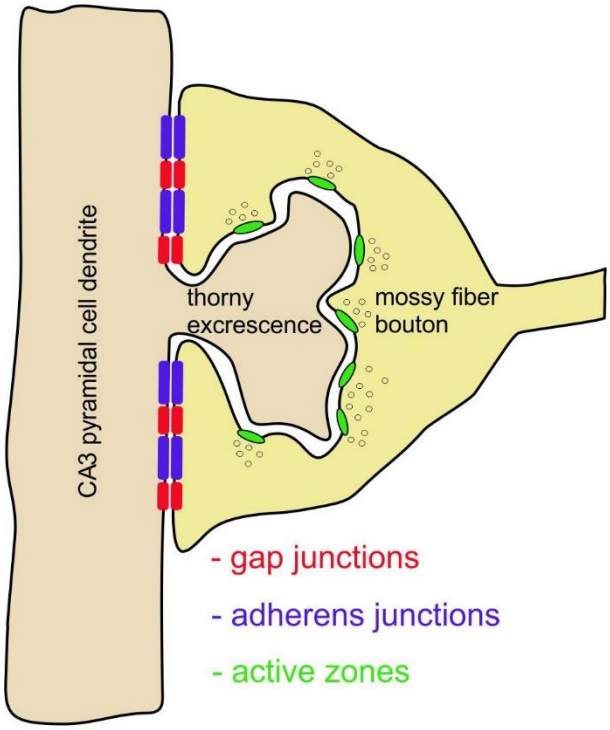
CA3 pyramidal cell dendrite
thorny excrescence
mossy fiber bouton
- gap junctions
- adherens junctions
- active zones

Fig. 8

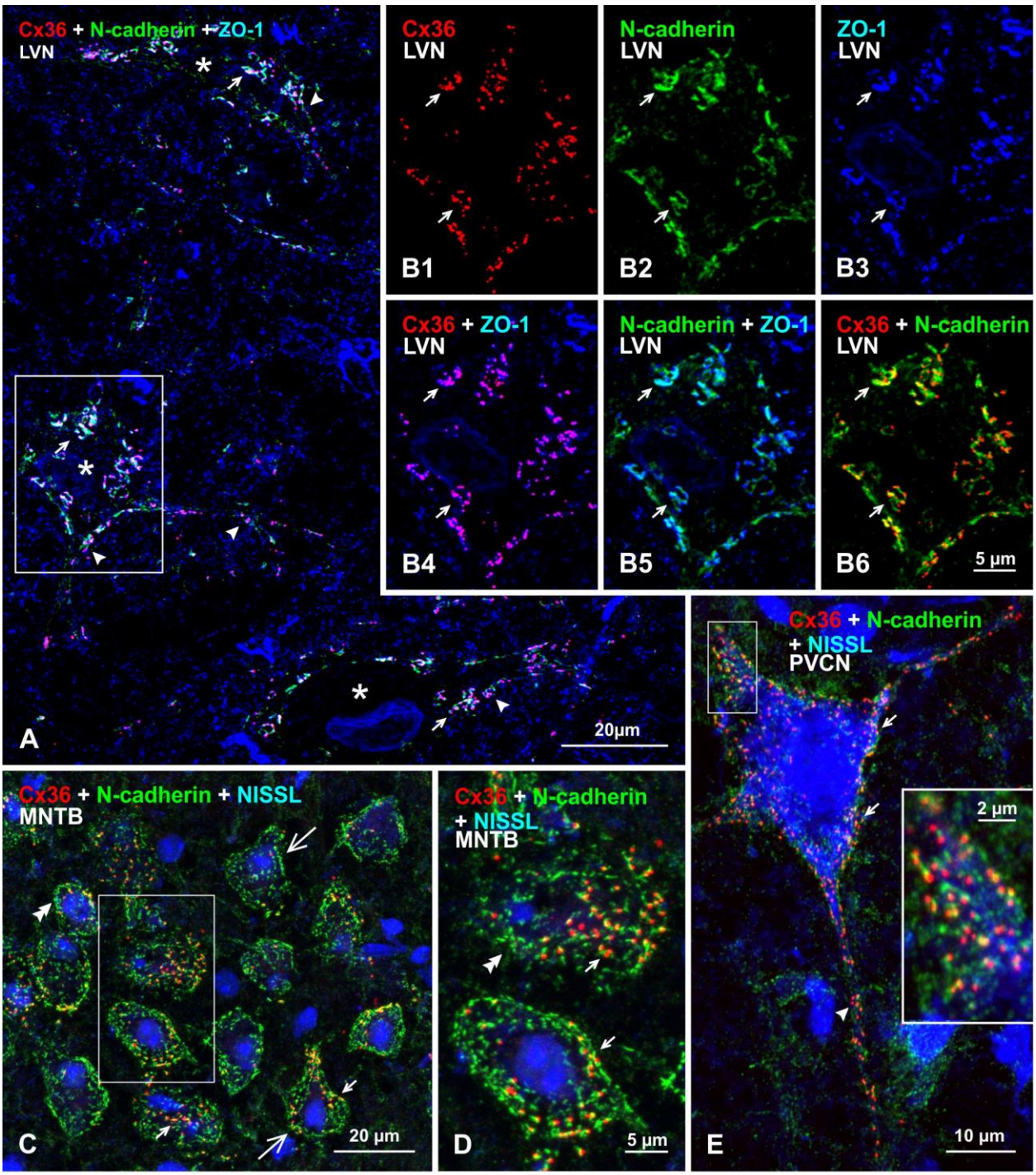
Cx36 + N-cadherin + ZO-1
LVN
Cx36
LVN
B1
N-cadherin
LVN
B2
ZO-1
LVN
B3
Cx36 + ZO-1
LVN
B4
N-cadherin + ZO-1
LVN
B5
Cx36 + N-cadherin
LVN
B6
5 µm
A
20µm
Cx36 + N-cadherin + NISSL
PVCN
2 µm
10 µm
E
Cx36 + N-cadherin + NISSL
MNTB
C
20 µm
Cx36 + N-cadherin
+ NISSL
MNTB
D
5 µm

Fig. 9

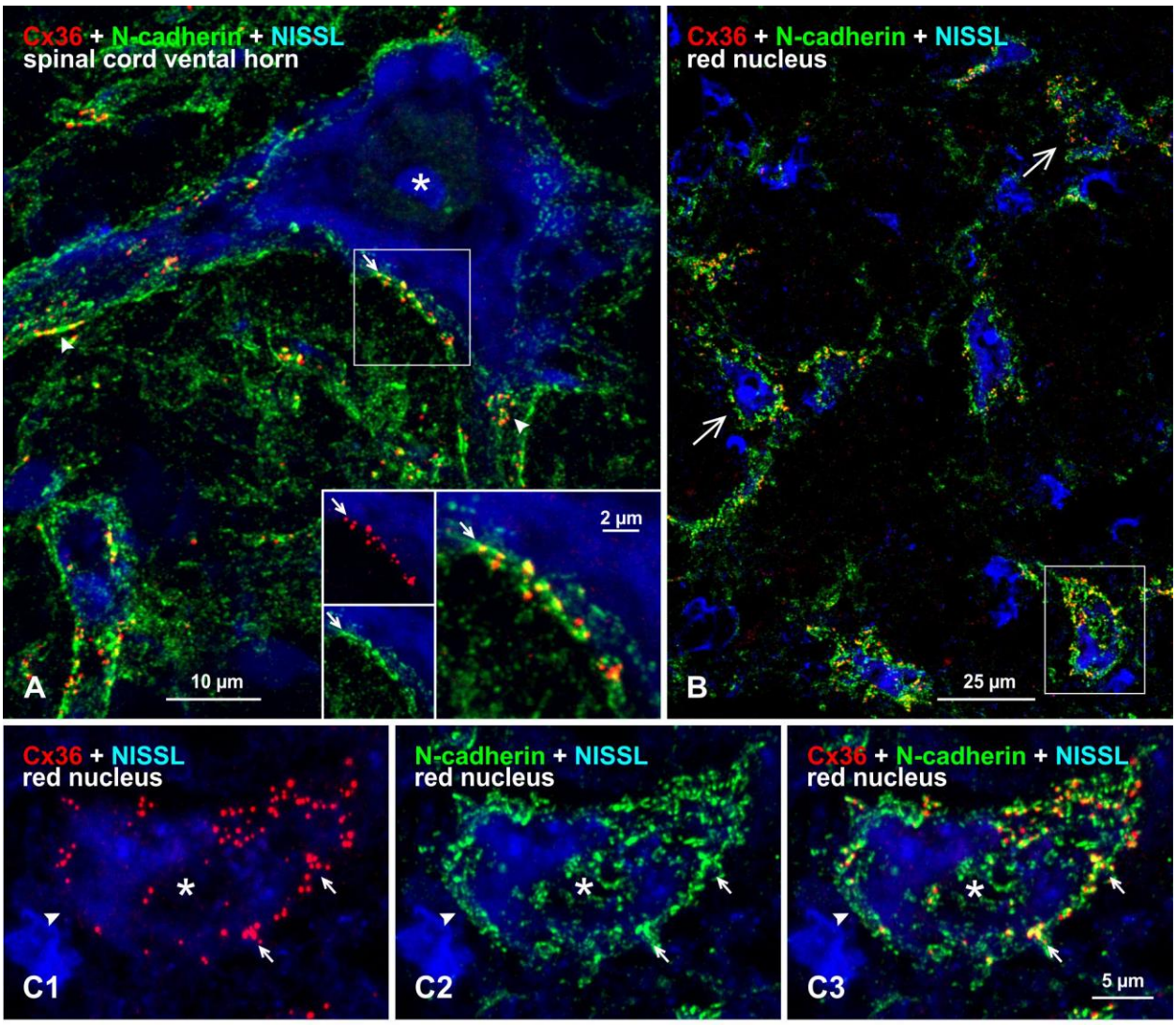
Cx36 + N-cadherin + NISSL
spinal cord ventral horn
2 µm
A
10 µm
Cx36 + N-cadherin + NISSL
red nucleus
B
25 µm
Cx36 + NISSL
red nucleus
C1
N-cadherin + NISSL
red nucleus
C2
Cx36 + N-cadherin + NISSL
red nucleus
C3
5 µm

Fig. 10

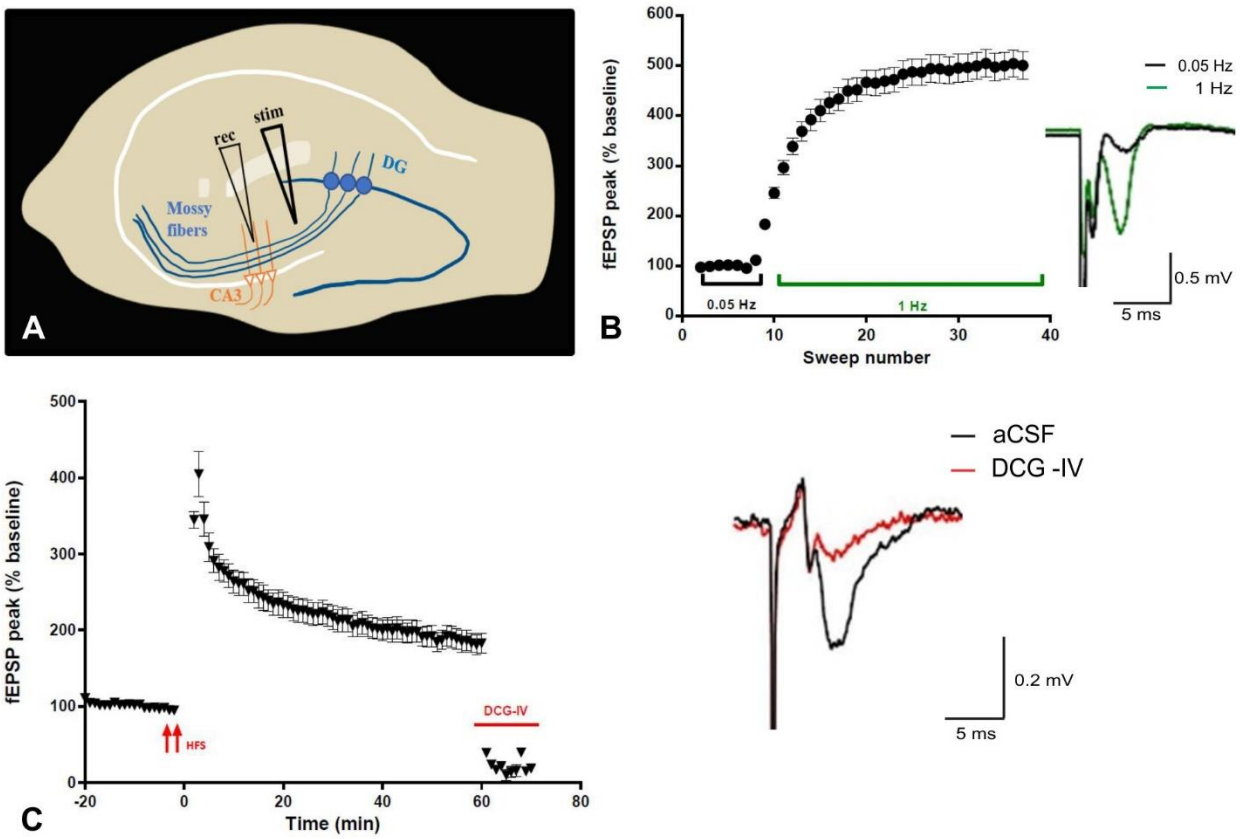
A
rec
stim
DG
Mossy fibers
CA3
B
fEPSP peak (% baseline)
Sweep number
0.05 Hz
1 Hz
0.5 mV
5 ms
C
fEPSP peak (% baseline)
Time (min)
HFS
DCG-IV
aCSF
DCG -IV
0.2 mV
5 ms

Fig. 11

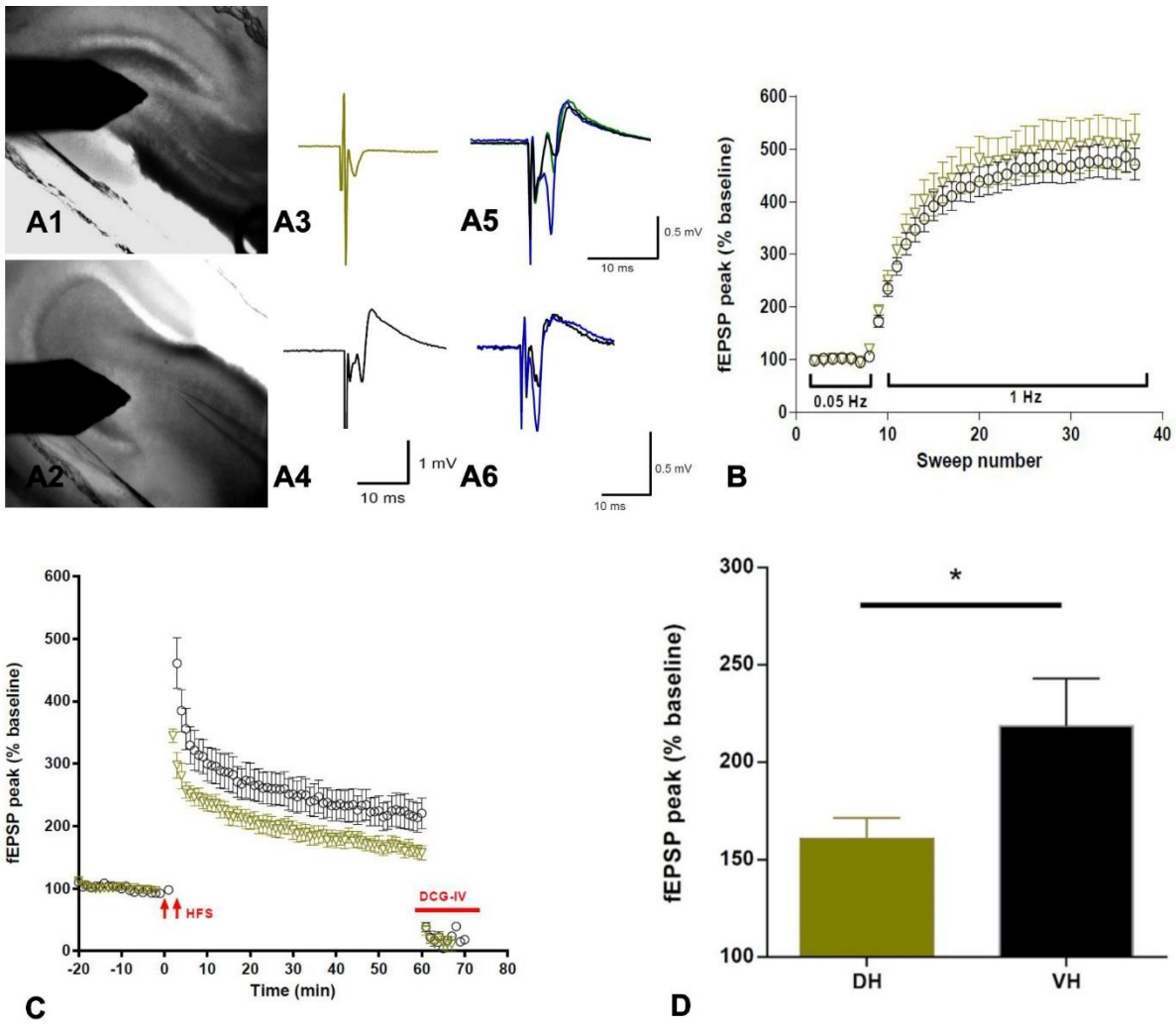
A1
A2
A3
A4
A5
A6
0.5 mV
10 ms
1 mV
10 ms
0.5 mV
10 ms
B
fEPSP peak (% baseline)
0.05 Hz
1 Hz
Sweep number
C
fEPSP peak (% baseline)
HFS
DCG-IV
Time (min)
D
fEPSP peak (% baseline)
*
DH
VH

Fig. 12

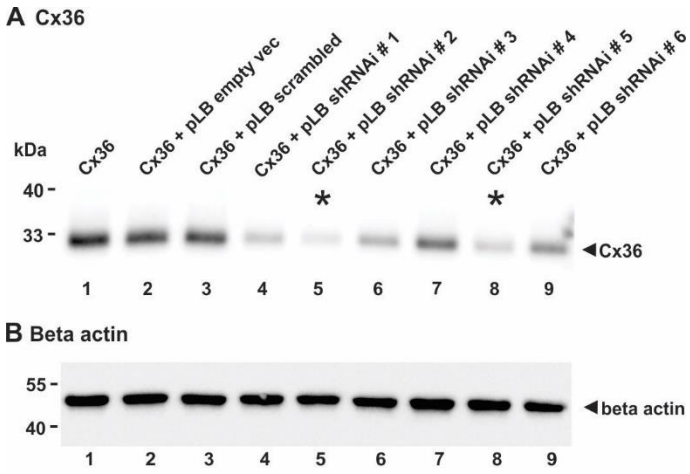
A Cx36
kDa
Cx36
Cx36 + pLB empty vec
Cx36 + pLB scrambled
Cx36 + pLB shRNAi # 1
Cx36 + pLB shRNAi # 2
Cx36 + pLB shRNAi # 3
Cx36 + pLB shRNAi # 4
Cx36 + pLB shRNAi # 5
Cx36 + pLB shRNAi # 6
40
33
*
*
Cx36
1 2 3 4 5 6 7 8 9
B Beta actin
55
40
beta actin
1 2 3 4 5 6 7 8 9

Fig. 13

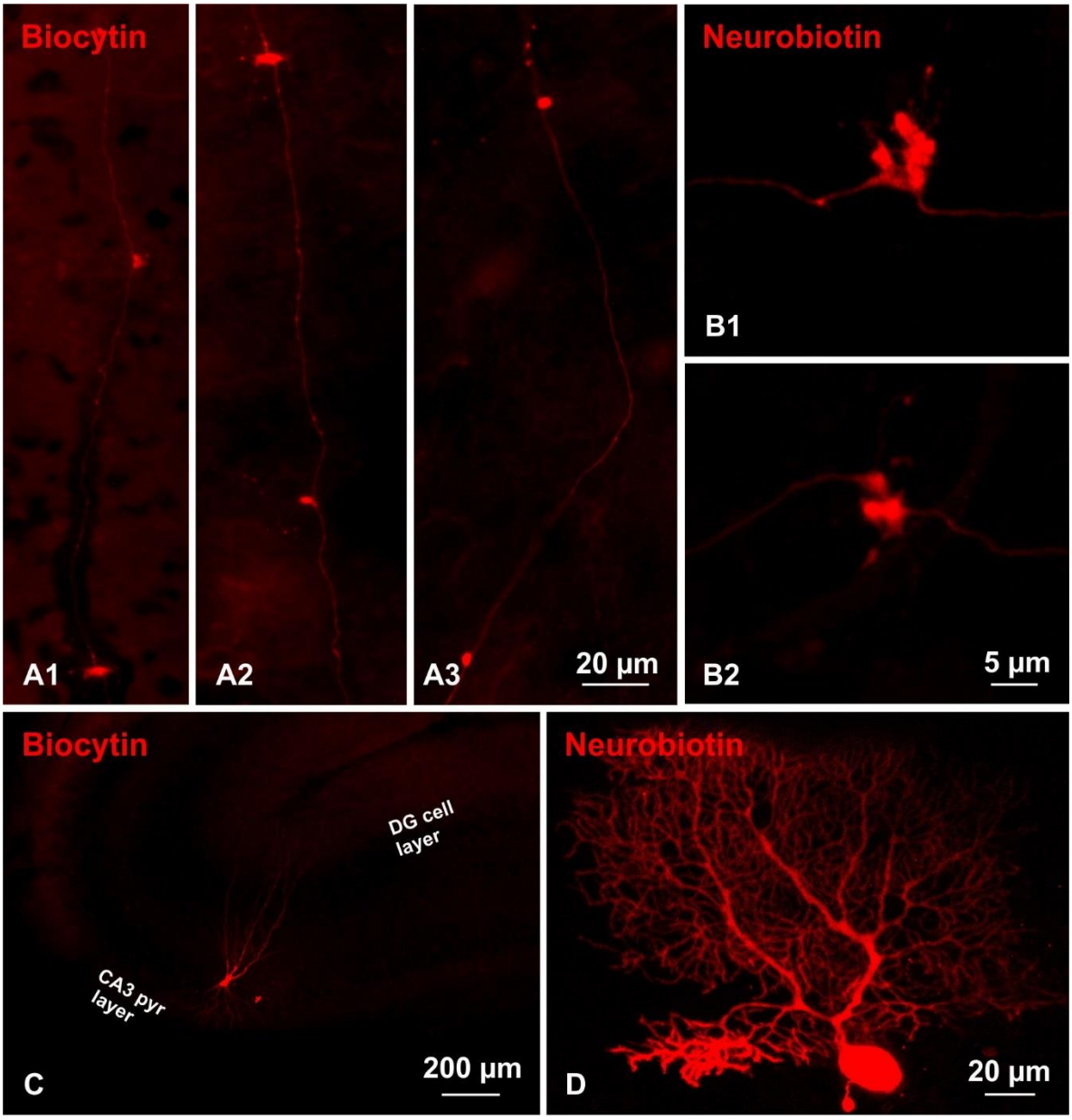

Supplementary fig. 1

Chapter 3: Conclusion

Despite the first reports demonstrating the occurrence of morphologically-identified mixed synapses in the mammalian CNS appearing a half century ago (Sotelo and Palay, 1970) and now culminating in recent discoveries of mixed synapses in a number of locations in mammalian brain and spinal cord (Nagy, 2012; Nagy et al., 2013; Bautista et al., 2014; Rubio and Nagy, 2015; Nagy et al., 2019), with some evidence that those synapses may have an electrical transmission component (Vivar et al., 2012; Ixmatlahua et al., 2020), the study of electrical transmission at these synapses is still in its infancy. Indeed, knowledge of normal physiological conditions under which the electrical component of these synapses may be functionally operative is entirely lacking. This is in stark contrast to nearly sixty years of work on mixed synapses in lower vertebrates where it appears that the majority of neuronal gap junctions occur at mixed synapses (Rash et al., 2015) and the functional contributions of those synapses are well understood (Pereda and Bennett, 2017). One of the difficulties that has plagued investigations of mixed synapses in mammalian systems is the ability to distinguish the electrical transmission component from the chemical component at these synapses. In contrast, in lower vertebrates mediation of transmission by the electrical component can readily be distinguished from the chemical component by virtue of the temporal separation of these components, arising in part from the lower speed of chemical transmission at the lower body temperature of fish. This has facilitated characterization of the properties of the electrical component, including the bi-directionality of electrical transmission identified as antidromically-transmitted responses that can be recorded in the presynaptic terminal (Furshpan, 1964; Pereda et al., 1995).

While combining electrical with chemical transmission is advantageous in cold-blooded vertebrates, where electrical synapses provide higher speed (shorter synaptic delay) and reliability (they are not probabilistic), and provide higher fidelity to networks that require fast signalling, these particular advantages are less relevant in mammals, where electrical and chemical synaptic delays can be similar (Bennett, 1997), making identification of the electrical component more difficult. This obstacle could be alleviated by dual cell recording from the postsynaptic and presynaptic elements at a mixed synapse as done in fish, which allows measures of bi-directional current flow via nGJs, but recording from nerve terminals is a heroic undertaking in mammalian systems. Interestingly, however, this has been achieved at mossy fiber terminals (Geiger and Jonas, 2000; Alle, 2006; Bischofberger et al., 2006b) and such an approach may one day be used to examine electrical transmission at these terminals. In lieu of the ability of all but a few to undertake

this approach, the identification of electrical responses in the form of spikelets generated in CA3 pyramidal cells as a consequence of electrical activity relayed via electrical synapses in response to mossy fiber stimulation, remains a mainstay for studies of these mixed synapses. Abolition of those spikelet responses by gap junction blocking agents has provided some support for mediation of electrical transmission by nGJs at mossy fiber terminals (Vivar et al., 2012), but the known non-specificity of those agents renders results less than compelling. Continuation of the work I have begun surrounding AAV-mediated knockdown of Cx36 in excitatory principle cells in the hippocampus represents a promising alternative to nGJ inhibitor agents, and can be used to study potential impairments in mossy fiber transmission after such knockdown of Cx36 in granule cells of the ventral hippocampus. Various possible functional roles of the electrical transmission component at mixed synapses have been discussed in detail elsewhere (Nagy et al., 2019) and these could be subject to tests at mossy fiber terminals after Cx36 knockdown. One possibility that has not yet been considered is the potential role of electrical synapses at these terminals in mediating transmission of signals arriving to them in an analog fashion, where subthreshold depolarizations of varying magnitude (hence the term analog *vs.* the all-or-none nature of action potentials) in granule cells below the level to generate action potentials are propagated along mossy fibers, creating subthreshold depolarizations of mossy fiber terminals (Alle, 2006). The low pass filtering properties of nGJs would be ideal for transmitting these low amplitude and relatively long duration depolarization to postsynaptic CA3 pyramidal cells. A further direction of studies should include identification of behavioral deficits resulting from this knockdown. With the AAV vector for achieving Cx36 knockdown now in-hand, I have conducted some initial work wherein the vector was administered stereotaxically into the granule cell region of the ventral hippocampus (coordinates relative to bregma, AP -5.7 mm, ML 4.6 mm, DV 7.2 mm) bilaterally in adult rats. Results are very preliminary with only a few animals (N=6) having been examined for behavioral deficits using the fear conditioning test. Contextual fear conditioning induces a robust form of emotional memory and requires the function of both amygdala and hippocampus (Restivo et al., 2009). There is evidence pointing out the role of ventral hippocampus in the formation and expression of contextual fear memory (Richmond et al., 1999; Zhang et al., 2001). So, we went ahead doing contextual fear memory test on a small sample of injected rats. Contextual fear conditioning involves linking a strong aversive stimulus (foot shock) with an environment context (shock chamber). Subsequent presentation of the context elicits a fear response presented as freezing behaviour, defined as the immobilization of the animal except for respiration. When fear

context is presented without the stimulus, there will be a reduction in the fear conditioned response on subsequent days, a process called fear extinction. A contextual fear conditioning protocol was performed on scrCx36 (N=3) and shCx36 (N=3) injected rats, followed by testing of fear extinction. I found the freezing time is reduced in rats injected with shCx36 compared with scrCx36, on day 1 post-application of foot shock (Fig. 15, 80.22 ± 4.98 *vs.*50.33 ± 9.00 %, * $p<0.05$, unpaired t test). The fear extinction test conducted from day 2 to day 6 did not show any significant difference between shCx36 and scrCx36 injected rats. Anatomical results confirming whether Cx36 knockdown in these animals was successful are not yet available, consequently, this aspect of my investigations was not included in this thesis. Further, my imminent departure from Winnipeg precluded completion of this work. Another future direction with the study will be to look at the electrophysiological parameters associated with mossy terminals in the sh- and scrCx36 injected rats. LTP analysis at mossy fiber pathway in rats from both virus injected groups will confirm the contribution of Cx36 containing gap junctions in maintaining plasticity at ventral hippocampus, as we see higher potentiation in rat ventral and not dorsal hippocampus. Mossy fibers being known as the detonator synapses for their high reliability to discharge postsynaptic CA3 neurons, analyzing the properties of their single unitary EPSPs will tell us the efficacy of individual mossy fiber connections and whether the absence of Cx36 will alter any of their properties in sh injected rats. Also, a comparative study of the current stimulation that is required to stimulate a single mossy fiber axon in both the virus injected groups will tell us whether the presence of electrical synapses at these terminals would allow more neuronal discharge with less stimulation, or in other words, whether the presence of electrical synapses would allow to reduce synaptic failures at these terminals thereby contributing to neurotransmission fidelity in a manner that impacts memory storage and retrieval. Thus, the study by utilizing histological, behavioural and electrophysiological techniques, would be the first to give an overall appreciation on the role of mixed chemical/electrical synapses in the mammalian CNS.

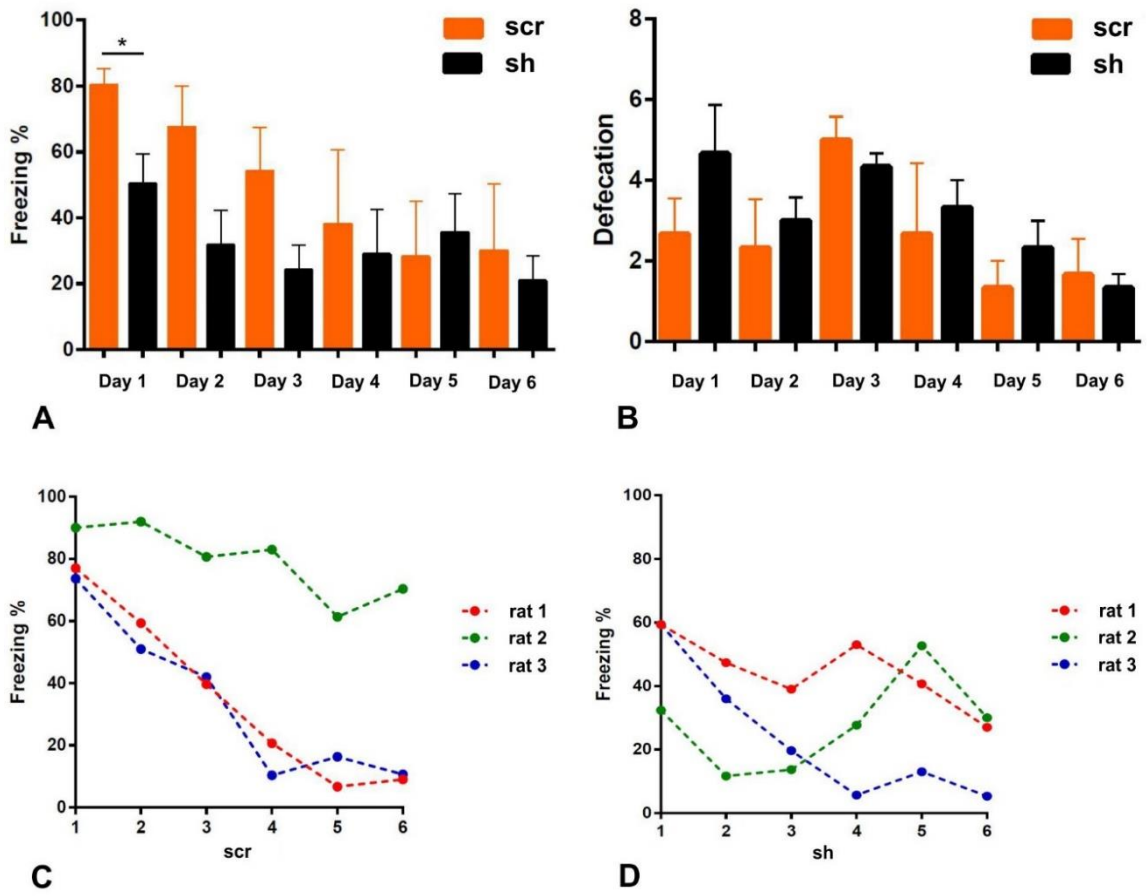
Freezing %
scr
sh
*
Day 1
Day 2
Day 3
Day 4
Day 5
Day 6
A
Defecation
B
rat 1
rat 2
rat 3
scr
C
sh
D

Fig. 15

Fig. 15. Contextual fear conditioning test performed in rats injected with AAV containing scrCx36 and shCx36 sequences. **(A)** Post-foot shock, the rats were analyzed for their freezing time (expressed as %) and defecation (feces counts) for the next six days. The freezing time in rats injected with AAV containing shCx36 was less on day 1 than the rats that got injected with scrCx36. There was no significant difference in the freezing time on the subsequent days. (B) The count of feces of all animals was noted when rats were inside the shock chamber. Graph shows no significant differences in the defecation counts between the groups. (C) A plot of freezing time (in %) in rats from both groups over the period of six days showing an overall decline in the freezing.

3.1. References

Alle H (2006) Combined Analog and Action Potential Coding in Hippocampal Mossy Fibers. Science (American Association for the Advancement of Science) 311:1290-1293.

Bautista W, McCrea DA, Nagy JI (2014) Connexin36 identified at morphologically mixed chemical/electrical synapses on trigeminal motoneurons and at primary afferent terminals on spinal cord neurons in adult mouse and rat. Neuroscience 263:159-180.

Bennett M (1997) Gap junctions as electrical synapses. Journal of Neurocytology 26:349-366.

Bischofberger J, Engel D, Li L, Geiger JRP, Jonas P (2006) Patch-clamp recording from mossy fiber terminals in hippocampal slices. Nature protocols 1:2075-2081.

Furshpan EJ (1964) "Electrical Transmission" at an Excitatory Synapse in a Vertebrate Brain. Science (American Association for the Advancement of Science) 144:878-880.

Geiger JRP, Jonas P (2000) Dynamic Control of Presynaptic Ca2+ Inflow by Fast-Inactivating K+ Channels in Hippocampal Mossy Fiber Boutons. Neuron (Cambridge, Mass) 28:927-939.

Ixmatlahua DJ, Vizcarra B, Gómez-Lira G, Romero-Maldonado I, Ortiz F, Rojas-Piloni G, Gutiérrez R (2020) Neuronal Glutamatergic Network Electrically Wired with Silent but Activatable Gap Junctions. The Journal of neuroscience 40:4661-4672.

Nagy JI (2012) Evidence for connexin36 localization at hippocampal mossy fiber terminals suggesting mixed chemical/electrical transmission by granule cells. Brain Res 1487:107-122.

Nagy JI, Pereda AE, Rash JE (2019) On the occurrence and enigmatic functions of mixed (chemical plus electrical) synapses in the mammalian CNS. Neurosci Lett 695:53-64.

Nagy JI, Bautista W, Blakley B, Rash JE (2013) Morphologically mixed chemical-electrical synapses formed by primary afferents in rodent vestibular nuclei as revealed by immunofluorescence detection of connexin36 and vesicular glutamate transporter-1. Neuroscience 252:468-488.

Pereda AE, Bennett MVL (2017) Electrical Synapses in Fishes: Their Relevance to Synaptic Transmission. In: Network Functions and Plasticity: Perspectives from Studying Neuronal Electrical Coupling in Microcircuits, pp 161-181.

Pereda AE, Bell TD, Faber DS (1995) Retrograde synaptic communication via gap junctions coupling auditory afferents to the Mauthner cell. Journal of Neuroscience 15:5943-5955.

Rash JE, Kamasawa N, Vanderpool KG, Yasumura T, O'Brien J, Nannapaneni S, Pereda AE, Nagy JI (2015) Heterotypic gap junctions at glutamatergic mixed synapses are abundant in goldfish brain. Neuroscience 285:166-193.

Restivo L, Vetere G, Bontempi B, Ammassari-Teule M (2009) The Formation of Recent and Remote Memory Is Associated with Time-Dependent Formation of Dendritic Spines in the Hippocampus and Anterior Cingulate Cortex. The Journal of neuroscience 29:8206-8214.

Richmond MA, Yee BK, Pouzet B, Veenman L, Rawlins JNP, Feldon J, Bannerman DM (1999) Dissociating Context and Space Within the Hippocampus: Effects of Complete, Dorsal, and Ventral Excitotoxic Hippocampal Lesions on Conditioned Freezing and Spatial Learning. Behavioral neuroscience 113:1189-1203.

Rubio ME, Nagy JI (2015) Connexin36 expression in major centers of the auditory system in the CNS of mouse and rat: Evidence for neurons forming purely electrical synapses and morphologically mixed synapses. Neuroscience 303:604-629.

Sotelo C, Palay SL (1970) The fine structure of the lateral vestibular nucleus in the rat. II. synaptic organization. Brain research 18:93-115.

Vivar C, Traub RD, Gutierrez R (2012) Mixed electrical-chemical transmission between hippocampal mossy fibers and pyramidal cells. Eur J Neurosci 35:76-82.

Zhang W-N, Bast T, Feldon J (2001) The ventral hippocampus and fear conditioning in rats: different anterograde amnesias of fear after infusion of N-methyl- d-aspartate or its noncompetitive antagonist MK-801 into the ventral hippocampus. Behavioural brain research 126:159-174.